Title	Discrete-Time Noncausal Linear Periodically Time-Varying Scaling for Robustness Analysis and Controller Synthesis(Dissertation_全文)
Author(s)	Hosoe, Yohei
Citation	Kyoto University (京都大学)
Issue Date	2013-09-24
URL	http://dx.doi.org/10.14989/doctor.k17889
Right	
Type	Thesis or Dissertation
Textversion	ETD

Discrete-Time Noncausal Linear Periodically Time-Varying Scaling for Robustness Analysis and Controller Synthesis

A Dissertation
Submitted to Kyoto University
in Partial Fulfillment of the Requirements
for the Degree of Doctor of Engineering

Yohei Hosoe

2013

Abstract

Since modeling of real plants inevitably gives rise to modeling errors regarded as uncertainties, considering robustness for the uncertainties is important in actual control problems. For tackling issues of analyzing robust stability of closed-loop systems in a less conservative fashion, the μ-analysis method is known to be effective. As an alternative approach to robust stability analysis, on the other hand, discrete-time noncausal linear periodically time-varying (LPTV) scaling has been proposed recently. This approach can be naturally introduced through the lifting-based treatment of systems, and the associated conservativeness can be reduced by increasing the period of lifting. This thesis is concerned with this lifting-based scaling approach.

In this thesis, we first review the definition and properties of noncausal LPTV scaling. This scaling approach is a generalization of the conventional causal linear time-invariant (LTI) scaling, and coincides with the latter scaling when we take the lifting period $N = 1$ (i.e., without lifting-based treatment). We call such a framework for robust stability analysis without lifting-based treatment the lifting-free framework, and that with lifting-based treatment the lifting-based framework. It is known that noncausal LPTV scaling induces dynamic causal LTI scaling in the lifting-free framework even if it is confined to static in the lifting-based framework. We show two theorems associated with this promising property, and confirm them numerically.

After such reviews, we consider applying static noncausal LPTV scaling to robust controller synthesis. If we take account of only robust stability in the synthesis, however, responses of the resulting control systems may become oscillatory at an unacceptable level. To avoid this problem, we develop a controller synthesis method taking account of not only robust stability but also robust H_∞ performance. Effectiveness of the developed method for robust control is discussed theoretically and numerically, and also demonstrated by experiments with a cart inverted pendulum whose length can be set from three choices (we regard the difference as the uncertainty in the experiments). The obtained results will indicate that the developed synthesis framework is indeed effective and practical in actual control problems.

Despite such advances for robust controller synthesis, however, comprehensive properties of noncausal LPTV scaling have not necessarily been revealed entirely. Hence, in this thesis, we also study further properties of noncausal LPTV scaling to exploit full potential of it. The missing arguments include, for example, an explicit characterization of the class of dynamic causal LTI scaling in the lifting-free framework that can equivalently be dealt with by working instead on static noncausal LPTV scaling in the lifting-based framework. We first introduce a concept called shift invariance with respect to timing of lifting, and give a partial answer to the above open problem. Regarding the introduced concept, we can show that noncausal LPTV scaling is not shift-invariant, in general, while causal scaling is. In addition, if we introduce the operation called shift-invariant reconstruction, we can naturally construct a class of shift-invariant scaling from (not necessarily shift-invariant) noncausal LPTV scaling in the lifting-based framework, which plays an essential role in the aforementioned characterization. The obtained theoretical results will be confirmed numerically.

To facilitate further studies on properties of noncausal LPTV scaling, we also apply another theoretical tool called an infinite matrix framework representing systems by infinite matrices. Since causal LTI and noncausal LPTV scaling approaches are defined in the different (lifting-free and -based) frameworks, direct comparison of their frequency-domain properties has not been very straightforward. Hence, we consider constructing a new unified framework that can equivalently deal with both the lifting-free and -based scaling approaches, and compare them in the unified framework. In particular, we introduce causal LTI and noncausal LPTV finite impulse response (FIR) scaling approaches in the lifting-free and -based frameworks, respectively, as practical and tractable classes of dynamic scaling approaches, and study their relationship with respect to the associated conservativeness in robust stability analysis. As a result of the comparison, we theoretically show the effect of employing the lifting technique in robust stability analysis for reducing the conservativeness. In this thesis, we also develop an explicit procedure for robust stability analysis based on dynamic noncausal LPTV FIR scaling, which enables us to numerically confirm the above theoretical results as well as the effectiveness of the developed analysis framework.

Through these theoretical and practical discussions, we develop a basis of robustness analysis and controller synthesis exploiting noncausal LPTV scaling. Noncausal LPTV scaling has interesting properties that differentiate it from the conventional causal LTI scaling, and is expected to be one of the effective tools for robust control. The results obtained in this thesis will thus be a step toward further developments in robust control theory.

Acknowledgments

First of all, I would like to express my sincere gratitude to Professor Tomomichi Hagiwara of Kyoto University for his supervision and constant support. Without his valuable advice and encouragement, this thesis would never have been completed.

I would also like to thank Associate Professor Yoshio Ebihara of Kyoto University. His thoughtfulness, as well as suggestive comments on robustness analysis and controller synthesis, was very helpful for my research activities in the laboratory.

My gratitude also goes to Professor Shinji Doi and Associate Professor Takashi Hisakado of Kyoto University for their kind support as co-supervisors. Their stimulating comments provided us with new viewpoints in this research.

Professor Anders Rantzer of Lund University also deserves my gratitude for his acceptance of my two-month stay in his department and suggestive advice. The stay was very exciting, and became a precious experience for me.

I would also like to thank Professor Takashi Hikihara of Kyoto University for giving me chances to study topics other than those in this thesis. The experiences let me have a wider view, and will provide new insights in my future work.

I am also grateful to Ms. Kei Katayama, a graduate student at Kyoto University, for her collaboration in a part of this research. She worked with me, and spent a lot of time on control experiments whose results are shown in this thesis.

Finally, I would like to thank all of my colleagues, friends and parents for their understanding and encouragement.

Contents

Chapter 1

Introduction

1.1 Background in robust control

When we apply control theory to real plants, it is generally required to identify them by some models. However, since real plants include factors difficult to deal with, such as nonlinearities and parameter variations, modeling of the plants inevitably gives rise to modeling errors regarded as uncertainties. If these uncertainties are not taken account of in the synthesis, the designed controllers may fail to control the real plants adequately. Therefore, ensuring robustness, which guarantees required performance of the closed-loop systems regardless of given classes of uncertainties, is quite important from the viewpoint of control applications.

The gain margins and the phase margins studied in the framework of classical control theory [6] are concepts related with robustness, and in this sense, the study of robust control has a long history. In 1966, the so-called small-gain theorem was proved by George Zames [46],[47], and it became easy to deal with the closed-loop system consisting of the nominal system and the uncertainty. In 1979, George Zames further gave a formulation of the H_∞ control problem [48],[49], and this became a trigger for the remarkable development of robust control theory ensuring worst-case performance of the systems whose gaps from the plants are explicitly extracted as H_∞-norm-bounded uncertainties. Since the problem of designing robust controllers satisfying the small-gain conditions can be regarded as a special case of the H_∞ control problems, the formulation attracted many researchers in those days. H_∞ control theory has been further developed [19],[12],[27], and employed to improve accuracy about products in manufacturing industry such as steel industry, and also applied to the attitude control of satellites, the head positioning control of disk drives, and so forth. Nowadays, H_∞ control is one of the representative methods in the field of robust control.

As mentioned above, H_∞ control theory has succeeded from the viewpoint of robust

control for norm-bounded uncertainties. However, as higher accuracy was required in actual control problems, it became insufficient to take account of only (unstructured) norm-bounded uncertainties. In most actual cases, we obtain a sort of information about the uncertainties (e.g., they are structured), and then robustness analysis and controller synthesis based on the basic H_∞ control theory naturally become conservative. It is quite important to reduce this conservativeness, and many researchers tackled this issue to make the robust control theory more practical.

As one of the robust control methods that enable us to deal with properties of uncertainties directly, the μ-analysis and synthesis approach [11],[32],[51] was studied extensively from the 1980s, with the research group of John C. Doyle in the lead. μ-analysis evaluates robust stability of the closed-loop system through calculating the structured singular values. Various methods were proposed to reduce conservativeness of robust stability analysis, associated with the development of μ-analysis. μ-synthesis is an extension of μ-analysis for controller synthesis, and a D-scaling-based algorithm is available in μ-Analysis and Synthesis Toolbox [2] on MATLAB. The μ-analysis and synthesis approach succeeded in reducing conservativeness of robustness analysis and controller synthesis for the systems with structured uncertainties, and thus is already one of the standard methods for robust control.

Typical frameworks for μ-analysis and synthesis, however, have a sort of numerical issue. More specifically, we often employ frequency gridding to calculate (an upper bound of) the structured singular value for μ-analysis and synthesis, since computing its response on the whole frequency range is generally difficult from the computational viewpoint. However, if we employ frequency gridding, we cannot evaluate the structured singular values that are not on the grid. Hence, the obtained results inevitably depend on the gridding taken in the analysis. This may cause an unfavorable situation that the obtained results indicate that the closed-loop system is robustly stable, even when it is not actually. Since processing power of computers is finite, this issue is essentially unsolvable, as far as the frequency gridding is employed.

From the 1990s, controller synthesis employing linear matrix inequalities (LMIs) was studied extensively [7],[9],[38],[29]. Since LMIs are globally solvable as convex optimization problems, they are quite suitable for computations, and enable us to systematically obtain globally optimal solutions without any manual adjustment. In addition, LMIs can easily deal with multivariable systems, and are also compatible with multiobjective controller synthesis. Hence, many researchers made efforts to convert various conventional results to the LMI counterparts. For example, the analysis condition in the framework of H_∞ control was known to reduce to an LMI by applying the bounded real lemma [1], and the analysis condition was further linearized for controller synthesis as discussed in [18],[38],[31]. Since the LMI-based

H_∞ controller synthesis provides globally optimal solutions for H_∞ control problems that ensure robust stability of the closed-loop systems in a sufficient fashion (through ignoring information about the uncertainties), it does not lead us to overestimate the stability region with respect to the uncertainties. In addition, conservativeness of the synthesis stemming from the ignored information of uncertainties can be reduced by introducing the scaling technique, as in the case with μ-synthesis.

In parallel with the above development of LMI-based controller synthesis, treatment of uncertainties was further studied. As one of the remarkable results, the integral quadratic constraint (IQC) theory was organized [30]. This theory enables us to directly deal with many kinds of norm-bounded uncertainties (e.g., static and dynamic, linear and nonlinear, time-invariant and time-varying, and so fourth), and we can reduce the conservativeness of the analysis and synthesis that arises in the treatment of uncertainties. The robustness analysis condition in the IQC theory can be reduced to an LMI by applying the Kalman-Yakubovich-Popov (KYP) lemma [43]–[45],[34], and the condition can be further linearized for controller synthesis by the same linearization technique described in [38],[31]. IQC theory unifies many kinds of control theory for the systems including norm-bounded uncertainties, and conventional methods such as the small-gain and passivity theorems, D-scaling, (D, G)-scaling and multiplier methods [42],[51],[13],[10],[37],[17] can be formulated as special cases of the IQC approach.

1.2 Motivation of this thesis

The purpose of this thesis is to develop a robustness analysis and synthesis method that is more practical and tractable compared with conventional methods. As already stated, the IQC theory unifies many kinds of conventional results, and is one of the most successful approaches for robust control. This thesis tackles the issue of how to efficiently reduce conservativeness of the robustness analysis and synthesis based on this theory. In particular, the thesis deals with the case of linear time-invariant (LTI) uncertainties, which naturally arise when the plants include parameter variations. In this case, the separator-type robust stability theorem [25] is known to further hold for robust stability of the closed-loop system. This theorem can be regarded as a special case of the IQC approach under the restriction on the class of uncertainties (to be LTI), and gives a condition not only sufficient but also necessary for robust stability, while the general IQC theory guarantees only sufficiency. Various types of robust stability conditions for LTI uncertainties are covered by the separator-type theorem, as well as the IQC theorem.

Robust stability can be analyzed by searching for the matrices in the separator-type

theorem called separators satisfying the robust stability condition therein (such separators are said to be eligible in the following). Eligible separators can be searched for by an LMI-based optimization through applying the KYP lemma, as in the IQC approach. To achieve nonconservative robust stability analysis, however, such a search must work on all frequency-dependent (i.e., dynamic) separators without any constraint, but this is not feasible from computational viewpoints. Thus, a tractable class of separators is introduced in practice, only on which the search of eligible separators is carried out. This generally results in conservativeness in robust stability analysis, as in the case with the IQC approach.

For reducing the conservativeness, discrete-time noncausal linear periodically time-varying (LPTV) scaling was introduced in [23]. This approach can be naturally introduced by employing the separator-type robust stability theorem via the lifting-based treatment [4], [5] of discrete-time systems. Since the separator-type robust stability theorems in the conventional lifting-free and new lifting-based scaling approaches give necessary and sufficient conditions for robust stability, both of these two scaling approaches can achieve exact robust stability analysis if an eligible (dynamic) separator could always be found whenever such a separator does exist. As mentioned above, however, such a search is computationally difficult, and to alleviate the difficulty in the search, one generally has to introduce a class of tractable separators from which an eligible separator is to be searched for, whichever of the two approaches one may take. Regarding the conservativeness of the analysis stemming from such a practical issue, the advantage of noncausal LPTV scaling over LTI scaling has been discussed in [23] through the frequency-domain analysis of the freedom provided by noncausal treatment of signals. For example, if we confine ourselves to static separators in both causal LTI and noncausal LPTV scaling approaches, it has been proved theoretically and confirmed numerically that static noncausal LPTV scaling is less (at least, no more) conservative than static causal LTI scaling.

In this thesis, we propose a robust performance controller synthesis method based on noncausal LPTV scaling, which has such promising properties, and demonstrate its effectiveness by control experiments with a cart-inverted pendulum. In addition, we further clarify the properties of noncausal LPTV scaling through introducing new theoretical tools, and guarantee that exploiting the lifting technique in robust stability analysis indeed contributes to reducing conservativeness of the analysis.

1.3 Contents of this thesis

This thesis is organized as follows. In Chapter 2, we first give a brief sketch of the famous robust stability analysis method called μ-analysis for facilitating the understanding

of a basis of the robust stability analysis problem with structured uncertainties. This chapter then introduces discrete-time noncausal LPTV scaling that plays the most important role throughout the thesis, as an alternative approach for robust stability analysis. This scaling approach can be naturally introduced through the technique called discrete-time lifting, and induces dynamic scaling in the lifting-free (i.e., original) framework even if it is confined to static in the lifting-based framework. By this property, static noncausal LPTV scaling is theoretically guaranteed to be less (at least no more) conservative in robust stability analysis than the conventional static causal LTI scaling without lifting-based treatment. This chapter reviews two theorems indicating this advantage, and numerically shows the validity.

In Chapter 3, we extend the lifting-based static noncausal LPTV scaling, which has such a promising property, to robust performance controller synthesis, and demonstrate its effectiveness by control experiments with a cart inverted pendulum. We first review and discuss advantages of static noncausal LPTV scaling in detail, and develop a synthesis procedure of robust performance controllers taking account of not only robust stability but also robust H_∞ performance. The reason why we deal with also robust H_∞ performance is that the responses of the controlled systems often become oscillatory at an unacceptable level, associated with periodicity of the controllers designed naturally under the lifting-based treatment. We numerically confirm by a simple mechanical system example that this extension indeed contributes to alleviating the oscillations in the responses without deteriorating the robustness for the uncertainties so much. Then, we further demonstrate effectiveness of the developed synthesis framework by control experiments with a cart inverted pendulum whose pendulum length can be set from three choices.

In Chapter 4, we aim at clarifying further properties of noncausal LPTV scaling, whose effectiveness has been already demonstrated from the practical viewpoint. As an open issue for the properties, for example, it is not clear yet what specific class of dynamic scaling is equivalent to static noncausal LPTV scaling (with respect to conservativeness of robust stability analysis), although a class of dynamic scaling is indeed known to be induced if we interpret the lifting-based static scaling in the lifting-free framework. In this chapter, we provide a partial answer to this issue by discussing the properties of noncausal LPTV scaling through introducing a concept called shift invariance with respect to timing of lifting. Regarding the concept, we see that noncausal LPTV scaling is not shift invariant, in general, while causal scaling is. In addition, we show that the lifting-based scaling obtained through applying what we call shift-invariant reconstruction to static noncausal LPTV scaling is completely equivalent to the (lifting-free) dynamic scaling induced by the same static scaling with respect to the conservativeness. These theoretical results will be a basis for exploiting full potential of noncausal LPTV scaling.

In Chapter 5, we discuss properties of noncausal LPTV scaling from another viewpoint. Specifically, we apply a framework of representing systems by infinite matrices, and clarify the relationship between lifting-based noncausal LPTV scaling and lifting-free causal LTI scaling through the infinite matrix framework. Since the two scaling approaches are defined in the different (lifting-free and -based) frameworks, their frequency-domain properties are not easy to compare in a straightforward fashion. However, the infinite matrix framework can unify the lifting-free and -based treatment of systems, and both the lifting-free and -based scaling approaches can be equivalently reduced to those in the infinite matrix framework. This enables us to compare the two scaling approaches in the infinite matrix framework very easily. For such discussions, we derive a robust stability condition in the infinite matrix framework. Then, we introduce causal LTI and noncausal LPTV finite impulse response (FIR) scaling approaches as examples of tractable and practical scaling classes, and study the relationship between the two scaling approaches with respect to the conservativeness through the infinite matrix framework. As a consequence of this comparison, we clarify the effect of employing the lifting technique in robust stability analysis.

In Chapter 6, we develop a method of exploiting noncausal LPTV FIR scaling in robust stability analysis. This scaling has a sort of frequency dependence (i.e., dynamics) in addition to time dependence related with the lifting-based treatment. Hence, exploiting it in robustness analysis and controller synthesis is generally difficult, compared with the case of static noncausal LPTV scaling mainly discussed in Chapters 2 and 3. As a future step toward controller synthesis, this chapter confines ourselves to robust stability analysis problems. The difficulty of exploiting noncausal LPTV FIR scaling is mainly attributed to the frequency dependence of the scaling. Hence we first resolve this difficulty for the lifting-free causal LTI FIR scaling, which is a special case of noncausal LPTV FIR scaling, and then extend the result toward the lifting-based scaling. The effectiveness of employing the lifting technique in robust stability analysis has already been confirmed theoretically in Chapter 5, and we demonstrate its validity by a numerical example.

In Chapter 7, we state the issues to be solved in each chapter again, and summarize the obtained results. We then give concluding remarks, and refer to future works for further developments in robust control theory.

Chapter 2

Review of μ-Analysis and Robust Stability Analysis Based on Noncausal LPTV Scaling

2.1 Introduction

Robust stability analysis for closed-loop systems with structured uncertainties becomes conservative, in general. As an approach for reducing this conservativeness, μ-analysis [11], [32],[51] is known to be effective. This approach exploits frequency-dependent (i.e., dynamic) scaling for robust stability analysis, through calculating the structured singular values. In [23], on the other hand, another approach for robust stability called noncausal linear periodically time-varying (LPTV) scaling was proposed. This approach can be naturally introduced through the lifting-based treatment of closed-loop systems, and the associated conservativeness can be reduced by increasing the period of lifting. This thesis studies the scaling approach from the viewpoints of the extension toward controller synthesis and the clarification of properties, to exploit potentials of the scaling approach as much as possible. As a preliminary step toward such studies, this chapter reviews a basis of noncausal LPTV scaling in robust stability analysis.

This chapter is organized as follows. In Section 2.2, we introduce the structured uncertainties, which are often dealt with to achieve more accurate analysis and synthesis for robust stability. We then briefly review a representative analysis approach for such uncertainties called μ-analysis. In Section 2.3, we state the robust stability analysis problem studied in this chapter, and review the discrete-time lifting technique and the separator-type robust stability theorem, both of which play essential roles in introducing noncausal LPTV scaling. In Section 2.4, we show the definitions of causal and noncausal LPTV scaling approaches, and state the reason why we call the introduced scaling *noncausal* LPTV scaling. In addition,

we apply the idea of (D, G)-scaling, and numerically confirm the effectiveness of noncausal LPTV scaling. In Section 2.5, we show theorems indicating that noncausal LPTV scaling is indeed effective for robust stability analysis of linear time-invariant (LTI) closed-loop systems, to which we essentially do not need to apply the lifting technique. We also confirm the validity of the theoretical result by numerical examples.

2.2 Structured uncertainty and μ-analysis

Since modeling of the plants inevitably gives rise to modeling errors regarded as uncertainties, we are often required in practice to deal with the system shown in Figure 2.1, where P denotes the generalized plant and Δ denotes the uncertainty. For this system (including the uncertainty), the controller Ψ is designed and connected from y to u (Figure 2.2). Then, through regarding the interconnection of P and Ψ as the nominal system G, we can obtain the closed-loop system Σ shown in Figure 2.3. Developing a method of deciding whether this Σ is robustly stable in the presence of the uncertainty Δ is an important issue for actual control problems. As an approach to robust stability analysis of the closed-loop system, the μ-analysis method [11],[32],[51] is known to be effective with respect to the conservativeness. Before proceeding to the discussions about noncausal LPTV scaling, which is the central concept in this thesis, we briefly review the conventional μ-analysis method in this section, associated with the so-called structured uncertainties.

Only in this section, we suppose that both G and Δ are *continuous-time* systems (hence the signals w and z in Figure 2.3 are continuous-time in this section). In addition, they are also supposed to be stable, finite-dimensional, LTI and have p inputs and outputs. We denote the (continuous-time) transfer matrices of G and Δ by $G(s)$ and $\Delta(s)$, respectively, with the variable s of Laplace transforms.

In most actual cases, we may obtain a sort of information about the uncertainties such as sources where they come from and properties that they have. With such information, we

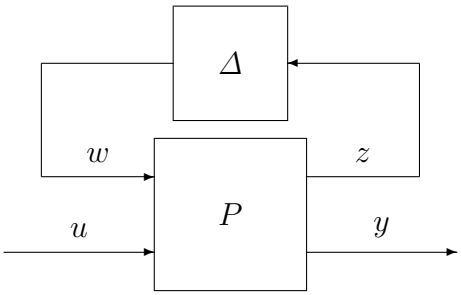

Figure 2.1: Generalized plant with uncertainty.

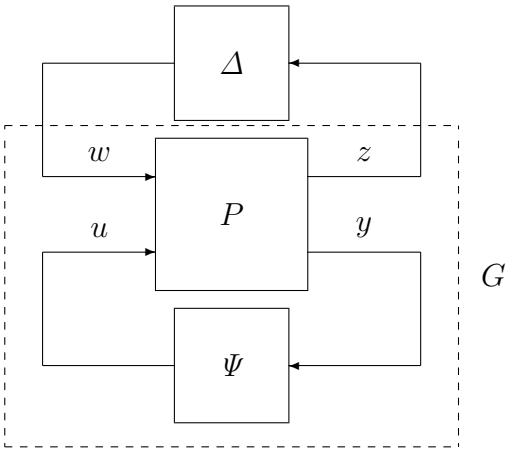

Figure 2.2: Feedback system.

only have to deal with the corresponding restricted classes of uncertainties, rather than the black box (i.e., completely full block) uncertainties. This idea naturally leads us to introduce the class of structured uncertainties given by

$$\boldsymbol{\Delta} = \{\mathrm{diag}[\delta_1(s)I_{r_1}, \cdots, \delta_Y(s)I_{r_Y}, \Delta_1(s), \cdots, \Delta_Z(s)]\}, \tag{2.1}$$

with $\delta_i(s) \in \mathbf{RH}_\infty$ $(i = 1, \ldots, Y)$ and $\Delta_j(s) \in \mathbf{RH}_\infty^{m_j \times m_j} (j = 1, \ldots, Z)$, where $\mathbf{RH}_\infty$ and $\mathbf{RH}_\infty^{m_j \times m_j}$ denote the set of proper and real rational stable transfer functions and matrices of the size $m_j \times m_j$, respectively. For example, taking $Y = 2$ and $Z = 0$ corresponds to the assumption that the plant has two independent (dynamic) scalar uncertainties.

Suppose that we have some information about the uncertainties, and thus only have to deal with the structured uncertainties described as (2.1). Then, if we analyze robust stability of the closed-loop system without taking account of the structure, the corresponding result inevitably becomes conservative, since the result does guarantee robust stability also for such uncertainties that are not required to be considered. Hence, reducing the conservativeness through taking account of the structure is very important in actual control problems. From the 1980s, the μ-analysis approach was extensively studied to tackle this issue. The μ-

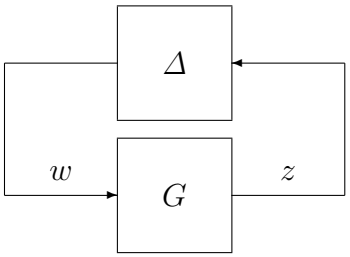

Figure 2.3: Closed-loop system Σ.

analysis approach analyzes robust stability through calculating what we call the structured singular values defined as follows.

Definition 2.1 For a given $G(s) \in \mathbf{RH}_\infty^{p\times p}$ and a given $s \in \mathbf{C}$, the structured singular value $\mu_{\boldsymbol{\Delta}}(G(s))$ is defined as

$$\mu_{\boldsymbol{\Delta}}(G(s)) := \frac{1}{\min\{\overline{\sigma}(\Delta(s)) : \Delta \in \boldsymbol{\Delta}, \det(I - G(s)\Delta(s)) = 0\}}, \tag{2.2}$$

unless no $\Delta \in \boldsymbol{\Delta}$ makes $I - G(s)\Delta(s)$ singular, in which case $\mu_{\boldsymbol{\Delta}}(G(s)) := 0$.

It is obvious from this definition that the structured singular value depends on the structure of the uncertainties. For this structured singular value, we have the following result [11],[32], [51].

Theorem 2.1 Let $\gamma > 0$. The closed-loop system consisting of $G(s)$ and $\Delta(s)$ is robustly well-posed and internally stable for all $\Delta \in \boldsymbol{\Delta}$ with $\|\Delta\|_\infty < 1/\gamma$ if and only if

$$\sup_{\omega\in\mathbf{R}} \mu_{\boldsymbol{\Delta}}(G(j\omega)) \le \gamma. \tag{2.3}$$

By this theorem, we can evaluate robust stability of the closed-loop system through calculating the structured singular values.

However, there is an issue that calculating the exact value of the structured singular value is difficult (it has been proved to be NP-hard in [33]). Hence we usually have to employ upper bounds of the structured singular values instead, to analyze robust stability. The maximum singular value $\overline{\sigma}(G(s))$ is one of the simplest upper bounds of $\mu_{\boldsymbol{\Delta}}(G(s))$. This upper bound, however, does not take account of the uncertainty structure, and thus results in providing no reduction of the conservativeness in the analysis. As one of the approaches to reducing this conservativeness, the D-scaling approach employing the following class of complex matrices has been proposed.

$$\begin{aligned}\boldsymbol{D} := \{&\mathrm{diag}[D_1, \cdots, D_Y, d_1 I_{m_1}, \cdots, d_Z I_{m_Z}] : D_i \in \mathbf{C}^{r_i\times r_i},\\ &D_i = D_i^* > 0, d_j \in \mathbf{R}, d_j > 0\}\end{aligned} \tag{2.4}$$

This class is determined associated with the class (2.1) of structured uncertainties, and leads us to the following relationship for a given $s \in \mathbf{C}$.

$$\mu_{\boldsymbol{\Delta}}(G(s)) = \mu_{\boldsymbol{\Delta}}(D^{1/2}G(s)D^{-1/2}),\ D \in \boldsymbol{D} \tag{2.5}$$

Hence, for a given $s \in \mathbf{C}$, we have

$$\mu_{\boldsymbol{\Delta}}(G(s)) \le \inf_{D\in\boldsymbol{D}} \overline{\sigma}(D^{1/2}G(s)D^{-1/2}). \tag{2.6}$$

By searching for some appropriate $D \in \boldsymbol{D}$, we can reduce the gap between $\mu_{\boldsymbol{\Delta}}(G(s))$ and $\overline{\sigma}(D^{1/2}G(s)D^{-1/2})$ (i.e., conservativeness in the analysis).

We have reviewed a basis of the conventional μ-analysis method. In the above discussions, we have dealt with the structured uncertainties given by (2.1) consisting of dynamic blocks. In actual cases, however, we may be able to further restrict (some of) the blocks in (2.1) to be static. Unfortunately, we cannot exploit this additional information if we employ only D-scaling, but its extended approach called (D, G)-scaling may enable us to deal with the information adequately. Although we omit the details here, we would like to emphasize that this thesis is actually interested in reducing conservativeness of the robust stability analysis for the structured uncertainties involving static blocks, and we will thus employ the notion of (D, G)-scaling in robust stability analysis based on noncausal LPTV scaling, whose basis is reviewed in the rest of this chapter.

2.3 Discrete-time lifting and separator-type robust stability theorem

In the preceding section, we reviewed one of the conventional robust stability analysis approaches called μ-analysis with the assumption that the closed-loop system is continuous-time; although we can also develop the discrete-time counterpart of the continuous-time method, we would like to omit it here. In the rest of this chapter, we revisit a new robust stability analysis approach called discrete-time noncausal LPTV scaling, which plays the most important role in this thesis. Before introducing the scaling approach, we devote this section to stating the robust stability analysis problem dealt with in this chapter, and reviewing the discrete-time lifting technique [4],[5] and the separator-type robust stability theorem [25] via the lifting-based treatment.

2.3.1 Robust stability analysis problem for discrete-time closed-loop systems

Let us consider the discrete-time closed-loop system Σ shown in Figure 2.3 consisting of the *discrete-time* nominal system G and the *discrete-time* uncertainty Δ. The nominal system G is assumed to be internally stable, finite-dimensional, linear N-periodic, and represented by

$$x_{k+1} = A_k x_k + B_k w_k, \quad z_k = C_k x_k + D_k w_k \tag{2.7}$$

where $x_k \in \mathbf{R}^n$, $w_k \in \mathbf{R}^p$, $z_k \in \mathbf{R}^p$, and A_k, B_k, C_k and D_k are N-periodic matrices. The uncertainty Δ is assumed to belong to a given set $\boldsymbol{\Delta}$ satisfying the following assumption.

Assumption 1 Every $\Delta \in \boldsymbol{\Delta}$ is stable, finite-dimensional and linear N-periodic, and $\boldsymbol{\Delta}$ is star-convex with a center at the origin (i.e., $k\Delta \in \boldsymbol{\Delta}$ whenever $\Delta \in \boldsymbol{\Delta}$ and $0 \leq k \leq 1$). In addition, every $\Delta \in \boldsymbol{\Delta}$ satisfies $\|\Delta\|_\infty < 1/\gamma$ for a given $\gamma > 0$.

We also prepare the following alternative assumption, which is a special case of the above assumption.

Assumption 2 Every $\Delta \in \boldsymbol{\Delta}$ is stable, finite-dimensional and LTI, and $\boldsymbol{\Delta}$ is star-convex with a center at the origin. In addition, every $\Delta \in \boldsymbol{\Delta}$ satisfies $\|\Delta\|_\infty < 1/\gamma$ for a given $\gamma > 0$.

It can also be the case that every $\Delta \in \boldsymbol{\Delta}$ is static, i.e., a periodically time-varying or a constant matrix. Furthermore, G is also allowed to be LTI; when Δ is N-periodic, we view an LTI system G as a special case of N-periodic systems. An LTI Δ is treated in a similar fashion (i.e., when G is N-periodic, we view the LTI Δ as a special case of N-periodic systems).

In this chapter, we study the problem of deciding whether the above closed-loop system is robustly stable for a given uncertainty class $\boldsymbol{\Delta}$. In particular, we are interested in reducing conservativeness of robust stability analysis when the uncertainties $\Delta \in \boldsymbol{\Delta}$ are structured and have static blocks.

2.3.2 Discrete-time lifting

This subsection reviews the discrete-time lifting technique [4],[5]. The operation of introducing new signal representations

$$\widehat{w}_\kappa := \left[w_{\kappa N}^T, w_{\kappa N+1}^T, \cdots, w_{\kappa N+N-1}^T\right]^T, \quad \widehat{z}_\kappa := \left[z_{\kappa N}^T, z_{\kappa N+1}^T, \cdots, z_{\kappa N+N-1}^T\right]^T \tag{2.8}$$

from the discrete-time signals w and z is called the lifting of signals, where κ denotes the variable of time steps on the lifted time axis. This converts the treatment of systems with input w and output z into that of systems with lifted input $\widehat{w}$ and lifted output $\widehat{z}$, and such treatment is called the lifting of systems. The resulting lifted representations of systems are called N-lifted systems. By defining $\widehat{x}_\kappa := x_{\kappa N}$, we can describe the N-lifted nominal system $\widehat{G}$ by

$$\widehat{x}_{\kappa+1} = \widehat{A}\widehat{x}_\kappa + \widehat{B}\widehat{w}_\kappa, \quad \widehat{z}_\kappa = \widehat{C}\widehat{x}_\kappa + \widehat{D}\widehat{w}_\kappa, \tag{2.9}$$

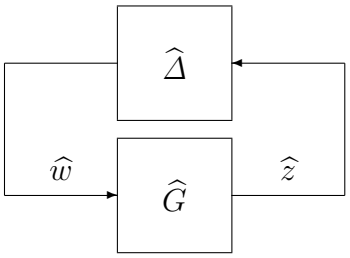

Figure 2.4: Lifted closed-loop system $\widehat{\Sigma}$.

where $\widehat{A}$, $\widehat{B}$, $\widehat{C}$ and $\widehat{D}$ are given as follows.

$$\widehat{A} = \prod_{k=0}^{N-1} A_k := A_{N-1} \cdots A_1 A_0, \tag{2.10}$$

$$\widehat{B} = \begin{bmatrix} \left(\prod_{k=1}^{N-1} A_k\right) B_0 & \left(\prod_{k=2}^{N-1} A_k\right) B_1 & \cdots & B_{N-1} \end{bmatrix}, \tag{2.11}$$

$$\widehat{C} = \begin{bmatrix} C_0 \\ C_1 A_0 \\ \vdots \\ C_{N-1} \prod_{k=0}^{N-2} A_k \end{bmatrix}, \quad \widehat{D} = \begin{bmatrix} D_0 & 0 & \cdots & 0 \\ C_1 B_0 & D_1 & \ddots & \vdots \\ \vdots & \ddots & \ddots & 0 \\ C_{N-1}\left(\prod_{k=1}^{N-2} A_k\right) B_0 & \cdots & C_{N-1}B_{N-2} & D_{N-1} \end{bmatrix} \tag{2.12}$$

Through this lifting-based treatment, we can regard the obtained system $\widehat{G}$ as an LTI system on the lifted time axis. Hence the transfer matrix of $\widehat{G}$ can be defined and is denoted by $\widehat{G}(z)$, which is called the N-lifted transfer matrix of G, where z denotes the variable of z-transforms under the lifting-based treatment. We can also obtain the N-lifted representation $\widehat{\Delta}$ and the N-lifted transfer matrix $\widehat{\Delta}(z)$ from Δ. Through these ideas, we can obtain the lifted representation $\widehat{\Sigma}$ (Figure 2.4) from the closed-loop system Σ.

2.3.3 Separator-type robust stability theorem via lifting-based treatment

This subsection reviews the separator-type robust stability theorem. It follows from the property of lifting that the closed-loop system Σ is robustly stable with respect to $\boldsymbol{\Delta}$ if and only if its lifted counterpart $\widehat{\Sigma}$ is. Hence, we have the following robust stability theorem via the lifting-based treatment [25],[23] (see also [21] for the classical well-posedness issue).

Theorem 2.2 Suppose that G is internally stable and N-periodic, and $\boldsymbol{\Delta}$ satisfies Assumption 1. Then, Σ is robustly (well-posed and) stable with respect to $\boldsymbol{\Delta}$ if and only if

there exists $\widehat{\Theta}(z) = \widehat{\Theta}(z)^*$ $(z \in \partial\mathbf{D})$ such that

$$\begin{bmatrix} I \\ \widehat{G}(z) \end{bmatrix}^* \widehat{\Theta}(z) \begin{bmatrix} I \\ \widehat{G}(z) \end{bmatrix} \leq 0 \quad (\forall z \in \partial\mathbf{D}), \tag{2.13}$$

$$\begin{bmatrix} \widehat{\Delta}(z) \\ I \end{bmatrix}^* \widehat{\Theta}(z) \begin{bmatrix} \widehat{\Delta}(z) \\ I \end{bmatrix} > 0 \quad \left(\begin{array}{l} \forall \Delta \in \boldsymbol{\Delta}, \\ \forall z \in \partial\mathbf{D} \end{array} \right), \tag{2.14}$$

where $\partial\mathbf{D} := \{z \in \mathbf{C} : |z| = 1\}$ denotes the unit circle.

We can analyze robust stability of the closed-loop system Σ by searching for the matrix $\widehat{\Theta}(z)$, called a separator, satisfying (2.13) and (2.14).

Note that this theorem reduces to the following usual (lifting-free) separator-type robust stability theorem [25],[21] by letting $N = 1$ when Σ is LTI, where ζ denotes the variable for z-transforms under the treatment without lifting, and $G(\zeta)$ and $\Delta(\zeta)$ denote the transfer matrices of LTI systems G and Δ, respectively.

Theorem 2.3 Suppose that G is internally stable and LTI, and $\boldsymbol{\Delta}$ satisfies Assumption 2. Then, Σ is robustly (well-posed and) stable with respect to $\boldsymbol{\Delta}$ if and only if there exists $\Theta(\zeta) = \Theta(\zeta)^*$ $(\zeta \in \partial\mathbf{D})$ such that

$$\begin{bmatrix} I \\ G(\zeta) \end{bmatrix}^* \Theta(\zeta) \begin{bmatrix} I \\ G(\zeta) \end{bmatrix} \leq 0 \quad (\forall \zeta \in \partial\mathbf{D}), \tag{2.15}$$

$$\begin{bmatrix} \Delta(\zeta) \\ I \end{bmatrix}^* \Theta(\zeta) \begin{bmatrix} \Delta(\zeta) \\ I \end{bmatrix} > 0 \quad \left(\begin{array}{l} \forall \Delta \in \boldsymbol{\Delta}, \\ \forall \zeta \in \partial\mathbf{D} \end{array} \right). \tag{2.16}$$

By Theorem 2.3, robust stability of LTI closed-loop systems can be analyzed without applying the lifting technique, and this is nothing but the conventional causal LTI scaling. We call such a framework for robust stability analysis the *lifting-free framework*. On the other hand, this thesis is rather interested in applying lifting-based Theorem 2.2 to the closed-loop system Σ (even when Σ is surely LTI), and we call such a framework the *lifting-based framework*.

In the following arguments, if a separator $\widehat{\Theta}(z)$ satisfies (2.13) and (2.14), then we say that it is eligible with respect to (2.13) and (2.14) (or simply in the lifting-based framework). Similarly, if $\Theta(\zeta)$ satisfies (2.15) and (2.16), then we say that it is eligible with respect to (2.15) and (2.16) (or in the lifting-free framework).

2.4 Causal and noncausal LPTV scaling

The preceding section reviewed the discrete-time lifting and the separator-type robust stability theorem via the lifting-based treatment. On the basis of those preparations, this

section introduces explicit definitions of causal and noncausal LPTV separators, and compares the corresponding two scaling approaches with respect to conservativeness of robust stability analysis by a numerical example.

2.4.1 Definitions of causal and noncausal LPTV separators

By Theorem 2.2, the robust stability problem of the closed-loop system $\widehat{\Sigma}$ (i.e., Σ) reduces to searching for separators $\widehat{\Theta}(z)$ satisfying (2.13) and (2.14) for the given $\boldsymbol{\Delta}$. This naturally leads to the idea of noncausal LPTV scaling reviewed in the following. For facilitating extensive discussions, however, it is important to introduce noncausal LPTV scaling in contrast with causal LPTV scaling. This is carried out by classifying the separators $\widehat{\Theta}(z)$ in Theorem 2.2 into two types [23].

First, causal LPTV separators are defined as follows.

Definition 2.2 We call a separator given by

$$\widehat{\Theta}(z) = \begin{bmatrix} \widehat{V}_1(z) & \widehat{V}_2(z) \end{bmatrix}^* \widehat{\Lambda} \begin{bmatrix} \widehat{V}_1(z) & \widehat{V}_2(z) \end{bmatrix} \tag{2.17}$$

a causal LPTV separator, where $\widehat{V}_1(z)$ and $\widehat{V}_2(z)$ are the N-lifted transfer matrices of causal N-periodic systems V_1 and V_2 with p inputs, respectively, and $\widehat{\Lambda} = \widehat{\Lambda}^*$ is a constant matrix of the form $\widehat{\Lambda} = \mathrm{diag}[\Lambda_1, \cdots, \Lambda_N]$ with the size of Λ_i being the same for all $i = 1, \ldots, N$. In particular, if we take static V_1 and V_2, then we call the corresponding separator a static causal LPTV separator.

The approach to robust stability analysis based on causal LPTV separators is called causal LPTV scaling.

On the other hand, more general noncausal LPTV separators have been defined as follows.

Definition 2.3 We call a separator given by

$$\widehat{\Theta}(z) = \widehat{V}(z)^* \Gamma \widehat{V}(z) \tag{2.18}$$

a noncausal LPTV separator, where $\widehat{V}(z)$ is the transfer matrix of a causal LTI system $\widehat{V}$ with $2Np$ inputs defined directly on the lifted time axis κ in (2.9)[1] and $\Gamma = \Gamma^*$ is a constant matrix. In particular, if we take a static $\widehat{V}$, then we call the corresponding separator a static noncausal LPTV separator.

[1]This means that $\widehat{V}$ is not required to be an N-lifted representation of a system in the original time axis k in (2.7) before the application of lifting.

The approach to robust stability analysis based on noncausal LPTV separators is called noncausal LPTV scaling. Even though Definition 2.3 is more general than Definition 2.2, they degenerate into an identical definition when $N = 1$. We refer to the degenerated separators as causal LTI separators (in the lifting-free framework).

2.4.2 Noncausal LPTV D-scaling

In the preceding subsection, we have reviewed the definitions of causal and noncausal LPTV separators, and the associated scaling approaches. In this subsection, we give some supplements about the reason why a separator given by Definition 2.3 is called a noncausal LPTV separator, through restricting separators to D-scaling type as an example.

Let us consider a typical separator of the form

$$\widehat{\Theta}(z) = \begin{bmatrix} -\gamma^2 \widehat{W}(z)^* \widehat{W}(z) & 0 \\ 0 & \widehat{W}(z)^* \widehat{W}(z) \end{bmatrix}, \tag{2.19}$$

corresponding to the D-scaling, where $\widehat{W}(z)$ is invertible for every $z \in \partial\mathbf{D}$ and γ is a positive scalar. Then, (2.13) and (2.14) are equivalent to the following conditions, respectively.

$$||\widehat{W}(z)\widehat{G}(z)\widehat{W}(z)^{-1}|| \leq \gamma \quad (\forall z \in \partial\mathbf{D}), \tag{2.20}$$

$$||\widehat{W}(z)\widehat{\Delta}(z)\widehat{W}(z)^{-1}|| < 1/\gamma \quad (\forall \Delta \in \boldsymbol{\Delta},\ \forall z \in \partial\mathbf{D}) \tag{2.21}$$

That is, taking the separator (2.19) corresponds to applying the small-gain condition [46], [47] scaled with $\widehat{W}(z)$. Suppose for simplicity that the scaling factor is independent of z and is thus a constant matrix $\widehat{W}$. If we interpret the corresponding scaling (i.e., the conditions (2.20) and (2.21)) in the time domain with respect to the lifting-free time axis, it is not hard to see that it generally leads to periodically time-varying scaling of the systems G and $\boldsymbol{\Delta}$ with some noncausal operation associated with the period of lifting N. In view of this observation, we say that the separator (2.19) generally induces *noncausal scaling* on LPTV systems G and $\boldsymbol{\Delta}$.

2.4.3 Noncausal LPTV (D, G)-scaling

We have viewed, with an example of D-scaling type noncausal LPTV separators (2.19), the reason why the lifting-based scaling associated with Definition 2.3 is called noncausal LPTV scaling. Since noncausal LPTV scaling is defined based on the separator-type robust stability theorem rather than the small-gain theorem [23], however, we can actually exploit separators more general than the D-scaling type one for robust stability. As one of such

classes, this subsection introduces the (D, G)-scaling type [13] noncausal LPTV separators given by

$$\widehat{\Theta}(z) = \begin{bmatrix} -\gamma^2 \widehat{W}(z)^* \widehat{W}(z) & \widehat{X}_G(z) \\ \widehat{X}_G(z)^* & \widehat{W}(z)^* \widehat{W}(z) \end{bmatrix}, \ \widehat{W}(z)^* \widehat{W}(z) > 0, \ \gamma > 0. \tag{2.22}$$

Then, (2.14) simplifies to $\|\widehat{\Delta}\|_\infty < 1/\gamma$, or equivalently $\|\Delta\|_\infty < 1/\gamma$, if $\widehat{W}(z)$ and $\widehat{X}_G(z)$ satisfy

$$\widehat{W}(z)\widehat{\Delta}(z) = \widehat{\Delta}(z)\widehat{W}(z) \ \ (\forall \Delta \in \boldsymbol{\Delta}), \tag{2.23}$$

$$\widehat{X}_G(z)^* \widehat{\Delta}(z) + \widehat{\Delta}(z)^* \widehat{X}_G(z) = 0 \ \ (\forall \Delta \in \boldsymbol{\Delta}), \tag{2.24}$$

respectively. Thus, we only have to search for $\widehat{\Theta}(z)$ satisfying (2.13), which is independent of the uncertainties, once we confine ourselves to the above (D, G)-scaling type noncausal LPTV separators. This approach to robust stability is called noncausal LPTV (D, G)-scaling.

Noncausal LPTV separators (2.22) satisfying (2.13) can be searched for through the linear matrix inequality (LMI) optimization. For simplicity, this section confines itself to static noncausal LPTV separators $\widehat{\Theta}$ (LMI optimization for dynamic noncausal LPTV scaling will be discussed in Chapter 6 in detail). Then, the KYP lemma [34] immediately leads us to the following result.

Lemma 2.1 Suppose that G (and thus $\widehat{G}$) is internally stable. Then, (2.13) holds if and only if there exists a real symmetric matrix $P \in \mathbf{R}^{n \times n}$ satisfying

$$\begin{bmatrix} \widehat{C} & \widehat{D} \\ 0 & I \end{bmatrix}^T \widehat{\Theta} \begin{bmatrix} \widehat{C} & \widehat{D} \\ 0 & I \end{bmatrix} \leq \begin{bmatrix} \widehat{A} & \widehat{B} \\ I & 0 \end{bmatrix}^T \begin{bmatrix} -P & 0 \\ 0 & P \end{bmatrix} \begin{bmatrix} \widehat{A} & \widehat{B} \\ I & 0 \end{bmatrix}. \tag{2.25}$$

Hence, given a scalar $\gamma > 0$, we can analyze robust stability of the closed-loop system by searching for a matrix P and a static (D, G)-scaling type separator (2.22) satisfying the LMI (2.25) under the restrictions (2.23) and (2.24) on the separator.

If $\widehat{\Delta}(z)$ is the structured uncertainty consisting only of dynamic blocks, it is generally difficult to find nonzero $\widehat{X}_G$ satisfying (2.24). However, for example, if $\widehat{\Delta}(z)$ is given by δI with a scalar $\delta \in \mathbf{R}$, this condition reduces to $\widehat{X}_G^T + \widehat{X}_G = 0$, which generally has nonzero solutions. Hence introducing (D, G)-scaling type separators can make sense when we deal with the structured uncertainties involving static blocks. In particular, this extension actually works very effectively in the case of noncausal LPTV scaling. In the following subsection, we confirm this fact, as well as the effectiveness of noncausal LPTV scaling itself, by a numerical example.

2.4.4 Numerical example

Consider the 3-periodic system G described by

$$A_0 = \begin{bmatrix} 0 & 1 & 0 & 0 \\ 0 & 0 & 1 & 0 \\ 0 & 0 & 0 & 1 \\ 0.1 & 0.1 & -0.8 & -1 \end{bmatrix}, \; A_1 = \begin{bmatrix} 0 & 1 & 0 & 0 \\ 0 & 0 & 1 & 0 \\ 0 & 0 & 0 & 1 \\ 0.2 & -0.4 & 0.01 & 0.2 \end{bmatrix},$$
$$A_2 = \begin{bmatrix} 0 & 1 & 0 & 0 \\ 0 & 0 & 1 & 0 \\ 0 & 0 & 0 & 1 \\ -0.4 & -0.3 & 0.3 & 0.5 \end{bmatrix}, \; B_0 = B_1 = B_2 = \begin{bmatrix} 0 & 0 & 0 & 1 \end{bmatrix}^T,$$
$$C_0 = \begin{bmatrix} 0.3 & 0.2 & 0.5 & 0.1 \end{bmatrix}, \; C_1 = \begin{bmatrix} 0.3 & 0.3 & 0.3 & 0.4 \end{bmatrix},$$
$$C_2 = \begin{bmatrix} 0.2 & 0.6 & 0.4 & 0.2 \end{bmatrix}, \; D_0 = D_1 = D_2 = 0, \tag{2.26}$$

which we can confirm is internally stable. In addition, we assume that the corresponding scalar uncertainties $\Delta = \delta$ are static and LTI. The problem we study here is to find the minimal $\gamma > 0$ such that the closed-loop system Σ is robustly stable for the uncertainty set $\boldsymbol{\Delta} = \{\delta : |\delta| < 1/\gamma\}$.

The analysis results obtained by static causal LPTV D-scaling and static noncausal LPTV D-scaling are shown in Table 2.1. Each value in the table denotes the reciprocal of the supremal value of $|\Delta|$ for those Δ such that the stability of the closed-loop system with G and Δ is ensured by each respective analysis method. The result of noncausal LPTV scaling can indeed be confirmed to be better than that by causal LPTV scaling.

Since we define noncausal (and causal) LPTV scaling based on the separator-type robust stability theorem (rather than the small-gain theorem), we can deal with (D, G)-scaling type separators, whose corresponding analysis results are also shown in Table 2.1 for both the causal and noncausal LPTV cases. According to the table, static noncausal (D, G)-scaling is surely more effective than static noncausal D-scaling, even though static causal (D, G)-scaling leads only to the same result as static causal D-scaling. To put it another way, the extension from D-scaling to (D, G)-scaling does not work within the framework of *causal* LPTV scaling but it does work effectively in the case of noncausal LPTV scaling. This is one of the important advantages of noncausal LPTV scaling (the details will be discussed in the following chapter).

Table 2.1: Results of robust stability analysis with different LPTV scaling approaches

	Causal-D	Noncausal-D	Causal-(D, G)	Noncausal-(D, G)
$1/\gamma$	0.4567	0.4962	0.4567	0.5292

2.5 Noncausal LPTV scaling applied to LTI systems

The preceding section introduced noncausal LPTV scaling, and numerically demonstrated its effectiveness in robust stability analysis of LPTV closed-loop systems. In this section, we review the properties of noncausal LPTV scaling in particular in the case of analyzing robust stability of LTI closed-loop systems. In that case, we have two alternatives for robust stability analysis as stated in Subsection 2.3.3: the lifting-based framework (i.e., noncausal LPTV scaling) and the lifting-free framework (i.e., causal LTI scaling). Whichever framework one may take, however, it is generally difficult to search for eligible separators, and thus one often introduces some tractable class of separators (such as static separators) within which the search of eligible separators is to be carried out. It should be remarked that, under such a restrictive search, the inequalities (2.13) and (2.14) as well as (2.15) and (2.16) in these theorems become a conservative sufficient condition for robust stability. With this in mind, the properties reviewed in this section are expected to be useful in clarifying the ability of noncausal LPTV scaling in reducing the aforementioned conservativeness in the analysis.

2.5.1 Theoretical results on static noncausal LPTV scaling

For simplicity, in this section, we introduce static scaling in both the lifting-free and lifting-based frameworks. Then, we review what class of scaling is induced in the lifting-based (resp. lifting-free) framework by static causal LTI (resp. noncausal LPTV) scaling defined in the lifting-free (resp. lifting-based) framework. Further results for dynamic scaling will be revisited and discussed in Chapter 4 later.

We first consider introducing static causal LTI scaling in the lifting-free framework. Then, the following theorem holds [23].

Theorem 2.4 Suppose that G is LTI, and $\boldsymbol{\Delta}$ satisfies Assumption 2. If a static causal LTI separator

$$\Theta = \begin{bmatrix} \Theta_{11} & \Theta_{12} \\ \Theta_{21} & \Theta_{22} \end{bmatrix} =: (\Theta_{ij})_{i,j=1,2} \tag{2.27}$$

is eligible in the lifting-free framework, the separator

$$\widehat{\Theta} = (I_N \otimes \Theta_{ij})_{i,j=1,2} \tag{2.28}$$

is eligible in the lifting-based framework, where $\otimes$ denotes the Kronecker product.

An important implication of the above theorem is that if we apply static causal/noncausal LPTV scaling to LTI systems, we can perform at least as good robust stability analysis as

static causal LTI scaling; we can see that the separator (2.28) satisfies the requirement about static causal LPTV scaling in Definition 2.2 (and thus that about static noncausal LPTV scaling in Definition 2.3).

Remark 2.1 The above theoretical result can be further generalized to the case of introducing dynamic causal LTI scaling in the lifting-free framework. The corresponding result will be discussed in Chapter 4 as Theorem 4.1 with an explicit proof. The extended result immediately leads us to the above theorem, and hence we omit the proof of the above theorem here.

We next consider introducing static noncausal LPTV scaling in the lifting-based framework. Then, the following theorem, which is closely related to the advantage of static noncausal LPTV scaling over static causal LTI scaling, holds [23] (this theorem is also an immediate consequence from Theorem 4.3 reviewed in Chapter 4).

Theorem 2.5 Suppose that G is LTI, and $\boldsymbol{\Delta}$ satisfies Assumption 2. If a static noncausal LPTV separator $\widehat{\Theta}$ is eligible in the lifting-based framework, the causal LTI separator

$$\Theta(\zeta) = \mathcal{T}(\zeta)^* \widehat{\Theta} \mathcal{T}(\zeta) \tag{2.29}$$

is eligible in the lifting-free framework, where

$$\mathcal{T}(\zeta) := \mathrm{diag}[T_p(\zeta), T_p(\zeta)], \quad T_p(\zeta) := \begin{bmatrix} \zeta^{-(N-1)} I_p \\ \vdots \\ \zeta^{-1} I_p \\ I_p \end{bmatrix}. \tag{2.30}$$

This theorem implies that if we find an eligible *static* separator $\widehat{\Theta}$ in the lifting-based framework, it immediately means that we have also found an eligible *dynamic* separator $\Theta(\zeta)$ in the lifting-free framework. This indicates that even static noncausal LPTV scaling can induce dynamic scaling if we interpret it in the lifting-free framework. Furthermore, it follows from Theorem 2.4 that the induced scaling in the lifting-free framework is ensured to be, at least, as effective as the static causal LTI scaling in that framework. This might suggest that static noncausal LPTV scaling could possibly replace dynamic causal LTI scaling, which sounds attractive because static separators are much more tractable than general dynamic separators.

Remark 2.2 We have also introduced static *causal* LPTV scaling as one of the lifting-based scaling approaches. However, such class of scaling cannot induce dynamic scaling in

the lifting-free framework actually. This can be easily confirmed by substituting a static causal LPTV separator into (2.29); the resulting $\Theta(\zeta)$ becomes a static matrix. From this fact, together with Theorem 2.4, we can see that static causal LPTV scaling is as conservative as static causal LTI scaling in robust stability analysis of LTI closed-loop systems.

2.5.2 Numerical example

We have reviewed the promising properties of static noncausal LPTV scaling in robust stability analysis of LTI closed-loop systems. This subsection numerically demonstrates their effectiveness in reducing conservativeness of the analysis.

Consider the LTI system G described by

$$\left[\begin{array}{c|c} A & B \\ \hline C & D \end{array}\right] = \left[\begin{array}{ccc|cc} 0 & 1 & 0 & 0 & 0 \\ 0 & 0 & 1 & 0 & 1 \\ -0.2 & 0.5 & 0.1 & 1 & 0 \\ \hline 0 & -1 & 0 & 0 & 0 \\ 0 & 0 & 1 & 0 & 0 \end{array}\right], \tag{2.31}$$

which we can confirm is internally stable. In addition, we assume that the corresponding uncertainties Δ are static and LTI and given by $\Delta = \delta I_2$ with a real scalar δ. The problem here is to compute (an upper bound of) the minimal $\gamma > 0$ such that the closed-loop system Σ is robustly stable for the uncertainty set $\boldsymbol{\Delta} = \{\Delta : ||\Delta|| < 1/\gamma\}$.

The analysis results obtained by static noncausal LPTV (D, G)-scaling under different lifting period N are shown in Table 2.2. Since noncausal LPTV scaling with $N = 1$ coincides with the lifting-free causal LTI scaling, the result $1/\gamma = 0.2761$ can be seen as that by static causal LTI scaling. Hence, this table shows that static noncausal LPTV scaling indeed outperforms static causal LTI scaling with respect to conservativeness in robust stability analysis of LTI systems. Note that this improvement is achieved by introducing noncausality into the scaling because *causal* LPTV scaling cannot outperform causal LTI scaling in this case, as stated in the preceding subsection.

Table 2.2: Static noncausal LPTV (D, G)-scaling for LTI system

N	1	2	4	8
$1/\gamma$	0.2761	0.9231	0.9231	0.9231

2.5.3 νN-lifted treatment of N-periodic systems

We have reviewed the promising properties of static noncausal LPTV scaling (i.e., Theorems 2.4 and 2.5) for LTI closed-loop systems, and numerically demonstrated their effectiveness with respect to conservativeness in robust stability analysis. Before closing this

section, we remark that the reviewed properties can be exploited even in the analysis of LPTV closed-loop systems.

Recall that the system obtained by applying the lifting technique to an N-periodic system with the same period N becomes LTI on the lifted time axis. Hence if we further apply lifting to the N-lifted LTI system with period $\nu \geq 2$ and analyze the robust stability by (static) noncausal LPTV scaling with the period νN, the properties about Theorems 2.4 and 2.5 can be exploited at least for the integer ν.

To demonstrate this fact, we consider the same example (a 3-periodic nominal system and an LTI uncertainty) studied in Subsection 2.4.4. We analyzed the minimal $\gamma > 0$ such that the closed-loop system is robustly stable by static noncausal LPTV (D, G)-scaling with the period νN $(N = 3)$ with increasing ν from 1 to 4. Then we obtained the results shown in Table 2.3. In this table, we can see that conservativeness of robust stability analysis is reduced when we increase ν. This result indeed demonstrates that Theorem 2.4 and 2.5 are useful also for robust stability analysis of LPTV systems.

Table 2.3: Static noncausal LPTV (D, G)-scaling with period νN for N-periodic system

ν	1	2	3	4
$1/\gamma$	0.5292	0.6516	0.7123	0.7123

2.6 Concluding remarks

In this chapter, we briefly reviewed a basis of μ-analysis with the treatment of the structured uncertainties. Then, as an alternative approach to less conservative robust stability analysis, we also reviewed noncausal LPTV scaling, which plays the most important role in the thesis. In particular, we showed two theorems closely related with the fact that even static noncausal LPTV scaling can induce dynamic scaling in the lifting-free framework, and outperform static causal LTI scaling with respect to conservativeness in robust stability analysis, when we deal with LTI closed-loop systems. Effectiveness of this property was also demonstrated numerically. In addition, we showed that this property can also be exploited in the analysis of LPTV closed-loop systems, through taking integers larger than the period of the LPTV systems as that for lifting-based treatment. The following chapter discusses robust performance controller synthesis based on static noncausal LPTV scaling exploiting the above promising property.

Chapter 3

Robust Controller Synthesis Based on Static Noncausal LPTV Scaling

3.1 Introduction

Ensuring robustness of control systems is one of the most important issues in control system analysis and synthesis. H_∞ control theory provides us with a powerful method for controller synthesis taking account of robustness for the uncertainties arising from the modeling errors of the plant. When there are multiple sources for the modeling errors, the uncertainties become structured, and the well-known μ-analysis and synthesis techniques [11],[32],[51] based on the H_∞ methodology and frequency-domain (or dynamic) scaling give an extended approach provided that the systems are linear time-invariant (LTI).

As an alternative approach to robustness analysis, noncausal LPTV scaling reviewed in the preceding chapter has been introduced in [23] for discrete-time systems, based on the lifting-based treatment of closed-loop systems. It introduces a sort of time-domain scaling in a noncausal fashion, in general, and thus is called *noncausal* LPTV scaling. An interesting feature of this approach is that even static noncausal LPTV scaling induces some frequency-dependent scaling when it is interpreted in the context of lifting-free treatment. This feature together with the fact that the uncertainties come to be dealt with in their lifted forms leads to an effective method for robust stability analysis through the KYP Lemma [34] and LMI optimization. Such a state-space approach could be an alternative to μ-analysis involving some frequency-domain treatment.

In this chapter, we extend such a promising approach of static noncausal LPTV scaling to a robust controller synthesis method. We theoretically discuss effectiveness of the synthesis method as well as static noncausal LPTV scaling itself, and numerically demonstrate it through the comparison with μ-synthesis. The LPTV controllers designed with the synthesis method, however, tend to produce oscillatory responses, as can be often the case with LPTV

controllers in general; the LPTV nature of the controllers contributing to achieving the control performance specification could excite the plant dynamics in an undesirable way and deteriorate another performance that has not been taken into consideration explicitly in the design process. Hence, this chapter in particular studies robust performance controller synthesis taking account of not only robust stability but also robust H_∞ performance to alleviate the possible oscillations in the responses of the resulting control systems. We demonstrate effectiveness of such controller synthesis by a numerical example, and also by control experiments with a cart inverted pendulum further.

This chapter is organized as follows. Section 3.2 reviews the basic ideas and frequency-domain properties of static noncausal LPTV scaling. Section 3.3 discusses the flexibility and effectiveness of noncausal LPTV scaling (compared with causal LPTV scaling, as well as the conventional lifting-free scaling), and classifies their sources in relation to the existence of different types of uncertainty blocks. Section 3.4 presents a robust performance controller synthesis method, as an extension of the robust stabilization method based on static noncausal LPTV scaling. The effectiveness of such an extended synthesis method is demonstrated with a numerical example in Section 3.5, in which it is also discussed how the properties of noncausal LPTV scaling play an important role in the LPTV controller synthesis for the robust performance problem. Effectiveness of the method is also demonstrated by control experiments with a cart inverted pendulum in Section 3.6, as an example of actual control problems.

3.2 Robust stability analysis based on static noncausal LPTV scaling

This chapter aims at studying robust performance controller synthesis based on static noncausal LPTV scaling reviewed in the preceding chapter. As a preliminary to such arguments, this section briefly reviews what has been clarified about the scaling approach in robust stability analysis of the feedback system Σ consisting of the nominal system G and the uncertainty Δ shown in Figure 2.3.

3.2.1 Separator-type theorem and static separators

Let us assume that the nominal system G is internally stable, finite-dimensional and LTI, and the uncertainty Δ belongs to a given set $\boldsymbol{\Delta}$ satisfying Assumption 2. Static noncausal LPTV scaling can be naturally introduced through the lifting-based treatment [4],[5] of these systems. We denote the lifted representations of G and Δ by $\widehat{G}$ and $\widehat{\Delta}$, respectively, and

the corresponding transfer matrices in the lifting-based framework by $\widehat{G}(z)$ and $\widehat{\Delta}(z)$. Then, regarding robust stability of the closed-loop system Σ, the following lifting-based separator-type theorem holds.

Theorem 3.1 Suppose that G is internally stable, and $\boldsymbol{\Delta}$ satisfies Assumption 2. Then, Σ is robustly (well-posed and) stable with respect to $\boldsymbol{\Delta}$ if there exists $\widehat{\Theta} = \widehat{\Theta}^T$ such that

$$\begin{bmatrix} I \\ \widehat{G}(z) \end{bmatrix}^* \widehat{\Theta} \begin{bmatrix} I \\ \widehat{G}(z) \end{bmatrix} \leq 0 \quad (\forall z \in \partial\mathbf{D}), \tag{3.1}$$

$$\begin{bmatrix} \widehat{\Delta}(z) \\ I \end{bmatrix}^* \widehat{\Theta} \begin{bmatrix} \widehat{\Delta}(z) \\ I \end{bmatrix} > 0 \quad \left(\begin{array}{l} \forall \Delta \in \boldsymbol{\Delta}, \\ \forall z \in \partial\mathbf{D} \end{array} \right), \tag{3.2}$$

where $\partial\mathbf{D} := \{z \in \mathbf{C} : |z| = 1\}$ denotes the unit circle.

This theorem is a restatement of Theorem 2.2 under the restriction on the matrix $\widehat{\Theta}$, called a noncausal LPTV separator, which is taken to be static. With this theorem, we can analyze robust stability of Σ for a given class $\boldsymbol{\Delta}$ through searching for the separator $\widehat{\Theta}$ satisfying (3.1) and (3.2). Such an approach to robust stability analysis is called static noncausal LPTV scaling, since taking a general matrix $\widehat{\Theta}$ corresponds to allowing a sort of noncausal operations of signals if the treatment is interpreted in the lifting-free framework.

However, no noncausal operations arise in the special case when $\widehat{\Theta} = (\widehat{\Theta})_{i,j=1,2}$ is restricted to such a form that $\widehat{\Theta}_{ij}$ $(i, j = 1, 2)$ are block-diagonal matrices consisting of N submatrices with size $p \times p$. Such a separator is called a static causal LPTV separator, and the approach to robust stability analysis with such separators is called static causal LPTV scaling. Note that when $N = 1$, (static) noncausal LPTV scaling and (static) causal LPTV scaling coincide with each other, and are nothing but the conventional (static) LTI scaling.

Noncausal LPTV scaling has remarkable frequency-domain properties that distinguish it clearly from causal LPTV scaling. They will be summarized in the following subsection.

Remark 3.1 We could consider the dynamic (i.e., z-dependent) $\widehat{\Theta}(z)$ instead of $\widehat{\Theta}$ in inequalities (3.1) and (3.2), as introduced in the preceding chapter. However, we confine ourselves to the case of the static separator $\widehat{\Theta}$ in the controller synthesis studied in this chapter unless stated otherwise. This is because the search of dynamic separators satisfying these inequalities is more difficult, in general, especially in the case of controller synthesis. Regarding robustness analysis, on the other hand, we will study a procedure of searching for dynamic separators in Chapter 6.

3.2.2 Frequency-domain properties of static noncausal LPTV scaling

This subsection summarizes the remarkable properties of static noncausal LPTV scaling reviewed in the preceding chapter, assuming for the moment that G and Δ are LTI. Note that G and Δ then have transfer matrices, so that we could also study the robust stability of Σ through the conditions (3.1) and (3.2) with $\widehat{G}(z)$ and $\widehat{\Delta}(z)$ obtained by taking $N = 1$, i.e., by dealing with Σ directly without applying lifting. We denote these transfer matrices by $G(\zeta)$ and $\Delta(\zeta)$, respectively, and the associated separator by Θ.

The following properties have been clarified about noncausal LPTV scaling [23].

(i) If there exists a separator $\Theta := (\Theta_{ij})_{i,j=1,2}$ in the lifting-free approach satisfying the conditions corresponding to inequalities (3.1) and (3.2), then the causal LPTV separator

$$\widehat{\Theta} = (I_N \otimes \Theta_{ij})_{i,j=1,2} \tag{3.3}$$

satisfies (3.1) and (3.2) in the lifting-based approach, where $\otimes$ denotes the Kronecker product of matrices.

(ii) If there exists a noncausal LPTV separator $\widehat{\Theta}$ satisfying (3.1) and (3.2), then the dynamic separator (recall Remark 3.1)

$$\begin{aligned} &\Theta(\zeta) = \mathcal{T}(\zeta)^* \widehat{\Theta} \mathcal{T}(\zeta), \\ &\mathcal{T}(\zeta) = \mathrm{diag}[T_p(\zeta), T_p(\zeta)], \quad T_p(\zeta) = \begin{bmatrix} \zeta^{-(N-1)} I_p \\ \vdots \\ \zeta^{-1} I_p \\ I_p \end{bmatrix} \end{aligned} \tag{3.4}$$

in the lifting-free approach satisfies the conditions corresponding to inequalities (3.1) and (3.2).

The first property implies that searching for a static noncausal LPTV separator in the lifting-based analysis is, at least, as effective as searching for a static separator in the conventional lifting-free LTI scaling. Furthermore, the second property implies that *noncausal* LPTV scaling corresponds to dynamic LTI scaling if it is interpreted in the lifting-free approach. Note that the latter is not the case for *causal* LPTV scaling, since the resulting $\Theta(\zeta)$ then degenerates to a constant matrix. Hence, these properties suggest that static *noncausal* LPTV scaling is more effective than the conventional static LTI scaling.

Note that this chapter studies the synthesis of LPTV controllers, and thus assuming G to be LTI as above is not directly suited to the situations in the following arguments. However, once we regard N-periodic systems as νN-periodic systems with some integer $\nu \geq 2$, the properties (i) and (ii) mean that noncausal LPTV scaling is effective also for periodic systems. This is because we could repeat the same arguments with N replaced by ν, if we start from the LTI systems $\widehat{G}$ and $\widehat{\Delta}$.

3.3 Flexibility of noncausal LPTV scaling and the classification of its sources

The preceding section reviewed the frequency-domain properties of noncausal LPTV scaling. These properties are closely related with the effectiveness of the design procedure of LPTV controllers based on noncausal LPTV scaling, as will be discussed in Section 3.5. Before such discussions, however, this section discusses another viewpoint: how the flexibility of noncausal LPTV scaling can be earned by the aspect that the LTI uncertainties are dealt with as the lifted form $\widehat{\Delta}$. In particular, we classify the sources of the flexibility of noncausal LPTV scaling (compared with causal LPTV scaling, which includes the conventional lifting-free scaling as a special case) in relation to the existence of different types of blocks in Δ.

3.3.1 Flexibility of noncausal LPTV scaling

In this chapter, we confine ourselves to the separators of the (D, G)-scaling type [13] given by

$$\widehat{\Theta} = \begin{bmatrix} -\gamma^2 W_{\mathrm{sq}} & X_G \\ X_G^T & W_{\mathrm{sq}} \end{bmatrix} \quad \begin{pmatrix} W_{\mathrm{sq}} > 0, \\ \gamma > 0 \end{pmatrix}. \tag{3.5}$$

Then, (3.2) simplifies to $\|\widehat{\Delta}(z)\|_\infty < 1/\gamma$, or equivalently $\|\Delta(\zeta)\|_\infty < 1/\gamma,\ \forall \Delta \in \boldsymbol{\Delta}$ if W_{sq} and X_G satisfy

$$W_{\mathrm{sq}}\widehat{\Delta}(z) = \widehat{\Delta}(z)W_{\mathrm{sq}},\ X_G^T\widehat{\Delta}(z) + \widehat{\Delta}(z)^* X_G = 0. \tag{3.6}$$

Hence, the basic idea for robust stability analysis is to search for $\widehat{\Theta}$ with as small γ as possible and with W_{sq} and X_G satisfying (3.6), under the constraint (3.1). Now, let us observe how noncausal LPTV scaling leads to crucial flexibility in the search of separators.

In the remainder of this chapter, we assume the structured LTI uncertainties described by

$$\Delta(\zeta) = \mathrm{diag}[\delta_1 I_{m_1}, \cdots, \delta_S I_{m_S}, \Delta_1, \cdots, \Delta_F, \Delta_1(\zeta), \cdots, \Delta_Z(\zeta)], \tag{3.7}$$

where $\delta_i \in \mathbf{R}$ $(i = 1, \ldots, S)$, $\Delta_i \in \mathbf{R}^{n_i \times n_i}$ $(i = 1, \ldots, F)$, $\Delta_i(\zeta) \in \mathbf{RH}_\infty^{l_i \times l_i}$ $(i = 1, \ldots, Z)$ and $\|\Delta(\zeta)\|_\infty < \bar{\delta}$ for some $\bar{\delta} > 0$. Although we have dealt with repeated dynamic blocks $\delta_1(s)I_{r_1}, \ldots, \delta_Y(s)I_{r_Y}$ in (2.1) (in the continuous-time case), we considered that assuming such blocks in the structured uncertainty is not realistic in actual problems, and omitted them (i.e., took $Y = 0$) in (3.7). Instead, we have newly introduced (repeated and full types of) static blocks in (3.7) that are considered to be natural to assume. For such structured uncertainties, let us first consider the static *causal* LPTV separator of the (D, G)-scaling type, which is (by definition) given by (3.5) with $W_{\rm sq}$ and X_G restricted to the diagonal forms

$$W_{\rm sq} = \mathrm{diag}[W_{{\rm sq},0}, \cdots, W_{{\rm sq},N-1}], \quad X_G = \mathrm{diag}[X_{G,0}, \cdots, X_{G,N-1}]. \tag{3.8}$$

Then, when $m_i = 1$ $(i = 1, \ldots, S)$, for example, it is hard to find a nonzero X_G satisfying (3.6). This means that in such a case we can apply only D-scaling if we are to apply the idea of *causal* LPTV scaling, whatever N we may take. Alternatively, when $S = 0$, $F = 1$ and $Z = 0$, it is hard to find $W_{\rm sq}$ satisfying (3.6) that is not a scalar times the identity, as well as nonzero X_G satisfying (3.6), regardless of N. This implies that no meaningful *causal* LPTV scaling exists.

However, it is important to note that, even in the cases mentioned above, the lifted $\widehat{\Delta}$ (after appropriate permutations of rows and columns) has blocks described as $\delta_i I_N$ $(i = 1, \ldots, S)$ and $I_N \otimes \Delta_i$ $(i = 1, \ldots, F)$. Since X_G and $W_{\rm sq}$ in *noncausal* LPTV scaling are free from the diagonal structures in (3.8), we can immediately take X_G that is nonzero, or $W_{\rm sq}$ that is not a scalar times the identity under the constraint (3.6). This clearly demonstrates the flexibility of noncausal LPTV scaling.

3.3.2 Classification of the sources of flexibility of noncausal LPTV scaling

From the observations in the preceding subsection, we can give Table 3.1 showing whether such more general forms of $W_{\rm sq}$ and X_G, other than the block diagonal forms given in (3.8), can indeed be taken under the constraint (3.6). The table is classified by the types of the diagonal subblocks in the uncertainty Δ in (3.7). In this table, 'e' denotes that introducing noncausality into scaling is 'effective' in the sense that the existence of the corresponding type of subblock always enables us to take non-block-diagonal $W_{\rm sq}$ or X_G under the constraint (3.6). When it is postfixed with '+' in the consideration on X_G, it means that the effectiveness is quite marked in the sense that, without introducing noncausality into scaling, it would have been restricted not only to a block-diagonal matrix but actually to the zero matrix.

Table 3.1: Effectiveness earned by the flexibility of noncausal LPTV scaling

type of subblock	$W_{\rm sq}$	X_G
$\delta_i I_{m_i} \quad (m_i = 1)$	e	e+
$\delta_i I_{m_i} \quad (m_i \geq 2)$	e	e
Δ_i	e	-
$\Delta_i(\zeta)$	-	-

Table 3.1 can be confirmed by observing general forms of $W_{\rm sq}$ and X_G in the noncausal LPTV separator $\widehat{\Theta}$ of (3.5) satisfying (3.6), which are given by

$$W_{\rm sq} = W_{\rm sq}^T \in \mathcal{R}^W, \tag{3.9}$$

$$X_G = -X_G^T \in \mathcal{R}^X, \tag{3.10}$$

where $\mathcal{R}^W$ is the set of all matrices

$$R_N = \begin{bmatrix} R_{11} & \cdots & R_{1N} \\ \vdots & \ddots & \vdots \\ R_{N1} & \cdots & R_{NN} \end{bmatrix}, \tag{3.11}$$

$$R_{ij} = \mathrm{diag}[R_{ij}^{(1)}, \cdots, R_{ij}^{(S)}, r_{ij}^{(1)} I_{n_1}, \cdots, r_{ij}^{(F)} I_{n_F}, \rho_{ij}^{(1)} I_{l_1}, \cdots, \rho_{ij}^{(Z)} I_{l_Z}],$$

$$R_{ij}^{(k)} \in \mathbf{R}^{m_k \times m_k}, \quad k = 1, \ldots, S, \tag{3.12}$$

with $\rho_{ij}^{(k)}$ $(k = 1, \ldots, Z)$ being scalars such that $\rho_{ij}^{(k)} = 0$ $(i \neq j)$ and $\rho_{11}^{(k)} = \rho_{22}^{(k)} = \cdots = \rho_{NN}^{(k)}$. Also, $\mathcal{R}^X$ is the set of all R_N with R_{ij} replaced by

$$R_{ij} = \mathrm{diag}[R_{ij}^{(1)}, \cdots, R_{ij}^{(S)}, 0_{n_1}, \cdots, 0_{n_F}, 0_{l_1}, \cdots, 0_{l_Z}]. \tag{3.13}$$

The advantages in the frequency domain suggested in the preceding section have been confirmed in [23] (and in the preceding chapter) with respect to numerical examples of robust stability analysis. However, the observations leading to Table 3.1 about the lifted treatment of Δ and the relevant arguments (which include giving the explicit forms (3.9) and (3.10) of $W_{\rm sq}$ and X_G) in the present subsection have not been discussed explicitly; only flexibility in some special case has been referred to (see Section 4.2 of [23]).

It is expected that these advantages can be exploited also in controller synthesis problems. The following section develops an explicit procedure of robust performance controller synthesis based on static noncausal LPTV scaling.

3.4 Robust H_∞ performance controller synthesis based on noncausal LPTV scaling

This section considers extending the robust stability analysis approach of static noncausal LPTV scaling to robust controller synthesis. The most natural and simplest extension from robust stability analysis is robust stabilization controller synthesis. One of our studies [24] has discussed such a direct extension in detail, whose summary will be given in Subsection 3.4.1. However, as will be confirmed and discussed in Subsection 3.5.2, taking account of only robust stability in controller synthesis may cause a problem that the responses of the resulting control systems become quite oscillatory at an unacceptable level. To avoid this problem, it is important to take account of not only robust stability but also robust H_∞ performance with some appropriate input-output settings aiming at alleviating the oscillations. Hence, in Subsections 3.4.2 and 3.4.3, we further develop a robust performance controller synthesis method based on static noncausal LPTV scaling.

3.4.1 Robust stabilization controller synthesis based on noncausal LPTV scaling

Let us consider the closed-loop system shown in Figure 2.2, where P represents the LTI generalized plant described by

$$\begin{bmatrix} x_{k+1} \\ z_k \\ y_k \end{bmatrix} = \begin{bmatrix} A & B_1 & B_2 \\ C_1 & D_{11} & D_{12} \\ C_2 & D_{21} & D_{22} \end{bmatrix} \begin{bmatrix} x_k \\ w_k \\ u_k \end{bmatrix}, \tag{3.14}$$

Δ represents the structured LTI uncertainty (3.7) belonging to the given uncertainty set $\boldsymbol{\Delta}$, and Ψ represents the controller. We assume $D_{22} = 0$ without loss of generality. The robust stabilization problem in this subsection is to design an N-periodic controller Ψ that robustly stabilizes the closed-loop system (Figure 2.2) with respect to $\boldsymbol{\Delta}$.

Given the controller Ψ, we can check robust stability of the closed-loop system by Theorem 3.1, through regarding the interconnection of P and Ψ as the nominal system G in Figure 2.3; although G naturally becomes N-periodic, its N-lifted counterpart can be dealt with in the same manner in Theorem 3.1, as that introduced in Section 3.2 (see the preceding chapter for more details). The basic idea of robust stabilization controller synthesis based on noncausal LPTV scaling is to apply the lifting technique (see Figure 3.1) and search for not only a noncausal LPTV separator $\widehat{\Theta}$ but also an LTI controller $\widehat{\Psi}$ of the form

$$\begin{aligned} \widehat{q}_{\kappa+1} &= A_{\widehat{\Psi}}\widehat{q}_\kappa + B_{\widehat{\Psi}}\widehat{y}_\kappa, \\ \widehat{u}_\kappa &= C_{\widehat{\Psi}}\widehat{q}_\kappa + D_{\widehat{\Psi}}\widehat{y}_\kappa, \end{aligned} \tag{3.15}$$

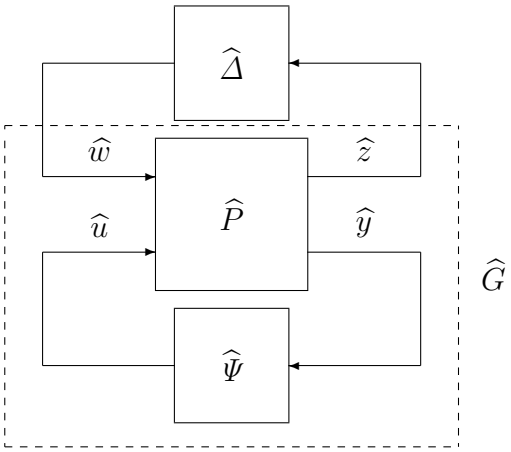

Figure 3.1: Lifted representation of feedback system.

which corresponds to an N-periodic controller Ψ in the lifting-free framework, satisfying inequalities (3.1) and (3.2). While (3.1) is relatively easy to deal with, (3.2) is generally difficult to directly deal with, since the condition consists of infinitely many inequalities with respect to $\boldsymbol{\Delta}$. To circumvent this difficulty, we confine separators to (D, G)-scaling type (3.5). Then, (3.2) simplifies to $\|\widehat{\Delta}(z)\|_\infty < 1/\gamma$ or equivalently $\|\Delta(\zeta)\|_\infty < 1/\gamma$, provided that $W_{\rm sq}$ and X_G satisfy (3.6). We thus only have to solve the remaining condition (3.1), as in the case of robust stability analysis, once separators are confined to (D, G)-scaling type satisfying (3.6).

Remark 3.2 Note that since the controller $\widehat{\Psi}$ will be directly computed in the lifting-based framework, the corresponding controller Ψ in the lifting-free framework may become noncausal. We thus confine the direct feedthrough matrix $D_{\widehat{\Psi}}$ of the controller $\widehat{\Psi}$ to an appropriate set $\mathcal{D}_l$ of block lower triangle matrices in the following, to ensure the implementability of the corresponding Ψ as a *causal* LPTV controller.

For P in (3.14), let us denote its lifted representation $\widehat{P}$ by

$$\begin{bmatrix} \widehat{x}_{\kappa+1} \\ \widehat{z}_\kappa \\ \widehat{y}_\kappa \end{bmatrix} = \begin{bmatrix} \widehat{A} & \widehat{B}_1 & \widehat{B}_2 \\ \widehat{C}_1 & \widehat{D}_{11} & \widehat{D}_{12} \\ \widehat{C}_2 & \widehat{D}_{21} & \widehat{D}_{22} \end{bmatrix} \begin{bmatrix} \widehat{x}_\kappa \\ \widehat{w}_\kappa \\ \widehat{u}_\kappa \end{bmatrix}. \tag{3.16}$$

It is known that the strict form

$$\begin{bmatrix} I \\ \widehat{G}(z) \end{bmatrix}^* \widehat{\Theta} \begin{bmatrix} I \\ \widehat{G}(z) \end{bmatrix} < 0 \quad (\forall z \in \partial\mathbf{D}) \tag{3.17}$$

of the inequality (3.1) can be reformulated as an LMI condition for controller synthesis [38], [31], once the separator $\widehat{\Theta}$ is fixed. This immediately leads us to the following theorem [24].

Theorem 3.2 There exists a controller $\widehat{\Psi}$, implementable as a causal LPTV controller Ψ in Figure 2.2, such that $\widehat{G}$ in Figure 3.1 is internally stable and satisfies (3.17), if and only if there exist real matrices $R \in \mathcal{D}_l$, $P = P^T$, $H = H^T$, J, X, Y, S, Q, F and L satisfying

$$\begin{bmatrix} P & J & \widehat{A}X + \widehat{B}_2 L & \widehat{A} + \widehat{B}_2 R \widehat{C}_2 & \widehat{B}_1 + \widehat{B}_2 R \widehat{D}_{21} & 0 \\ * & H & Q & Y\widehat{A} + F\widehat{C}_2 & Y\widehat{B}_1 + F\widehat{D}_{21} & 0 \\ * & * & X + X^T - P & I + S^T - J & -(\widehat{C}_1 X + \widehat{D}_{12} L)^T X_G^T & (\widehat{C}_1 X + \widehat{D}_{12} L)^T W_{\mathrm{sq}} \\ * & * & * & Y + Y^T - H & -(\widehat{C}_1 + \widehat{D}_{12} R \widehat{C}_2)^T X_G^T & (\widehat{C}_1 + \widehat{D}_{12} R \widehat{C}_2)^T W_{\mathrm{sq}} \\ * & * & * & * & \gamma^2 W_{\mathrm{sq}} - \mathcal{H} & (\widehat{D}_{11} + \widehat{D}_{12} R \widehat{D}_{21})^T W_{\mathrm{sq}} \\ * & * & * & * & * & W_{\mathrm{sq}} \end{bmatrix} > 0,$$

$$\mathcal{H} = \mathrm{He}\{X_G(\widehat{D}_{11} + \widehat{D}_{12} R \widehat{D}_{21})\}. \tag{3.18}$$

When the above inequality holds, $S - YX$ is nonsingular, and with any nonsingular matrices V and U such that $VU = S - YX$, one such controller $\widehat{\Psi}$ is given by

$$\begin{aligned} &A_{\widehat{\Psi}} = A^0_{\widehat{\Psi}} - B^0_{\widehat{\Psi}} \widehat{D}_{22} (I + D^0_{\widehat{\Psi}} \widehat{D}_{22})^{-1} C^0_{\widehat{\Psi}}, \quad B_{\widehat{\Psi}} = B^0_{\widehat{\Psi}} - B^0_{\widehat{\Psi}} \widehat{D}_{22} (I + D^0_{\widehat{\Psi}} \widehat{D}_{22})^{-1} D^0_{\widehat{\Psi}}, \\ &C_{\widehat{\Psi}} = (I + D^0_{\widehat{\Psi}} \widehat{D}_{22})^{-1} C^0_{\widehat{\Psi}}, \quad D_{\widehat{\Psi}} = (I + D^0_{\widehat{\Psi}} \widehat{D}_{22})^{-1} D^0_{\widehat{\Psi}}, \\ &\begin{bmatrix} A^0_{\widehat{\Psi}} & B^0_{\widehat{\Psi}} \\ C^0_{\widehat{\Psi}} & D^0_{\widehat{\Psi}} \end{bmatrix} = \begin{bmatrix} V^{-1} & -V^{-1} Y \widehat{B}_2 \\ 0 & I \end{bmatrix} \begin{bmatrix} Q - Y\widehat{A}X & F \\ L & R \end{bmatrix} \begin{bmatrix} U^{-1} & 0 \\ -\widehat{C}_2 X U^{-1} & I \end{bmatrix}. \end{aligned} \tag{3.19}$$

To achieve better control performance, however, it is important to optimize not only parameters for the controller $\widehat{\Psi}$ but also the separator $\widehat{\Theta}$, and this situation causes (3.18) to be a bilinear matrix inequality (BMI). Since it is difficult to obtain an optimal solution to BMIs, we solve it with an iterative method described as follows.

Robust stabilization controller synthesis method:

A1. Construct the lifted representation $\widehat{P}$ from P with the given N.

A2. With fixed W_{sq} and X_G, search for $R \in \mathcal{D}_l$, P, H, J, X, Y, S, Q, F and L in (3.18) minimizing γ, through LMI optimization, where the initial W_{sq} and X_G may be given arbitrarily within the structures shown in the equations in Subsection 3.3.2 (e.g., $W_{\mathrm{sq}} = I$, $X_G = 0$).

A3. Minimize γ with a bisection method with respect to (3.18) as follows: each time γ is fixed, fix also X, L and R, and search for P, H, J, Y, S, Q, F, W_{sq} and X_G satisfying (3.18) within the above constraints on the structure of W_{sq} and X_G.

A4. Repeat A2. and A3. to obtain as small γ as possible.

3.4.2 Robust performance problem and its reduction to robust stabilization problem

The preceding subsection discussed robust stabilization controller synthesis based on non-causal LPTV scaling (associated with the feedback system shown in Figure 2.2). Let us next consider the feedback system shown in Figure 3.2. In the figure, P denotes the generalized plant represented by (3.14) with $D_{22} = 0$ and with $w = [w_{\mathrm{u}}^{\mathrm{T}}, w_{\mathrm{d}}^{\mathrm{T}}]^{\mathrm{T}}$ and $z = [z_{\mathrm{u}}^{\mathrm{T}}, z_{\mathrm{d}}^{\mathrm{T}}]$, where w_{d} and z_{d} denote the disturbance input and the performance output, respectively. Δ_{u} is an uncertainty that lies in the given connected uncertainty set $\boldsymbol{\Delta}_{\mathrm{u}}$ ($\ni 0$) such that every $\Delta_{\mathrm{u}} \in \boldsymbol{\Delta}_{\mathrm{u}}$ is finite-dimensional, LTI, and stable. The robust performance controller synthesis problem in this chapter is to design an N-periodic controller Ψ that robustly stabilizes the closed-loop system (Figure 3.2) for the uncertainty class $\boldsymbol{\Delta}_{\mathrm{u}}$ and suppresses the worst-case H_∞-norm from w_{d} to z_{d} as much as possible.

Suppose we consider the lifted system shown in Figure 3.3, where $\widehat{P}$, $\widehat{\Delta}_{\mathrm{u}}$ and $\widehat{\Psi}$ denote the lifted representations of P, Δ_{u} and Ψ, respectively. The stability of feedback systems is retained by the application of lifting, and the H_∞-norm of an LPTV system is equivalent to that of the lifted equivalent LTI system. Hence, we can readily restate our problem into that of designing the LTI controller (3.15) such that it robustly stabilizes the above lifted feedback system and makes the worst-case H_∞-norm from $\widehat{w}_{\mathrm{d}}$ to $\widehat{z}_{\mathrm{d}}$ less than γ_{d} for as small $\gamma_{\mathrm{d}} > 0$ as possible, provided that $D_{\widehat{\Psi}}$ is confined to belong to an appropriate set $\mathcal{D}_l$ of block lower triangle matrices ensuring the implementability of $\widehat{\Psi}$ as Ψ, a *causal* LPTV controller.

Since the mapping from $\widehat{w}_{\mathrm{d}}$ to $\widehat{z}_{\mathrm{d}}$ is LTI, it is known that the H_∞-norm between $\widehat{w}_{\mathrm{d}}$ and $\widehat{z}_{\mathrm{d}}$ is less than or equal to γ_{d} if and only if the closed-loop system obtained by letting $\widehat{w}_{\mathrm{d}} = \widehat{\Delta}_{\mathrm{d}}\widehat{z}_{\mathrm{d}}$ is stable for all $\widehat{\Delta}_{\mathrm{d}} \in \widehat{\boldsymbol{\Delta}}_{\mathrm{d}}$, where $\widehat{\boldsymbol{\Delta}}_{\mathrm{d}}$ denotes the set of all dynamic stable LTI $\widehat{\Delta}_{\mathrm{d}}$ whose H_∞-norm is less than $1/\gamma_{\mathrm{d}}$. Hence, by defining $\widehat{\Delta} := \mathrm{diag}[\widehat{\Delta}_{\mathrm{u}}, \widehat{\Delta}_{\mathrm{d}}]$, we can reduce the problem to that of designing $\widehat{\Psi}$ such that the system shown in Figure 3.1 is robustly stable

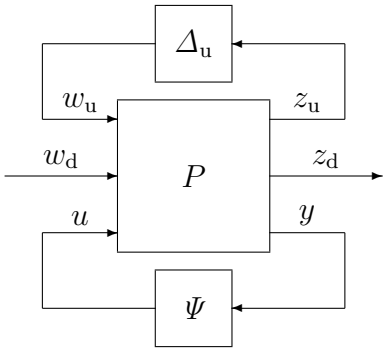

Figure 3.2: Robust performance problem.

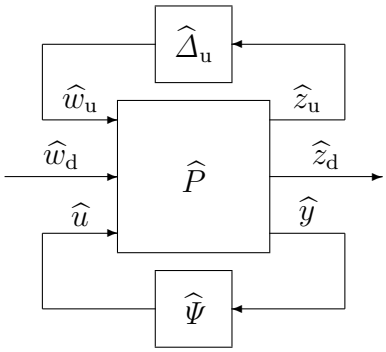

Figure 3.3: Lifted representation of feedback system for robust performance problem.

with respect to $\Delta_{\mathrm{u}} \in \boldsymbol{\Delta}_{\mathrm{u}}$ and $\widehat{\Delta}_{\mathrm{d}} \in \widehat{\boldsymbol{\Delta}}_{\mathrm{d}}$. This fact can be summarized as follows.

Theorem 3.3 Suppose the closed-loop system shown in Figure 3.3 is given. The H_∞-norm between $\widehat{w}_{\mathrm{d}}$ and $\widehat{z}_{\mathrm{d}}$ is less than or equal to γ_{d} for all $\Delta_{\mathrm{u}} \in \boldsymbol{\Delta}_{\mathrm{u}}$ such that $\|\Delta_{\mathrm{u}}\|_\infty < 1/\gamma_{\mathrm{u}}$ if and only if the closed-loop system given by Figure 3.1 is robustly stable with respect to $\{\widehat{\Delta} = \mathrm{diag}[\widehat{\Delta}_{\mathrm{u}}, \widehat{\Delta}_{\mathrm{d}}] \;\big|\; \Delta_{\mathrm{u}} \in \boldsymbol{\Delta}_{\mathrm{u}}, \|\Delta_{\mathrm{u}}\|_\infty < 1/\gamma_{\mathrm{u}}, \widehat{\Delta}_{\mathrm{d}} \in \widehat{\boldsymbol{\Delta}}_{\mathrm{d}}\}$.

To facilitate the explanation of the basic idea for reducing the robust performance controller synthesis problem to the robust stabilization controller synthesis problem, let us for the moment replace $\widehat{\boldsymbol{\Delta}}_{\mathrm{d}}$ with the set of the lifted representations of LTI Δ_{d} whose H_∞-norm is less than $1/\gamma_{\mathrm{d}}$ (even though it is in fact much smaller than the actual $\widehat{\boldsymbol{\Delta}}_{\mathrm{d}}$). Then, $\widehat{\Delta}$ can be regarded as the lifted representation of $\Delta = \mathrm{diag}[\Delta_{\mathrm{u}}, \Delta_{\mathrm{d}}]$, and once γ_{d} is fixed, appropriately scaling the output (or input) signals of P allows us to assume without loss of generality that the above $\Delta = \mathrm{diag}[\Delta_{\mathrm{u}}, \Delta_{\mathrm{d}}]$ is given by (3.7) for some $\overline{\delta} > 0$. More precisely, by scaling the output z_{d} of P and the associated input of Δ_{d} by the factors $\gamma_{\mathrm{u}}/\gamma_{\mathrm{d}}$ and $\gamma_{\mathrm{d}}/\gamma_{\mathrm{u}}$, respectively, and regarding the output-scaled generalized plant and the input-scaled uncertainty as P and Δ_{d}, respectively, we can see that $\Delta = \mathrm{diag}[\Delta_{\mathrm{u}}, \Delta_{\mathrm{d}}]$ is given by (3.7) with $\overline{\delta} = 1/\gamma_{\mathrm{u}}$ and that the corresponding Δ_Z in (3.7) equals Δ_{d}. This situation is compatible with the assumption in the robust stability analysis of the closed-loop system via noncausal LPTV scaling.

In the above description of the basic idea, we have introduced some rough treatment of $\widehat{\boldsymbol{\Delta}}_{\mathrm{d}}$; it does not always correspond to the set of the lifted representations of LTI Δ_{d} but is related also to N-periodic dynamic Δ_{d}, actually. Hence, we have to deal with periodic and dynamic uncertainties when we consider exploiting noncausal LPTV scaling in robust performance controller synthesis. Fortunately, noncausal LPTV scaling can in fact deal with such uncertainties, too, as long as the freedom in the scaling is adequately restricted about N-periodic uncertainty blocks; in the present situation, no scaling is allowed for the N-periodic dynamic block Δ_{d} ($\widehat{\Delta}_{\mathrm{d}} \in \widehat{\boldsymbol{\Delta}}_{\mathrm{d}}$). This constraint is indeed satisfied automatically

by the form of $\rho_{ij}^{(Z)} I_{l_Z}$, $i, j = 1, \ldots, N$ in (3.12) and the restriction 0_{l_Z} in (3.13). Taking this observation into account, the above reduction to robust stabilization controller synthesis problem is rigorous even when we deal with such a synthesis problem through the lifting technique to exploit noncausal LPTV scaling.

Following the basic idea shown above, we can construct an explicit robust performance controller synthesis method based on static noncausal LPTV scaling, as will be described in the following subsection.

3.4.3 Explicit procedure of robust performance controller synthesis based on noncausal LPTV scaling

An explicit robust performance controller synthesis method based on noncausal LPTV scaling is given in this subsection. A remark on its relationship with the robust stabilization controller synthesis method in Subsection 3.4.1 will be given after stating the procedure.

Robust performance controller synthesis method:

B1. Initialization steps

B1-1. Denote the original given generalized plant (3.14) by the new symbol P_0, and take the initial $\gamma_{\rm d} > 0$ and $\gamma > \gamma_{\rm u}$ large enough.

B1-2. Multiply the output $z_{\rm d}$ of P_0 by $\gamma/\gamma_{\rm d}$ (so that we can regard the norm of the inversely scaled fictitious uncertainty to be less than $1/\gamma$, rather than $1/\gamma_{\rm d}$). Denote, for notational simplicity, the resulting scaled generalized plant by the same symbol P (which in the beginning was used to denote the original generalized plant); we assume that (3.14) now represents this modified P rather than the original P_0. Construct the lifted representation $\widehat{P}$ from the modified generalized plant with the given N.

B1-3. Consider the augmented structured uncertainty Δ consisting of the plant uncertainty $\Delta_{\rm u}$ and the scaled fictitious uncertainty; when Δ is described in the form (3.7), we assume that the last block $\Delta_Z(\zeta)$ corresponds to the scaled fictitious uncertainty and that the norm of Δ is less than $1/\gamma$ (since $1/\gamma < 1/\gamma_{\rm u}$, this implies that we are taking account of only a subset of $\boldsymbol{\Delta}_{\rm u}$ at this initial stage).

B1-4. For the augmented structured uncertainty Δ, take the initial $W_{\rm sq}$ and X_G arbitrarily within the structures shown in the equations in Subsection 3.3.2 (e.g., $W_{\rm sq} = I$, $X_G = 0$).

B2. Robust stabilization steps

B2-1. Minimize γ with a bisection method with respect to (3.18) as follows: each time γ is fixed,

(i) Apply Step B1-2. with the new γ;

(ii) Fix also $W_{\rm sq}$ and X_G, and search for $R \in \mathcal{D}_l$, P, H, J, X, Y, S, Q, F and L satisfying

(3.18).

B2-2. Minimize γ with a bisection method with respect to (3.18) as follows: each time γ is fixed,

(i) Apply Step B1-2. with the new γ;

(ii) Fix also X, L and R, and search for P, H, J, Y, S, Q, F, $W_{\rm sq}$ and X_G satisfying (3.18) within the constraints on the structure of $W_{\rm sq}$ and X_G given by the equations in Subsection 3.2.2.

B2-3. Repeat Steps B2-1. and B2-2. until $\gamma \leq \gamma_{\rm u}$ is achieved. If this is achieved eventually, it implies that robust stabilization with respect to $\boldsymbol{\Delta}_{\rm u}$ ($\|\Delta_{\rm u}\|_\infty < 1/\gamma_{\rm u}$, $\forall \Delta_{\rm u} \in \boldsymbol{\Delta}_{\rm u}$) has been succeeded in with the worst case H_∞-performance less than the initial level $\gamma_{\rm d}$, and thus let $\gamma = \gamma_{\rm u}$ and go to the next step to optimize the worse case H_∞-performance. Otherwise, regard the robust performance controller synthesis problem to be infeasible with the present method or the present initial $\gamma_{\rm d}$, $W_{\rm sq}$ and X_G.

B3. H_∞-performance optimization steps

B3-1. Minimize $\gamma_{\rm d}$ with a bisection method[1] as follows: (i) Take new $\gamma_{\rm d} > 0$ determined by the bisection scheme, and apply Step B1-2. with the new $\gamma_{\rm d}$;

(ii) Fix γ, $W_{\rm sq}$ and X_G, and search for $R \in \mathcal{D}_l$, P, H, J, X, Y, S, Q, F and L satisfying (3.18);

(iii) Repeat (i) and (ii) to minimize, by a bisection method, $\gamma_{\rm d}$ under the constraint that the resulting (3.18) is feasible.

B3-2. Minimize $\gamma_{\rm d}$ with a bisection method as follows:

(i) Take new $\gamma_{\rm d} > 0$ determined by the bisection scheme, and apply Step B1-2. with the new $\gamma_{\rm d}$;

(ii) Fix γ, X, L and R, and search for P, H, J, Y, S, Q, F, $W_{\rm sq}$ and X_G satisfying (3.18) within the constraints on the structure of $W_{\rm sq}$ and X_G given by the equations in Subsection 3.2.2;

(iii) Repeat (i) and (ii) to minimize, by a bisection method, $\gamma_{\rm d}$ under the constraint that the resulting (3.18) is feasible.

B3-3. Repeat B3-1. and B3-2. to obtain as small $\gamma_{\rm d}$ as possible.

The above procedure leads to a robust performance controller $\widehat{\Psi}$ given by (3.19) such that the worst-case H_∞-performance is less than $\gamma_{\rm d}$ under the uncertainties $\boldsymbol{\Delta}_{\rm u}$.

Remark 3.3 In Steps B2-1., B2-2., B3-1. and B3-2. of the above procedure, it is repeatedly required to apply Step B1-2. (in which the lifted representation $\widehat{P}$ is to be constructed from

[1]Unlike in Step B2-1., this bisection method is with respect to $\gamma_{\rm d}$ rather than γ. Similarly for Step B3-2. below. Note that γ has been set to $\gamma_{\rm u}$ and will not be changed in Step B3.

the modified P in the respective stage). However, it is obvious that in each of these steps, $\widehat{P}$ can actually be constructed simply by appropriately scaling the lifted representation $\widehat{P}_0$ of the original generalized plant. Hence, it actually suffices to apply lifting only once for the original P_0.

This robust performance controller synthesis method is an extension of the robust stabilization controller synthesis method shown in Subsection 3.4.1 in the following sense. First of all, except for minor modifications, Steps B2-1. and B3-1. in this subsection correspond to Step A2. in Subsection 3.4.1, while Steps B2-2. and B3-2. to Step A3. in Subsection 3.4.1. Hence, an essential difference of the above robust performance synthesis method from the one in Subsection 3.4.1 is that robust stabilization (without paying attention to robust performance) is first achieved in Step B2., and then robust performance is improved in Step B3. Because of this two stage structure, Step B2. only aims at reducing γ down to γ_{u} (rather than minimizing γ), and this leads to minor modifications. On the other hand, Step B3. aims at improving the robust performance level γ_{d} as much as possible. Hence, Step B3. is essentially the same as Steps A2. to A4. in Subsection 3.4.1, even though their explicit descriptions look rather different. This is simply because the target γ_{d} for minimization in Steps B3. does not appear explicitly in the LMI (3.18), so that we had to describe the explicit relation between γ_{d} and the LMI (3.18) in the above procedure.

3.5 Numerical example and discussions

This section shows with a numerical example the effectiveness of noncausal LPTV scaling for robust controller synthesis. In particular, it is demonstrated that attempting not only robust stabilization but also robust performance can successfully alleviate the oscillations in the responses of the closed-loop system that are supposed to be descendent from the periodicity of the controller. Furthermore, a methodology is suggested for monotonically improving the performance of the closed-loop system through a sequential design procedure; it involves a sequential increase of the period of the LPTV controller by an integer multiple, in which the frequency-domain properties of noncausal LPTV scaling summarized in Subsection 3.2.2 play an important role for performance improvement.

3.5.1 Example: A simple mechanical system

This subsection first introduces a simple mechanical system as a numerical example studied throughout this section. It consists of a rod whose mass can be neglected and a point mass attached on one end of the rod. The other end of the rod is the pivot at which a

torque τ can be applied to the rod as the control input, where the rod is assumed to rotate within a vertical plane (see Figure 3.4). The length r of the rod is 0.2 and the nominal value M of the point mass is 1. The control objective is to regulate around 0 the angle θ of the rod from the vertically inverted attitude in the presence of the uncertainty in M.

The equation of motion for the above system is given by

$$\tau + Mgr\sin\theta = Mr^2\ddot{\theta}, \tag{3.20}$$

where $g = 9.8$ denotes the gravitational acceleration. We can obtain a continuous-time state equation by linearizing (3.20) around $(\theta, \dot{\theta}) = (0, 0)$ and defining the state variables $\xi_1 := \theta$, $\xi_2 := \dot{\theta}$, the input $u := \tau$ and the output $y := \theta$. By discretizing the associated transfer function via the zero-order hold with sampling period $T_\mathrm{s} = 0.1$ and realizing the result (with states taken independently of ξ_1 and ξ_2), we can obtain

$$\begin{bmatrix} x_{1,k+1} \\ x_{2,k+1} \end{bmatrix} = \begin{bmatrix} 0 & 1 \\ -1 & \alpha \end{bmatrix} \begin{bmatrix} x_{1,k} \\ x_{2,k} \end{bmatrix} + \begin{bmatrix} 0 \\ 1 \end{bmatrix} u_k, \tag{3.21}$$

$$y_k = \begin{bmatrix} (\alpha-2)\beta & (\alpha-2)\beta \end{bmatrix} \begin{bmatrix} x_{1,k} \\ x_{2,k} \end{bmatrix} \tag{3.22}$$

where $\alpha := e^{\sqrt{\frac{g}{r}}T_\mathrm{s}} + e^{-\sqrt{\frac{g}{r}}T_\mathrm{s}}$ and $\beta := \frac{1}{2Mgr}$. Since M in fact includes uncertainty, we consider replacing β by $\beta = (1+\delta)\beta_0$ with the real scalar uncertainty δ and the nominal value β_0, while the (nominal) value of α is denoted by α_0. We then separate δ from (3.21) and (3.22) so that the system can be described with the generalized plant

$$P : \left[\begin{array}{cc:c:c} 0 & 1 & 0 & 0 \\ -1 & \alpha_0 & 0 & 1 \\ \hdashline \beta_0 & \beta_0 & 0 & 0 \\ \hdashline (\alpha_0-2)\beta_0 & (\alpha_0-2)\beta_0 & \alpha_0-2 & 0 \end{array}\right] \tag{3.23}$$

and the uncertainty $\Delta_\mathrm{u} = \delta$.

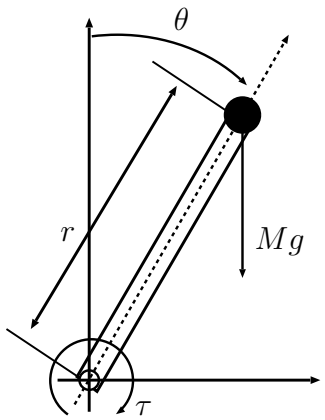

Figure 3.4: Simple mechanical system.

3.5.2 Results of robust stabilization controller synthesis and discussions

In this subsection, we first design robust stabilization controllers for the uncertainties δ such that $|\delta| < 1/\gamma_{\mathrm{u}}$ for as small γ_{u} as possible, based on static noncausal LPTV scaling through the method given in Subsection 3.4.1 with γ set to γ_{u}. The minimum value of γ_{u} achieved by the LPTV controller based on noncausal LPTV scaling with each N is shown in Table 3.2. In addition to γ_{u}, we also show $\gamma_{\mathrm{u,anal}}$ in Table 3.2 for each N, which denotes the minimum value of γ_{u} for which robust stability of the closed-loop system with the designed LPTV controller is ensured for the uncertainties $|\delta| < 1/\gamma_{\mathrm{u}}$ *through the 'post-synthesis' analysis based on static noncausal LPTV scaling with* $N = 6$. Such analysis is introduced here because the method for controller synthesis involves iterative solutions of LMIs and thus is not ensured to lead to the theoretical minimum of γ_{u}. Hence, the minimum value of γ_{u} obtained in the synthesis step is generally conservative, so that the mere comparison of the values of γ_{u} for different values of N may not be meaningful enough. The comparison of the values of $\gamma_{\mathrm{u,anal}}$ aims at alleviating the issue since the post-synthesis analysis is carried out with a common value $N = 6$ regardless of N used in the synthesis step.

As shown in Table 3.2, the synthesis results based on noncausal LPTV scaling are surely improved by increasing the period N of the controller. We stress here that such improvement is earned not only (i) by the increase in the controller period or the associated expansion of the controller classes but also (ii) by the enhanced ability of noncausal LPTV scaling with larger N, whose frequency-domain interpretation has been provided in Subsection 3.2.2. Regarding (i), it should be recalled that, because of the difficulty in simultaneously optimizing noncausal LPTV scaling and the controller, the design results are not ensured to be globally optimal. Hence, it is not an obvious theoretical consequence that increasing N leads to a better result. This observation implies that the above point (ii) is indeed closely related with the improvement that we have obtained by increasing N. This is because a larger N generally gives a less conservative result for robust stability analysis under a fixed controller (recall the relevant frequency-domain arguments in Section 3.2.2, that is, noncausal LPTV scaling with larger N is more flexible), and this aspect is obviously inherited also to the case in which noncausal LPTV scaling is employed in controller synthesis.

Table 3.2: Design results for robust stabilization with noncausal LPTV scaling

N	1	2	3	6
γ_{u}	2.0141	1.5936	1.4673	1.3546
$\gamma_{\mathrm{u,anal}}$	2.0139	1.5934	1.4670	1.3546

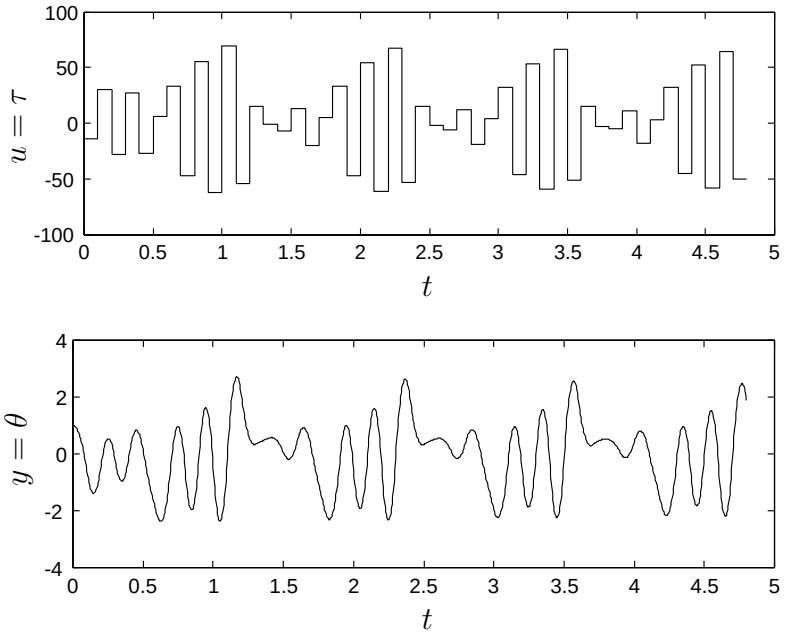

Figure 3.5: Initial value responses under the robust stabilization controller $\widehat{\Psi}$ with $N = 6$ when $\xi(0) = [1, 0]$.

We also remark that the minimum value of γ_{u} obtained by the conventional D-scaling-based μ-synthesis coincides with that for $N = 1$ in Table 3.2. This is obvious from the following two facts: (i) no (dynamic) D-scaling is meaningful for the scalar uncertainty δ here, so that μ-synthesis reduces to unscaled H_∞ synthesis; (ii) when $N = 1$, static noncausal LPTV (D, G)-scaling reduces to D-scaling for the scalar uncertainty δ (recall the relevant arguments in Subsection 3.3.1), which also reduces to unscaled H_∞ synthesis. Hence, we can confirm through this example the effectiveness of noncausal LPTV scaling over the conventional μ-synthesis approach in robust stabilization controller synthesis. In particular, the best result $\gamma_{\mathrm{u,anal}} = 1.3546$ with noncausal LPTV scaling is quite marked because μ-synthesis can only achieve $\gamma_{\mathrm{u,anal}} = 2.0139$.

However, feedback systems with periodic controllers often tend to produce oscillatory responses, and the closed-loop systems with the controllers designed here are no exception. In fact, the initial value responses of the 6-periodic feedback system, corresponding to the value of $\gamma_{\mathrm{u,anal}} = 1.3546$ in Table 3.2 obtained by total optimization in the synthesis step, are shown in Figure 3.5, where we only consider the nominal case of $\delta = 0$. They are obviously unacceptable (even though terminating the optimization in the synthesis step at a moderate level could somewhat reduce the oscillations). This seems to be attributed to the fact that the periodicity of the LPTV controller excites the high frequency dynamics of the plant and deteriorates the control performance that has not been taken explicitly into

consideration in the controller synthesis. Thus, to sophisticate the synthesis method based on noncausal LPTV scaling to a more practical one, we have to tackle the issue of alleviating oscillatory responses. The following subsection demonstrates that the robust performance controller synthesis method in Section 3.4 can surely alleviate the oscillatory responses while retaining the effectiveness of noncausal LPTV scaling, provided that the method is applied appropriately.

3.5.3 Results of robust performance controller synthesis and discussions

We have observed that robust stabilization with noncausal LPTV scaling could lead to the oscillations in the responses of the closed-loop system, which are supposed to be descendent from the periodicity of the controller itself. To alleviate such oscillations while exploiting the advantages of noncausal LPTV scaling, we consider applying the robust performance controller synthesis method presented in Section 3.4.

More precisely, we consider the generalized plant P for the robust performance problem shown in Figure 3.6, where P_{stab} denotes the one used in the robust stabilization problem, i.e., (3.23). Roughly speaking, this modified generalized plant takes the control input u as the performance output z_{d}. This is intended to be helpful in suppressing the oscillations of the control input (see Figure 3.5), which are presumed to be the main cause in the overall oscillatory responses of the closed-loop system. We also consider the disturbance w_{d} that contaminates the control input, and consider the problem of reducing the robust H_∞ performance from w_{d} to z_{d}. More precisely, we assume here that the uncertainties satisfy $|\delta| < 1/\gamma_{\mathrm{u}}$ for $\gamma_{\mathrm{u}} = 1.7$, and consider minimizing the worse-case H_∞ performance for such uncertainties through the robust performance controller synthesis method based on noncausal LPTV scaling presented in Section 3.4.

The initial value responses of the 6-periodic feedback system, obtained by minimizing the robust H_∞ performance with such synthesis, are shown in Figure 3.7 for the nominal value of M and for the maximum and minimum values of the uncertainty δ. Compared with the re-

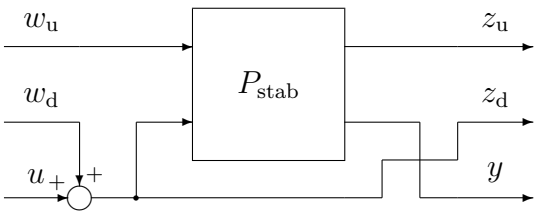

Figure 3.6: Generalized plant for robust performance problem.

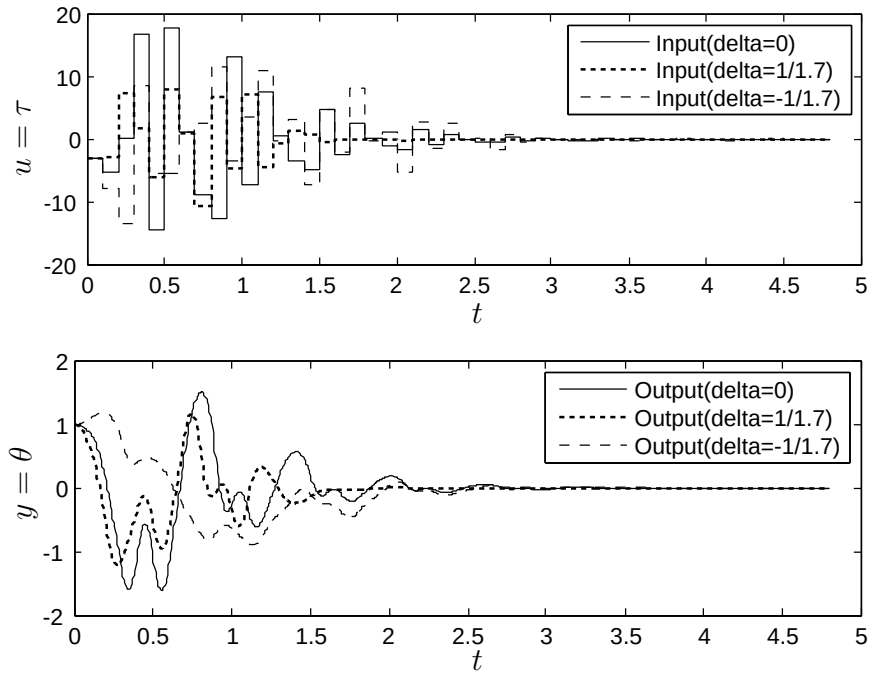

Figure 3.7: Initial value responses under the robust performance controller $\widehat{\Psi}$ with $N = 6$ when $\xi(0) = [1, 0]$.

sponses shown in Figure 3.5, these responses demonstrate that the oscillations are drastically suppressed. This implies that an adequate use of the robust stabilization controller synthesis method with noncausal LPTV scaling (i.e., the method presented in Subsection 3.4.3) can take account of robust performance issues too, and can thus give a practically attractive controller. As we try to achieve robust stabilization for larger uncertainties, it may become harder to suppress oscillatory responses, but what should be stressed here is our success in achieving satisfactory closed-loop responses for such uncertainties for which the conventional μ-synthesis fails to achieve even robust stabilization; recall that μ-synthesis can achieve robust stabilization only for $|\delta| < 1/\gamma_{\rm u} = 0.4965$ (with $\gamma_{\rm u} = 2.0139$), which is much smaller than the current value $1/\gamma_{\rm u} = 0.5882$ (with $\gamma_{\rm u} = 1.7$).

Remark 3.4 It has been shown in [14],[50] that no LPTV controllers can outperform LTI controllers in the H_∞-norm minimization problem for LTI plants. The examples studied in this section by no means contradict this result. This is because the result of [14], [50] is concerned only with the H_∞-norm performance of a nominal system (i.e., without uncertainties), or equivalently, the robust stability problem for unstructured dynamic uncertainties. The problems we have studied in this section involve an uncertainty that is *static*. Furthermore, the robust performance problem in this subsection considers both the uncertainties of the plant and the closed-loop performance, and thus leads equivalently to a

structured uncertainty (see Theorem 3.3). The results of the above examples are in fact quite natural since, for static and/or structured uncertainties, it is well known (see, e.g., [26]) that LPTV controllers could often outperform LTI controllers.

3.5.4 Remark on extension to sequential design procedure

It is obvious that the powerful properties of noncausal LPTV scaling reviewed in Subsection 3.2.2 and discussed in Section 3.3, which played an important role in the robust stabilization controller synthesis in Subsection 3.5.2, are inherited also to the case of robust performance controller synthesis. These properties can be exploited further, for example, when we sequentially increase the period of the LPTV controller by an integer multiple (i.e., $\nu \times N$ for some $\nu \geq 2$). Indeed, we can make the H_∞ performance monotonically improved (or non-degraded, more precisely speaking) by an appropriate choice of the initial separator for the νN-periodic controller design, in spite of the use of an iterative design procedure without guaranteed global optimality.

This can be seen from the following two facts: (i) if there exists $\widehat{\Theta}$ ensuring a certain level of robust performance under the N-periodic controller Ψ, then by the property (i) stated in Subsection 3.2.2, it follows that the separator $(I_\nu \otimes \widehat{\Theta}_{ij})_{i,j=1,2}$ under the lifting period νN ensures the same level of robust performance for the same controller viewed as a νN-periodic controller (denoted by Ψ_ν); (ii) under a fixed separator, Theorem 3.2 gives a *necessary and sufficient* condition for the existence of a controller satisfying the required conditions, and hence a controller achieving at least the same level of robust performance as the above Ψ_ν can surely be designed on the basis of Theorem 3.2 by taking the separator $(I_\nu \otimes \widehat{\Theta}_{ij})_{i,j=1,2}$.

3.6 Demonstrating effectiveness of noncausal LPTV scaling through experiments

In the preceding section, we demonstrated by a simple numerical example the effectiveness of the robust performance controller synthesis method based on static noncausal LPTV scaling developed in Section 3.4. In this section, we further demonstrate the effectiveness by control experiments with a cart inverted pendulum.

3.6.1 Model of cart inverted pendulum

We show in Figure 3.8 a schematic picture of the cart inverted pendulum used for demonstrating the effectiveness of our robust performance controller synthesis approach. In this picture, the cart can move along a horizontal line driven with a DC motor, and r denotes

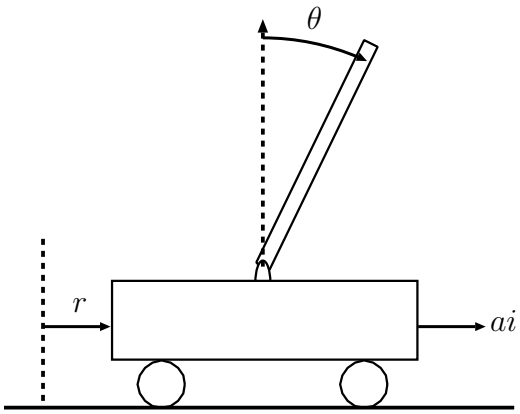

Figure 3.8: Schematic picture of cart inverted pendulum.

the distance of the cart from its initial position. The pendulum attached on the cart can rotate within the upper-half vertical plane including the horizontal line along which the cart can move, and θ denotes the angle of the pendulum from the vertically inverted attitude. The current i of the DC motor is controlled by an inner-loop PI controller. For simplicity, we assume that the current i immediately follows the reference input of the PI controller, and identify the latter outer-loop control input with the current i.

When we take the state vector $x_{\rm c} = [r, \theta, \dot{r}, \dot{\theta}]$ and the control input $u_{\rm c} = i$, the state equation of the cart inverted pendulum can be described as

$$
\begin{aligned}
&\dot{x}_{\rm c} = A_{\rm c} x_{\rm c} + B_{\rm c} u_{\rm c}, \\
&A_{\rm c} = \begin{bmatrix} 0 & 0 & 1 & 0 \\ 0 & 0 & 0 & 1 \\ 0 & -\frac{m^2 l^2 g}{X} & -\frac{f_{\rm c}}{X}(J_p + ml^2) & \frac{cml}{X} \\ 0 & \frac{mgl}{X}(M_{\rm c} + m + \frac{J_{\rm c}}{r_{\rm c}^2}) & \frac{f_{\rm c} ml}{X} & -\frac{c}{X}(M_{\rm c} + m + \frac{J_{\rm c}}{r_{\rm c}^2}) \end{bmatrix}, \\
&B_{\rm c} = \begin{bmatrix} 0 \\ 0 \\ \frac{a}{X}(J_p + ml^2) \\ -\frac{mla}{X} \end{bmatrix},
\end{aligned}
\tag{3.24}
$$

where $X = kM_{\rm c}J_p + M_{\rm c}ml^2 + mJ_p + J_{\rm c}J_p/r_{\rm c}^2 + J_{\rm c}ml^2/r_{\rm c}^2$ (see Table 3.3 for the meaning of each parameter, and its actual value for the case $l = 0.2\,{\rm m}$).

Remark 3.5 In the actual situation, the kinetic friction force $F_{\rm c}\,{\rm sgn}(\dot{r})$ would arise to the cart against the direction of its movement. To cancel this force in the experiments, we add $F_{\rm c}\,{\rm sgn}(\dot{r})/a$ to the control input generated by the controller.

We suppose that the pendulum length includes uncertainty, and is represented by $2(1+\delta)l$ with an uncertain parameter δ. Then, the parameters depending on the pendulum length

Table 3.3: Parameters of the cart inverted pendulum under pendulum length $2l = 0.4\,\mathrm{m}$

Physical quantity	Notation and value
Length from the pivot to the center of the pendulum	$l = 0.200$ m
Mass of the pendulum	$m = 5.36 \times 10^{-2}$ kg
Mass of the cart	$M_\mathrm{c} = 0.686$ kg
Radius of the wheels	$r_\mathrm{c} = 2.49 \times 10^{-2}$ m
Gain from the current of the DC motor to the force to the cart	$a = 1.92$ N/A
Moment of inertia of the wheels and the armature of the motor	$J_\mathrm{c} = 1.34 \times 10^{-4}$ kg $\cdot$ m^2
Moment of inertia of the pendulum around the center	$J_p = 7.15 \times 10^{-4}$ kg $\cdot$ m^2
Equivalent viscous friction coefficient in the direction of the cart movement	$f_\mathrm{c} = 0.360$ kg/s
Viscous friction coefficient of the shaft between the cart and the pendulum	$c = 1.50 \times 10^{-3}$ kg $\cdot$ m^2/s
Acceleration of gravity	$g = 9.807$ m/s^2

in (3.24) (i.e., l, m and J_p) are supposed to be replaced by the associated representations including δ. Under this treatment, we extract the uncertain part from (3.24), and construct a model represented by the linear fractional transformation consisting of the following continuous-time generalized plant P_c and Δ_c.

$$P_\mathrm{c} \;:\; \begin{cases} \dot{x}_\mathrm{c} &= A_\mathrm{c}x_\mathrm{c} + B_{\mathrm{c}1}w_\mathrm{c} + B_{\mathrm{c}2}u_\mathrm{c} \\ z_\mathrm{c} &= C_{\mathrm{c}1}x_\mathrm{c} + D_{\mathrm{c}11}w_\mathrm{c} + D_{\mathrm{c}12}u_\mathrm{c} \\ y_\mathrm{c} &= C_{\mathrm{c}2}x_\mathrm{c} \end{cases} \tag{3.25}$$

$$\Delta_\mathrm{c} \;:\; w_\mathrm{c} = \delta I_5 z_\mathrm{c} \tag{3.26}$$

Since noncausal LPTV scaling is to be applied for discrete-time systems, we discretize (3.25) and (3.26). For simplicity, we apply the zero-order hold discretization with sampling period 0.01 s, which is determined by the hardware.

Our cart inverted pendulum actually has three choices 0.3 m, 0.4 m and 0.5 m for the pendulum length. In this chapter, we regard the variation in the pendulum length as the uncertainty, and consider designing a single controller independent of the pendulum length. We take 0.4 m as the nominal value of the pendulum length $2l$, and consider the (discrete-time) uncertainty set

$$\boldsymbol{\Delta}_\mathrm{u} := \left\{ \Delta_\mathrm{u} \mid \Delta_\mathrm{u} = \delta I_5,\ |\delta| < \bar{\delta} \right\} \tag{3.27}$$

for a given $\bar{\delta}$ satisfying $\bar{\delta} > 0.25$. Since the uncertain representation $2(1+\delta)l$ of the pendulum

length covers all the three choices for the pendulum length under this set, it suffices for us to design a controller that robustly stabilizes the closed-loop system for the above $\boldsymbol{\Delta}_{\mathrm{u}}$ (assuming that the effect of discretizing Δ_{c} into Δ_{u} can be ignored).

3.6.2 Generalized plant and controller synthesis

This section demonstrates the effectiveness of robust controller synthesis based on non-causal LPTV scaling through experiments with the cart inverted pendulum. As a step toward such discussions, this subsection first introduces a generalized plant suitable for our controller synthesis, based on the model given in the preceding subsection.

Let us consider the generalized plant shown in Figure 3.9 for robust performance controller synthesis. The system P_{stab} in the figure denotes the discrete-time counterpart of the continuous-time generalized plant P_{c} given in the preceding subsection. We suppose that a disturbance contaminates the control input u. We denote the disturbance by w_{d} in Figure 3.9, which is scaled by the weight q_1 for adjusting its ratio to u. As the control output z_{d} for the generalized plant, we take the sum of the control input contaminated by the disturbance and the state x of P_{stab} evaluated through the weight q_2^{T}. Taking such w_{d} and z_{d} for robust H_∞ performance is expected to lead to controllers adequately suppressing the control input and state responses. We next discuss how to adjust the weights q_1 and q_2^{T} to have satisfactory performance.

Regarding q_1, we take $q_1 = 0.01$ since the disturbance w_{d} seems relatively small compared with the input u.

Regarding q_2^{T}, we consider taking its first entry large enough to suppress the response of the cart position r. However, only taking account of the response of r often causes unacceptable oscillations in the response of θ, which seems to be sensitively induced by the movement of the cart. To avoid this problem, we also take the third entry of q_2^{T} large enough to suppress the response of the velocity $\dot{r}$. The second and fourth entries of q_2^{T} are also adjusted simultaneously to suppress the responses of the angle θ and the angular velocity

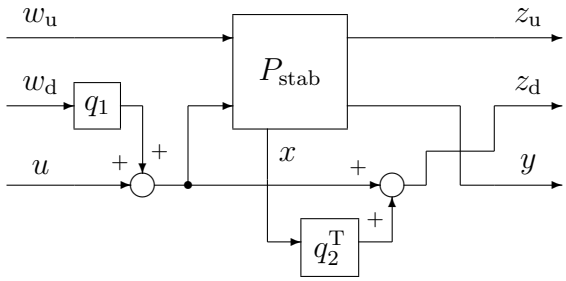

Figure 3.9: Generalized plant for suppressing control input and state responses.

$\dot{\theta}$ directly. Following these ideas, we tuned the value of q_2^{T} in a trial-and-error fashion; for fixed q_2^{T}, we designed robust performance controllers with $N = 1, 2$ and 4, all with the initial value of the separator given by $W_{\mathrm{sq}} = I$ and $X_{\mathrm{G}} = 0$, and compared the design results through simulations. After a trial-and-error process for tuning q_2^{T}, we found an adequate weight $q_2^{\mathrm{T}} = [1.3, 0.5, 1.0, 0.5]$ for our design. Under this q_2^{T}, the control input is kept, for most of the times, within the range of the current that the motor can accept without causing saturation (approximately between $-1.4\,\mathrm{A}$ and $1.4\,\mathrm{A}$), and the oscillations of r and θ are adequately suppressed for all of $N = 1, 2$ and 4.

Having introduced a generalized plant independent of the lifting period N suitable for our design as described above, we take only the results for $N = 1$ (discarding those for $N = 2$ and 4) and initiate our design of robust performance controllers based on noncausal LPTV scaling with the lifting period $N = 2$ and 4 as discussed in Subsection 3.5.4. Then, we obtained the minimum values of γ_{d} as shown in Table 3.4. We can see that the results monotonically improve (at least do not degrade) as N is increased, as is theoretically guaranteed. The minimum values of γ_{d} obtained at the synthesis stage could be conservative, in general, because of the use of an iterative method. Hence, Table 3.4 also shows $\gamma_{\mathrm{d,anal}}$, which is the minimum value of γ_{d} for which robust stability of the closed-loop system with the designed controller is ensured; this is obtained by the analysis based on noncausal LPTV scaling with $N = 4$ (regardless of N used in the controller synthesis).

Table 3.4: Design results by noncausal LPTV scaling

N	1	2	4	4*
γ_{d}	1.373	0.451	0.451	0.451
$\gamma_{\mathrm{d,anal}}$	0.122	0.041	0.046	0.055

3.6.3 Robust performance control experiments

With the controllers of $N = 1, 2$ and 4 designed in the preceding subsection, we performed control experiments, and confirmed that all the controllers successfully kept the pendulum in an inverted position when its length is 0.4 m. The obtained time responses of r and θ under the LTI controller (i.e., $N = 1$) are shown in Figure 3.10 with dashed lines. As shown in this figure, r and θ continued to oscillate in the experiment, even after a sufficiently long time. To evaluate these oscillations quantitatively, we show in Table 3.5(a) the standard deviations of r and θ calculated from the data of their time responses from 10 to 60 s.

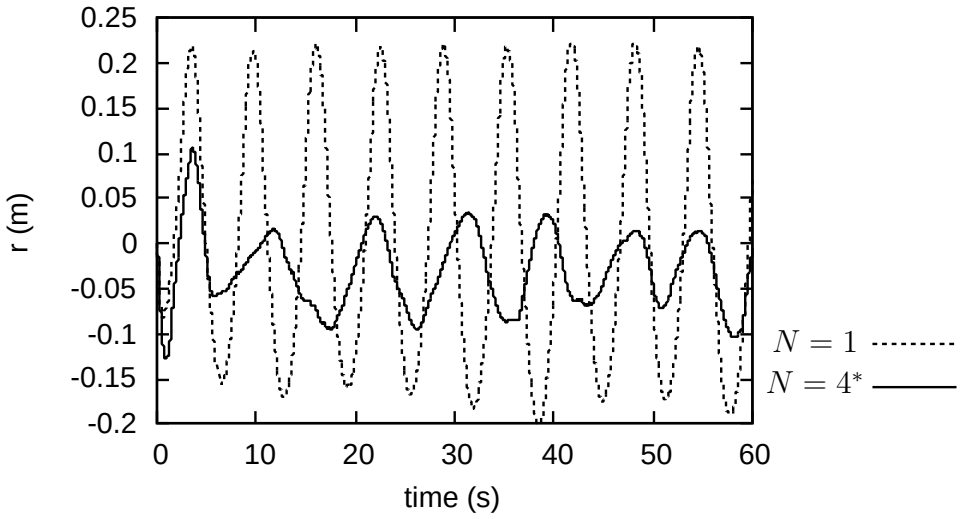

(a) Time responses of r

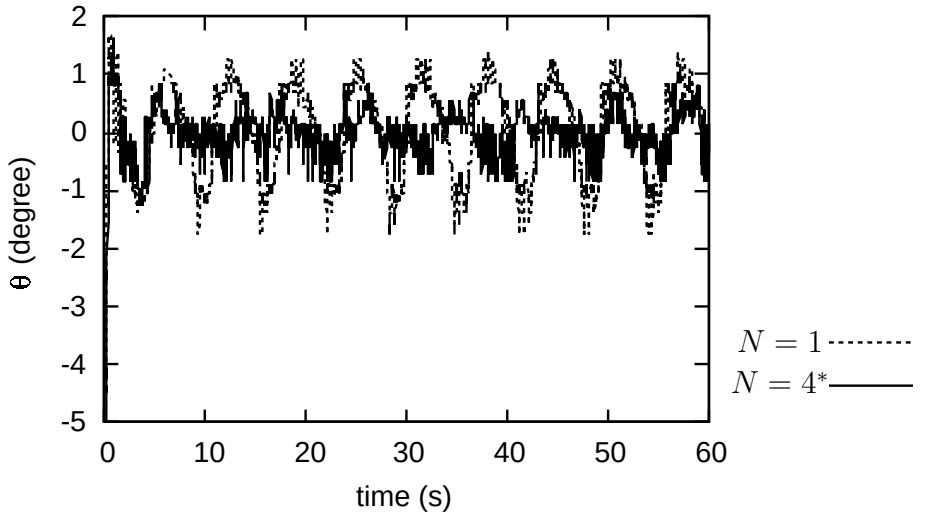

(b) Time responses of θ

Figure 3.10: Experiment results of r and θ.

By the advantage of noncausal LPTV scaling, it is expected that the control performance monotonically improves by increasing N. However, Table 3.5(a) shows a sort of mismatch against this expectation in the comparison between the cases of $N = 2$ and 4 (the result of $N = 2$ looks better than that of $N = 4$). To find the cause of this outcome, we examined the responses of the feedback systems in experiments, and found that the control input u in the case of $N = 4$ seriously exceeded the acceptable range of the current (see Figure 3.11(a)). Since the values of r and θ obtained at each sampling instant inevitably include noises, the cause could be attributed to some of the gains in the designed controller whose absolute

values are relatively large; the input u would become quite sensitive to the noises in the sampled values associated with such gains, and could easily exceed the acceptable range. In fact, the absolute values of some entries in the direct feedthrough matrix $D_{\widehat{\Psi}}$ were quite large in the case of $N = 4$, compared with the cases of $N = 1$ and 2. We presumed that this is the essential reason why the performance deteriorated in $N = 4$, and considered restricting the direct feedthrough matrix $D_{\widehat{\Psi}}$ for the case of $N = 4$ so that the absolute values of its entries do not exceed 1000. We refer to the controller obtained through such a restriction, which can be handled directly by dealing with an associated constraint on R in the LMI condition, as the controller with $N = 4^*$. The response of u under this controller shown in Figure 3.11(b) successfully lies within the acceptable range of the current. Furthermore, the corresponding responses of r and θ, shown in Figure 3.10 with solid lines, are successfully suppressed in terms of the amplitudes, compared with the cases of $N = 1$ and $N = 2$; see their standard deviations shown in Table 3.5(a).

To demonstrate robustness of the feedback systems, we further performed control experiments changing the pendulum length into 0.3 m and 0.5 m. Then, we confirmed that all the four controllers designed so far successfully kept the pendulum in an inverted position even for these different pendulums. Tables 3.5(b) and 3.5(c) show the standard deviations of r and θ in the experiments for the pendulum length 0.3 m and 0.5 m, respectively. From Table 3.5, we could say that the controller $N = 4^*$ has achieved the highest performance among the four controllers, and that it has achieved almost the same performance, regardless of the pendulum length.

Table 3.5: Experiment results: Standard deviations of r and θ

(a) Pendulum length 0.4 m

N	1	2	4	4^*
r	13.571 cm	4.486 cm	5.310 cm	3.958 cm
θ	0.784°	0.603°	0.729°	0.343°

(b) Pendulum length 0.3 m

N	1	2	4	4^*
r	15.433 cm	3.857 cm	7.234 cm	4.115 cm
θ	1.138°	0.753°	0.818°	0.454°

(c) Pendulum length 0.5 m

N	1	2	4	4^*
r	17.721 cm	4.678 cm	6.793 cm	3.936 cm
θ	1.132°	0.580°	0.747°	0.532°

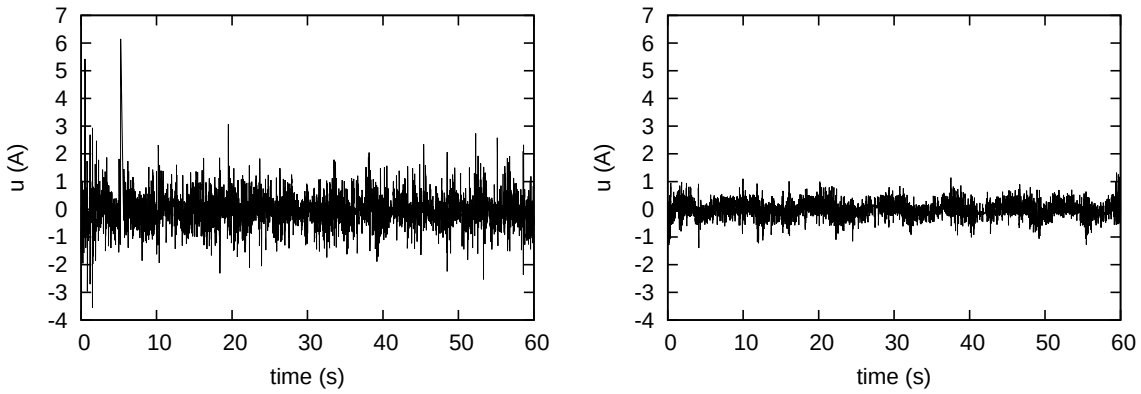

(a) Time response of u ($N = 4$)

(b) Time response of u ($N = 4^*$)

Figure 3.11: Experiment results of u.

3.7 Concluding remarks

In this chapter, we first reviewed the properties of static noncausal LPTV scaling in robust stability analysis. The properties are indeed effective also for robust stabilization controller synthesis. However, it was observed in this chapter that the synthesis taking account of only robust stabilization may suffer from some drawback; the designed controllers may produce oscillations in the closed-loop system responses because of their own periodicity. To alleviate such oscillations and have satisfactory performance, this chapter also discussed robust performance controller synthesis based on static noncausal LPTV scaling. More precisely, we showed that an adjusted use of the robust stabilization controller synthesis method can deal with robust performance controller synthesis. Then, we demonstrated with a numerical example that, through such a robust performance controller synthesis method, a practical design of LPTV controllers can be achieved for such uncertainties for which μ-synthesis with LTI controllers fails to achieve even robust stabilization. We further demonstrated the effectiveness of the developed synthesis method by control experiments with a cart inverted pendulum.

Chapter 4

Properties of Noncausal LPTV Scaling and Their Relationship with Lifting Timing

4.1 Introduction

In this chapter, we discuss properties of discrete-time noncausal LPTV scaling. The lifting technique enables us to treat discrete-time LPTV systems as if they were LTI. Hence, given an LPTV system (or an LTI system as a special case), we can analyze its robust stability by applying the separator-type robust stability theorem (see Theorem 2.2) to the lifted LTI system. Noncausal LPTV scaling is an idea that can be introduced quite naturally in such an analysis by allowing some noncausal operations of signals through the lifting-based treatment. Noncausality thus introduced in the scaling approach has been demonstrated to be effective for reducing the conservativeness in the robustness analysis of LTI and LPTV systems both theoretically and numerically, as reviewed in Chapter 2. In particular, as far as LTI systems are concerned, it has been proved that even if we confine ourselves to *static* noncausal LPTV scaling, it induces some dynamic causal LTI scaling when it is interpreted in the lifting-free (i.e., conventional) treatment. This property endows (even static) noncausal LPTV scaling with a promising ability in achieving less conservative analysis, in spite of its simple treatment. Such a feature of noncausal LPTV scaling can be exploited also in the development of robust controller synthesis methods, and their effectiveness has been demonstrated by numerical examples and also control experiments, as discussed in the preceding chapter.

Despite the promising properties on the practical side of noncausal LPTV scaling described above as a new approach to robust control, however, its comprehensive properties have not necessarily been revealed entirely. The missing arguments include, e.g., the char-

acterization of the class of dynamic causal LTI scaling in the lifting-free treatment that can equivalently be dealt with by working instead on *static* noncausal LPTV scaling in the lifting-based treatment; or what theoretical differences there are between noncausal LPTV scaling and the conventional causal LTI scaling. These issues must be resolved for further clarifying the advantages (or drawbacks) of noncausal LPTV scaling compared with the conventional method and thus establishing a further solid theoretical basis for noncausal LPTV scaling. This chapter aims at making a step forward to such issues by clarifying further properties of noncausal LPTV scaling. In particular, as a key idea, we introduce the notion of the timing of lifting into the framework of noncausal LPTV scaling. The effect of shifting the lifting timing can be studied easily by using what we call the timing-shift matrix, and thus this matrix plays an important role throughout the chapter. More precisely, this chapter introduces through this matrix the notion called shift invariance (with respect to lifting timing) of the separator in the robust stability theorem, as well as that notion of a class of separators. It is then shown that this notion plays a crucial role in revealing the properties of noncausal LPTV scaling through its theoretical comparisons with *causal* LPTV scaling and causal LTI scaling.

This chapter is organized as follows. Section 4.2 confines itself to the robust stability analysis of LTI systems, and revisits and slightly extends the existing results about the relationship between causal/noncausal LPTV scaling and the conventional causal LTI scaling. Section 4.3 introduces the timing shift about lifting and the timing-shift matrix, as well as the shift invariance notion of a separator and a class of separators, and then discusses the implication of the presence (or lack) of shift invariance on the properties of noncausal LPTV scaling. Section 4.4 introduces shift-invariant reconstruction of a given class of noncausal LPTV separators that is not necessarily shift-invariant, and shows an important equivalence relationship between the two approaches: one is noncausal LPTV scaling with the reconstructed class of separators, while the other is the dynamic causal LTI scaling (in the lifting-free framework) with the associated separator class induced by the given class of noncausal LPTV separators. The implication of such a relationship is further discussed, and important observations are given on the properties of noncausal LPTV scaling.

In the following arguments, if the separator $\widehat{\Theta}(z)$ satisfies (2.13) and (2.14) in lifting-based Theorem 2.2, then we say that it is eligible with respect to (2.13) and (2.14) (or simply in the lifting-based framework). Similarly, if $\Theta(\zeta)$ satisfies (2.15) and (2.16) in lifting-free Theorem 2.3, then we say that it is eligible with respect to (2.15) and (2.16) (or in the lifting-free framework). In addition, if there exists an eligible $\Theta(\zeta) \in \boldsymbol{\Theta}(\zeta)$ (or $\widehat{\Theta}(z) \in \widehat{\boldsymbol{\Theta}}(z)$), then we say that the separator class $\boldsymbol{\Theta}(\zeta)$ (or $\widehat{\boldsymbol{\Theta}}(z)$) is eligible.

4.2 Revisit to noncausal LPTV scaling applied to LTI systems

This chapter discusses the properties of noncausal LPTV scaling that follows naturally from Theorem 2.2 as a method for robust stability analysis, where we place particular emphasis on (but do not limit our attention exclusively to) the case when Σ is LTI. In that case, we have two alternatives for robust stability analysis: lifting-based framework (i.e., noncausal LPTV scaling) and lifting-free framework (i.e., the conventional causal LTI scaling). Whichever framework one may take, however, it is generally difficult to search for eligible separators, and thus one often introduces some tractable class of separators within which the search of eligible separators is to be carried out. It should be remarked that, under such a restrictive search, inequalities (2.13) and (2.14) as well as (2.15) and (2.16) in these theorems become a conservative sufficient condition for robust stability. With this in mind, this chapter aims at studying the properties of noncausal LPTV scaling that are expected to be useful in clarifying its ability in reducing the aforementioned conservativeness in the analysis, particularly in comparison with the conventional causal LTI scaling.

To facilitate the arguments that motivate the study in the remainder of this chapter, this section first introduces some important results suggesting possible advantages of noncausal LPTV scaling over causal LTI scaling, assuming that both the nominal system G and the uncertainty Δ in the closed-loop system Σ (Figure 2.3) are stable and LTI. Some of these results have in fact been reported in existing studies (with or without proof), but such remarks will be deferred to the end of this section to avoid distracting the attention of the reader. Instead, we opt to suggest immediately after these results some open problems that are not covered by these results. These problems will motivate further discussions about the properties of noncausal LPTV scaling studied in the remainder of this chapter.

The first result is as follows.

Theorem 4.1 Suppose that G is LTI, and $\boldsymbol{\Delta}$ satisfies Assumption 2. If there exists an eligible causal LTI separator $\Theta(\zeta)$ in the lifting-free framework, there exists an eligible causal LPTV separator $\widehat{\Theta}(z)$ in the lifting-based framework. In particular, if a causal LTI separator given by

$$\Theta(\zeta) = (\Theta_{ij}(\zeta))_{i,j=1,2} = (V_i(\zeta)\Lambda V_j(\zeta))_{i,j=1,2} \tag{4.1}$$

in the lifting-free framework is eligible, the separator

$$\widehat{\Theta}(z) = \left(\frac{1}{N}\widehat{V}_i(z)^*\widehat{\Lambda}\widehat{V}_j(z)\right)_{i,j=1,2} \tag{4.2}$$

is eligible in the lifting-based framework.

Proof. Let $\phi := \exp(2\pi \mathrm{i}/N)$, where i denotes the imaginary unit. Let us define the matrix

$$U_p(\zeta) := \frac{1}{\sqrt{N}} \begin{bmatrix} T_p(\zeta) & T_p(\phi\zeta) & \cdots & T_p(\phi^{N-1}\zeta) \end{bmatrix}, \tag{4.3}$$

where $T_p(\zeta)$ is given by (2.30). It follows that $U_p(\zeta)$ is a unitary matrix for $\zeta \in \partial\mathbf{D}$. Since

$$\widehat{G}(\zeta^N) T_p(\zeta) = T_p(\zeta) G(\zeta) \tag{4.4}$$

holds [40],[5], we immediately see that

$$\widehat{G}(\zeta^N) U_p(\zeta) = U_p(\zeta) \underline{G(\zeta)}, \tag{4.5}$$

where given a ζ-dependent matrix $M(\zeta)$, we use the shorthand notation

$$\underline{M(\zeta)} = \mathrm{diag}[M(\zeta), M(\phi\zeta), \cdots, M(\phi^{N-1}\zeta)]. \tag{4.6}$$

We now proceed to the proof. Let us take an eligible causal LTI separator given by (4.1), where V_1 and V_2 are LTI systems with p inputs. Since it satisfies (2.15) and (2.16) and since $\phi \in \partial\mathbf{D}$, it also satisfies these two inequalities with ζ replaced by $\phi^i\zeta$ $(i = 1, \ldots, N-1)$. In other words, we have

$$\underline{\begin{bmatrix} I \\ G(\zeta) \end{bmatrix}^* \Theta(\zeta) \begin{bmatrix} I \\ G(\zeta) \end{bmatrix} \le 0} \quad (\forall \zeta \in \partial\mathbf{D}), \tag{4.7}$$

$$\underline{\begin{bmatrix} \Delta(\zeta) \\ I \end{bmatrix}^* \Theta(\zeta) \begin{bmatrix} \Delta(\zeta) \\ I \end{bmatrix} > 0} \quad \left(\begin{array}{l} \forall \Delta \in \boldsymbol{\Delta}, \\ \forall \zeta \in \partial\mathbf{D} \end{array} \right). \tag{4.8}$$

Through appropriate permutations of rows and columns, (4.7) and (4.8) are equivalently transformed into

$$\begin{bmatrix} \underline{I} \\ \underline{G(\zeta)} \end{bmatrix}^* \left(\underline{\Theta_{ij}(\zeta)} \right)_{i,j=1,2} \begin{bmatrix} \underline{I} \\ \underline{G(\zeta)} \end{bmatrix} \le 0 \quad (\forall \zeta \in \partial\mathbf{D}), \tag{4.9}$$

$$\begin{bmatrix} \underline{\Delta(\zeta)} \\ \underline{I} \end{bmatrix}^* \left(\underline{\Theta_{ij}(\zeta)} \right)_{i,j=1,2} \begin{bmatrix} \underline{\Delta(\zeta)} \\ \underline{I} \end{bmatrix} > 0 \quad \left(\begin{array}{l} \forall \Delta \in \boldsymbol{\Delta}, \\ \forall \zeta \in \partial\mathbf{D} \end{array} \right). \tag{4.10}$$

Let us define

$$\mathcal{U}(\zeta) = \mathrm{diag}[U_p(\zeta), U_p(\zeta)]. \tag{4.11}$$

Then, by applying the congruence transformation with $U_p(\zeta)^*$ on (4.9) and (4.10), and by noting the relation (4.5), we have

$$\begin{bmatrix} I \\ \widehat{G}(\zeta^N) \end{bmatrix}^* \mathcal{U}(\zeta) \underline{\Theta}(\zeta) \mathcal{U}(\zeta)^* \begin{bmatrix} I \\ \widehat{G}(\zeta^N) \end{bmatrix} \le 0 \quad (\forall \zeta \in \partial\mathbf{D}), \tag{4.12}$$

$$\begin{bmatrix} \widehat{\Delta}(\zeta^N) \\ I \end{bmatrix}^* \mathcal{U}(\zeta) \underline{\Theta}(\zeta) \mathcal{U}(\zeta)^* \begin{bmatrix} \widehat{\Delta}(\zeta^N) \\ I \end{bmatrix} > 0 \quad \left(\begin{array}{l} \forall \Delta \in \boldsymbol{\Delta}, \\ \forall \zeta \in \partial\mathbf{D} \end{array} \right). \tag{4.13}$$

Regarding the separator in (4.12) and (4.13), we have the following again from (4.5).

$$\begin{aligned} U_p(\zeta)\underline{\Theta_{ij}(\zeta)}U_p(\zeta)^* =& U_p(\zeta)\underline{V_i(\zeta)}^*\underline{\Lambda}\underline{V_j(\zeta)}U_p(\zeta)^* \\ =& \widehat{V}_i(\zeta^N)^* U_p(\zeta)\underline{\Lambda} U_p(\zeta)^*\widehat{V}_j(\zeta^N) \\ =& \widehat{V}_i(\zeta^N)^*\widehat{\Lambda}U_p(\zeta)U_p(\zeta)^*\widehat{V}_j(\zeta^N) \\ =& \widehat{V}_i(\zeta^N)^*\widehat{\Lambda}\widehat{V}_j(\zeta^N) \quad (\forall \zeta \in \partial\mathbf{D}). \end{aligned} \tag{4.14}$$

This implies that the separator (4.2) is eligible in the lifting-based framework. Q.E.D.

An important implication of the above theorem is that if we apply causal/noncausal LPTV scaling to LTI systems, we can perform at least as good robust stability analysis as causal LTI scaling. The separator in the lifting-based framework given in this theorem, i.e., (4.2), satisfies the requirement in Definition 2.2 in a particular way, that is, with LTI systems V_1 and V_2, and with the constraint $\Lambda_i = \Lambda_j$ $(i, j = 1, \ldots, N)$. Hence, we refer to the separator of the form (4.2) constructed from the causal LTI separator (4.1) (in the lifting-free framework) as an *equivalent* causal LTI separator *in the lifting-based framework*. We denote such an embedding mapping from (4.1) to (4.2) by $\widehat{\Theta}(z) = \widehat{\mathrm{E}}[\Theta(\zeta)]$. Similarly, we call the treatment with such separators causal LTI scaling *in the lifting-based framework*. The validity of introducing such terms can be verified in a strong sense since not only Theorem 4.1 but also a sort of its converse holds as follows.

Theorem 4.2 Suppose that G is LTI, $\boldsymbol{\Delta}$ satisfies Assumption 2, and a causal LTI separator $\Theta(\zeta)$ described by (4.1) is given. If the embedded separator $\widehat{\Theta}(z) = \widehat{\mathrm{E}}[\Theta(\zeta)]$ equivalent to $\Theta(\zeta)$ is eligible in the lifting-based framework, $\Theta(\zeta)$ is eligible in the lifting-free framework.

Proof. Suppose that $\widehat{\Theta}(z) = \widehat{\mathrm{E}}[\Theta(\zeta)]$ given by (4.2) satisfies (2.13) and (2.14). Then, by post-multiplying (resp. pre-multiplying) these inequalities with $T_p(\zeta)$ (resp. its complex conjugate transpose) and by noting (4.4), we have

$$\begin{bmatrix} I \\ G(\zeta) \end{bmatrix}^* \Theta_{T_p}(\zeta) \begin{bmatrix} I \\ G(\zeta) \end{bmatrix} \le 0 \quad (\forall \zeta \in \partial\mathbf{D}), \tag{4.15}$$

$$\begin{bmatrix} \Delta(\zeta) \\ I \end{bmatrix}^* \Theta_{T_p}(\zeta) \begin{bmatrix} \Delta(\zeta) \\ I \end{bmatrix} > 0 \quad \left(\begin{array}{c} \forall \Delta \in \boldsymbol{\Delta}, \\ \forall \zeta \in \partial\mathbf{D} \end{array} \right), \tag{4.16}$$

where

$$\Theta_{T_p}(\zeta) = \left(\frac{1}{N} T_p(\zeta)^* \widehat{V}_i(\zeta^N)^* \widehat{\Lambda} \widehat{V}_j(\zeta^N) T_p(\zeta) \right)_{i,j=1,2}. \tag{4.17}$$

Regarding the above separator $\Theta_{T_p}(\zeta)$, we have

$$\frac{1}{N}V_i(\zeta)^* T_p(\zeta)^* \widehat{\Lambda} T_p(\zeta) V_j(\zeta) = V_i(\zeta)^* \Lambda V_j(\zeta) \quad (\forall \zeta \in \partial \mathbf{D}) \tag{4.18}$$

by (4.4), since $\widehat{V}_i$ $(i = 1, 2)$ are the lifted representations of the LTI systems V_i $(i = 1, 2)$, and $\widehat{\Lambda} = \mathrm{diag}[\Lambda, \cdots, \Lambda]$. That is, $\Theta_{T_p}(\zeta)$ is nothing but the causal LTI separator in the lifting-free framework underlying (4.2). This completes the proof. Q.E.D.

Remark 4.1 Even though this section is confined to the case of LTI Σ, we can similarly define causal LTI scaling for LPTV systems; such scaling refers to the approach in the lifting-based framework that uses only equivalent causal LTI separators constructed from causal LTI separators in the lifting-free framework. The properties of causal LTI scaling for LPTV systems will be discussed in Section 4.3.

The following is another important result closely related to the advantage of noncausal LPTV scaling over causal LTI scaling.

Theorem 4.3 Suppose that G is LTI, and $\boldsymbol{\Delta}$ satisfies Assumption 2. If a noncausal LPTV separator $\widehat{\Theta}(z)$ is eligible in the lifting-based framework, the causal LTI separator

$$\Theta(\zeta) = \mathcal{T}(\zeta)^* \widehat{\Theta}(\zeta^N) \mathcal{T}(\zeta) \tag{4.19}$$

is eligible in the lifting-free framework, where $\mathcal{T}(\zeta)$ is given by (2.30).

Proof. It can be confirmed by post-multiplying (resp. pre-multiplying) (2.13) and (2.14) with $\mathcal{T}(\zeta)$ (resp. its complex conjugate transpose) and by noting (4.4), under $z = \zeta^N$. Q.E.D.

This theorem implies that if we find an eligible separator $\widehat{\Theta}(z)$ in the lifting-based framework, it immediately means that we have also found an eligible separator $\Theta(\zeta)$ in the lifting-free framework. In particular, even if we were to confine ourselves to the search of *static* noncausal LPTV separators $\widehat{\Theta}$ (which is nothing but a constant matrix) in the lifting-based framework, it would induce some frequency-dependent scaling (i.e., dynamic causal LTI scaling) in the lifting-free framework (recall Theorem 2.5).

However, Theorems 4.1 and 4.3 alone are deficient in the theoretical depth for affirming the above prospect. In other words, the properties of noncausal LPTV scaling have not been

revealed completely, and there still remain important issues that should be investigated much further. For example, let us take a class $\widehat{\boldsymbol{\Theta}}_0^{\text{noncausal}}(z)$ of noncausal LPTV separators, and denote by

$$\boldsymbol{\Theta}(\zeta) := \left\{ \mathcal{T}(\zeta)^* \widehat{\Theta}(\zeta^N) \mathcal{T}(\zeta) \;\middle|\; \widehat{\Theta}(z) \in \widehat{\boldsymbol{\Theta}}_0^{\text{noncausal}}(z) \right\} \tag{4.20}$$

the class of separators $\Theta(\zeta)$ in the lifting-free framework given by (4.19) with $\widehat{\Theta}(z) \in \widehat{\boldsymbol{\Theta}}_0^{\text{noncausal}}(z)$. An important unresolved issue is whether the eligibility of the class $\boldsymbol{\Theta}(\zeta)$ always implies that of the original class $\widehat{\boldsymbol{\Theta}}_0^{\text{noncausal}}(z)$, or to put it another way, whether it is ensured that we can convert the problem of searching for an eligible $\Theta(\zeta) \in \boldsymbol{\Theta}(\zeta)$ equivalently into that of searching for an eligible noncausal LPTV separator $\widehat{\Theta}(z) \in \widehat{\boldsymbol{\Theta}}_0^{\text{noncausal}}(z)$. If this question has an affirmative answer, then the prospect mentioned above is also resolved affirmatively by taking $\widehat{\boldsymbol{\Theta}}_0^{\text{noncausal}}(z)$ to be the set of static separators.

This chapter aims at making a step forward to answering the question raised above by revealing further properties of noncausal LPTV scaling. To proceed in that direction, the idea of shifting the timing of lifting (timing-shift of lifting) plays a crucial role. Hence, we first study in the following section some fundamental properties of noncausal LPTV scaling with respect to the timing-shift of lifting, where we deal with N-periodic systems as well as LTI systems. We then proceed the arguments about the timing-shift in Section 4.4 for the special case when Σ is LTI. In particular, we discuss further relationship and difference between noncausal LPTV scaling and the conventional causal LTI scaling, and provide a partial answer to the question raised above.

Before closing this section, we give some remarks about the above theorems. Regarding Theorem 4.1, its special case confining only to *static* separators has been given in [23] in a less explicit form; see Theorem 2 and its proof therein. A similar but again less explicit assertion has been given about a general case in [22], in which the proof was omitted because of limited space. Hence, the proof of this theorem was given, which is indeed important in the following arguments because the ideas therein are closely related with the discussions of this chapter (in particular, Theorem 4.5 to be derived later). On the other hand, Theorem 4.2 is asserted for the first time in this chapter (except for the case of static separators, which is again asserted by Theorem 2 in [23] in an implicit way). Finally, Theorem 4.3 is nothing but Theorem 1 in [23], which, together with the other two theorems, strongly motivates the further studies in the remainder of this chapter.

4.3 Timing-shift in noncausal LPTV scaling

The preceding section confined itself to the case when Σ is LTI. This section returns to the treatment of N-periodic systems, introduces the idea of timing-shift about the lifting treatment in noncausal LPTV scaling, and discusses the properties of noncausal LPTV scaling in connection with timing-shift.

4.3.1 Timing-shift matrix and its properties

To begin with, the timing of lifting (or lifting timing for short) means the basic time instant that we take in the lifting-based treatment of signals and systems. For example, for a signal f_k related with an N-periodic system H, the lifted representation of f_k is usually given by $\widehat{f}_\kappa = [f_{\kappa N}^T, f_{\kappa N+1}^T, \cdots, f_{\kappa N+N-1}^T]^T$. However, when we consider the lifting timing denoted by l, then by definition, the lifted representation is given by $\widehat{f}_\kappa^{(l)} = [f_{\kappa N+l}^T, f_{\kappa N+1+l}^T, \cdots, f_{\kappa N+N-1+l}^T]^T$. Under the lifting timing l, we denote the resulting lifted system by $\widehat{H}^{(l)}$, and its associated transfer matrix by $\widehat{H}^{(l)}(z)$. Obviously, it is enough to consider the lifting timing l only in $\{0, 1, \ldots, N-1\}$, and if H is LTI, its lifted representation $\widehat{H}^{(l)}$ obtained by regarding H as N-periodic is independent of the lifting timing l. However, this is not the case if H is not LTI. Hence, we can easily see that lifting timing could be an important factor to study especially when the system Σ is LPTV. We will eventually see that it is equally important even when Σ is LTI.

Even though shifting the lifting timing is equivalent to shifting signals before applying the standard lifting with $l = 0$, its effect can easily be treated in the lifting-based framework (i.e., after lifting has been applied) by introducing the (backward) timing-shift matrix

$$S_p(z) := \begin{bmatrix} 0 & z^{-1}I_p \\ I_{(N-1)p} & 0 \end{bmatrix}. \tag{4.21}$$

Let us denote the z-transform of the lifted signal $\widehat{f}_\kappa^{(l)}$ by $\widehat{F}^{(l)}(z)$. Then, ignoring the influence of the "initial value f_l," we readily have $\widehat{F}^{(l)}(z) = S_p(z)\widehat{F}^{(l+1)}(z)$. This immediately leads to

$$\widehat{H}^{(l+1)}(z) = S_p(z)^{-1}\widehat{H}^{(l)}(z)S_p(z). \tag{4.22}$$

It is immediate from the definition that the timing-shift matrix $S_p(z)$ has the properties

$$S_p(z)S_p(z)^* = S_p(z)^*S_p(z) = I \quad (z \in \partial\mathbf{D}), \quad S_p(z)^N = z^{-1}I. \tag{4.23}$$

4.3.2 Effect of timing-shift in noncausal LPTV scaling

By applying the congruence transformation by the matrix $S_p(z)$ on the conditions in Theorem 2.2 and noting (4.22), we are led to the following theorem.

Theorem 4.4 Suppose that G is N-periodic, and $\boldsymbol{\Delta}$ satisfies Assumption 2. Let us define

$$\mathcal{S}(z) := \mathrm{diag}[S_p(z), S_p(z)]. \tag{4.24}$$

Then, $\widehat{\Theta}(z) = \widehat{\Theta}(z)^*$ $(\forall z \in \partial\mathbf{D})$ satisfies

$$\begin{bmatrix} I \\ \widehat{G}^{(0)}(z) \end{bmatrix}^* \widehat{\Theta}(z) \begin{bmatrix} I \\ \widehat{G}^{(0)}(z) \end{bmatrix} \leq 0 \quad (\forall z \in \partial\mathbf{D}), \tag{4.25}$$

$$\begin{bmatrix} \widehat{\Delta}^{(0)}(z) \\ I \end{bmatrix}^* \widehat{\Theta}(z) \begin{bmatrix} \widehat{\Delta}^{(0)}(z) \\ I \end{bmatrix} > 0 \quad \left(\begin{array}{l} \forall \Delta \in \boldsymbol{\Delta}, \\ \forall z \in \partial\mathbf{D} \end{array} \right) \tag{4.26}$$

under the standard lifting timing $l = 0$ if and only if it satisfies

$$\begin{bmatrix} I \\ \widehat{G}^{(l)}(z) \end{bmatrix}^* (\mathcal{S}(z)^l)^* \widehat{\Theta}(z) \mathcal{S}(z)^l \begin{bmatrix} I \\ \widehat{G}^{(l)}(z) \end{bmatrix} \leq 0 \quad (\forall z \in \partial\mathbf{D}), \tag{4.27}$$

$$\begin{bmatrix} \widehat{\Delta}^{(l)}(z) \\ I \end{bmatrix}^* (\mathcal{S}(z)^l)^* \widehat{\Theta}(z) \mathcal{S}(z)^l \begin{bmatrix} \widehat{\Delta}^{(l)}(z) \\ I \end{bmatrix} > 0 \quad \left(\begin{array}{l} \forall \Delta \in \boldsymbol{\Delta}, \\ \forall z \in \partial\mathbf{D} \end{array} \right) \tag{4.28}$$

under at least one lifting timing $l = 0, \ldots, N-1$, and also if and only if it satisfies (4.27) and (4.28) under all $l = 0, 1, \ldots, N-1$.

According to this theorem, if we take a set of some tractable (e.g., static) separators denoted by $\widehat{\boldsymbol{\Theta}}_0(z)$, the approach under the lifting timing $l = 0$ that searches for eligible separators $\widehat{\Theta}(z) \in \widehat{\boldsymbol{\Theta}}_0(z)$ is, if it is interpreted under another lifting timing l, equivalent to the approach of searching for eligible separators $(\mathcal{S}(z)^l)^* \widehat{\Theta}(z) \mathcal{S}(z)^l$ such that $\widehat{\Theta}(z) \in \widehat{\boldsymbol{\Theta}}_0(z)$. Hence, it is not obvious, in general, whether the approach of searching for eligible separators $\widehat{\Theta}(z) \in \widehat{\boldsymbol{\Theta}}_0(z)$ under $l = 0$ is equivalent to that under another l that searches for eligible separators $\widehat{\Theta}(z)$ within the same class $\widehat{\boldsymbol{\Theta}}_0(z)$. That is, even if we were to search for eligible separators within the common tractable class $\widehat{\boldsymbol{\Theta}}_0(z)$ regardless of l, the effects obtained by noncausal LPTV scaling might vary in general, depending on the underlying lifting timing l. If this is indeed the case, it would be related with the fact that an eligible separator $\widehat{\Theta}(z) \in \widehat{\boldsymbol{\Theta}}_0(z)$ under some lifting timing l may not satisfy

$$\widehat{\Theta}(z) = \mathcal{S}(z)^* \widehat{\Theta}(z) \mathcal{S}(z) \ (z \in \partial\mathbf{D}). \tag{4.29}$$

Hence, the remainder of this section is devoted to discussing the properties of causal LTI, causal LPTV and noncausal LPTV scaling approaches, all in connection with the condition (4.29). In particular, we suggest that noncausal LPTV scaling has different properties in this respect from the other two approaches.

In the rest of this chapter, we regard that separators are defined only on the unit circle $\partial\mathbf{D}$, and identify an operator with another if they take the same value for every z (or ζ) on the unit circle. For example, I and $z^* z I$ are regarded as the same separator.

(a) **Causal LTI scaling** We first consider causal LTI scaling (in the lifting-based framework, i.e., in the sense of Remark 4.1), assuming that Σ is N-periodic, in general. A causal LTI separator (4.2) in the lifting-based framework is described by $\widehat{V}_1$, $\widehat{V}_2$ and $\widehat{\Lambda}$, which are the lifted representations of the LTI systems V_1, V_2 and Λ, respectively (hence, $\widehat{V}_i = \widehat{V}_i^{(0)} = \widehat{V}_i^{(l)},\ l = 0, 1, \ldots, N-1$). This, together with (4.22), leads to

$$\begin{aligned}(S_p(z)^l)^* \widehat{\Theta}_{ij}(z) S_p(z)^l =& (1/N)(S_p(z)^l)^* \widehat{V}_i(z)^* \widehat{\Lambda} \widehat{V}_j(z) S_p(z)^l \\ =& (1/N) \widehat{V}_i(z)^* (S_p(z)^l)^* \widehat{\Lambda} S_p(z)^l \widehat{V}_j(z) \\ =& (1/N) \widehat{V}_i(z)^* \widehat{\Lambda} \widehat{V}_j(z) = \widehat{\Theta}_{ij}(z) \quad (i, j = 1, 2). \end{aligned} \tag{4.30}$$

This in particular implies that (4.29) holds, and it, together with Theorem 4.4, immediately leads to the fact that a causal LTI separator in the lifting-based framework is eligible under one lifting timing l if and only if it is under every timing.

If a separator $\widehat{\Theta}(z)$ satisfies (4.29), we say that it is shift-invariant (with respect to lifting timing). Similarly, we say that the separator class $\widehat{\boldsymbol{\Theta}}_0(z)$ is shift-invariant if

$$\widehat{\boldsymbol{\Theta}}_0(z) = \{\mathcal{S}(z)^* \widehat{\Theta}(z) \mathcal{S}(z) \mid \widehat{\Theta}(z) \in \widehat{\boldsymbol{\Theta}}_0(z)\}. \tag{4.31}$$

In particular, if every $\widehat{\Theta}(z) \in \widehat{\boldsymbol{\Theta}}_0(z)$ is shift-invariant, we say that the separator class $\widehat{\boldsymbol{\Theta}}_0(z)$ is strongly shift-invariant. Having introduced these terms, we readily see that any class consisting of causal LTI separators is strongly shift-invariant, and thus causal LTI scaling in the lifting-based framework leads to the same analysis results regardless of the lifting timing l.

(b) **Causal LPTV scaling** We next consider causal LPTV scaling. Then, it turns out that the eligibility of a causal LPTV separator given by Definition 2.2 depends generally on lifting timing. This is because the systems $\widehat{V}_1$, $\widehat{V}_2$ and $\widehat{\Lambda}$ in Definition 2.2 are the lifted representations of N-periodic systems for which (4.30) fails, in general. However, this only means that the eligibility of a given causal LPTV separator depends on lifting timing, and does not necessarily mean that the eligibility of a class of causal LPTV separators does. For example, let us take the class $\widehat{\boldsymbol{\Theta}}_{\mathrm{static}}^{\mathrm{causal}}$ of static LPTV separators, and consider the static causal LPTV scaling based on $\widehat{\boldsymbol{\Theta}}_{\mathrm{static}}^{\mathrm{causal}}$. By Definition 2.2, this class coincides with the set of matrices in the form of

$$\widehat{\Theta}_{\mathrm{static}} = \left(\mathrm{diag}[X_{ij}^1, X_{ij}^2, \cdots, X_{ij}^N]\right)_{i,j=1,2} \tag{4.32}$$

where X_{ij}^k $(i = 1, 2;\ j = 1, 2;\ k = 1, \ldots, N)$ are constant matrices of the same size. Hence

$$\mathcal{S}(z)^* \widehat{\Theta}_{\mathrm{static}} \mathcal{S}(z) = \left(\mathrm{diag}[X_{ij}^2, \cdots, X_{ij}^N, X_{ij}^1]\right)_{i,j=1,2} \in \widehat{\boldsymbol{\Theta}}_{\mathrm{static}}^{\mathrm{causal}}, \tag{4.33}$$

and thus $\widehat{\boldsymbol{\Theta}}^{\mathrm{causal}}_{\mathrm{static}}$ is a (non-strongly) shift-invariant class. This means that whether $\widehat{\boldsymbol{\Theta}}^{\mathrm{causal}}_{\mathrm{static}}$ is eligible does not depend on lifting timing. Even when we consider *dynamic* causal LPTV separators, a naturally constructed separator class would also become (non-strongly) shift-invariant unless the LPTV systems V_1 and V_2 and the constant matrix $\widehat{\Lambda}$ in the causal LPTV separator are restricted to some "distorted sets" that fail to be invariant under the one-step shift in the lifting-free time axis k; considering such distorted sets would never sound sensible, and thus would be unnatural. Hence, the eligibility of a natural class of causal LPTV separators is independent of lifting timing, and hence causal LPTV scaling also leads virtually to the same analysis results regardless of the lifting timing l.

(c) **Noncausal LPTV scaling** We have so far discussed the relationship of lifting timing to two types of causal scaling approaches. We have then observed that all natural classes of causal separators are shift-invariant, and thus their eligibility is virtually independent of the lifting timing l. However, noncausal LPTV scaling exhibits a different aspect, which could be attributed to the fact that taking a general LTI systems $\widehat{V}$ in noncausal LPTV separators (recall Definition 2.3) corresponds to ignoring causality to some limited extent, where causality is meant here with respect to the original lifting-free time axis k rather than the lifting-based time axis κ in (2.9). To confirm the different aspect, let us take, for example, the class $\widehat{\boldsymbol{\Theta}}^{\mathrm{noncausal}}_{\mathrm{static}}$ of static noncausal LPTV separators, and consider the static noncausal LPTV scaling based on $\widehat{\boldsymbol{\Theta}}^{\mathrm{noncausal}}_{\mathrm{static}}$. By Definition 2.3, this class coincides with the set of constant matrices. Hence, it follows that the z-dependent factors in $\mathcal{S}(z)^*\widehat{\Theta}_{\mathrm{static}}\mathcal{S}(z)$ do not vanish, in general, and thus it does not belong to $\widehat{\boldsymbol{\Theta}}^{\mathrm{noncausal}}_{\mathrm{static}}$. That is, the class $\widehat{\boldsymbol{\Theta}}^{\mathrm{noncausal}}_{\mathrm{static}}$ of static noncausal LPTV separators is not shift-invariant with respect to lifting timing. This fact is much different from that for static *causal* LPTV separators shown in (4.33).

4.3.3 Numerical confirmation of theoretical results

An outcome of the property of static noncausal LPTV scaling about the lack of shift invariance, stated in the preceding subsection, should also be easy to confirm numerically by observing the dependency of analysis results on the lifting timing l. In fact, however, an example in that direction can never be constructed if Σ is confined to be LTI. This is because the static noncausal LPTV separator $\widehat{\Theta}$ is eligible if and only if $\mathcal{S}(z)^*\widehat{\Theta}\mathcal{S}(z)$ is, since $\widehat{G}^{(1)} = \widehat{G}^{(0)}$ and $\widehat{\Delta}^{(1)} = \widehat{\Delta}^{(0)}$ in Theorem 4.4 when Σ is LTI; due to this coincidence, the lack of shift invariance in the class of static noncausal LPTV separator does not lead to difference in the analysis results with respect to the shift in the lifting timing. We thus consider an example with an LPTV system Σ.

Example: Consider the 3-periodic system G given by (2.26) in Subsection 2.4.4. In addition,

we assume that the corresponding scalar uncertainty $\Delta = \delta$ is static and LTI. The problem we study here is to find (a lower bound of) the maximal $\overline{\delta}$ such that the closed-loop system Σ is robustly stable with respect to the uncertainty set $\boldsymbol{\Delta} = \{\delta : |\delta| < \overline{\delta}\}$.

The analysis results of the maximal $\overline{\delta}$ obtained by static causal/noncausal LPTV scaling are shown in Table 4.1, where we confined ourselves to the class of (D, G)-scaling type separators [13] in both approaches (this treatment of separators was discussed in detail in Subsection 2.4.3 and Section 3.3). Such analysis can be carried out through the KYP lemma [34] (see Lemma 2.1) and LMI optimization, as reviewed in Subsection 2.4.3.

Table 4.1 shows that the analysis results of $\overline{\delta}$ obtained by noncausal LPTV scaling depend much on the lifting timing l. In contrast, we can confirm, also numerically, that the analysis results of $\overline{\delta}$ obtained by causal LPTV scaling are completely independent of l.

Table 4.1: Robust stability analysis considering lifting timing l

Timing l	Noncausal-(D, G)	Causal-(D, G)
0	0.5292	0.4567
1	0.6032	0.4567
2	0.6293	0.4567

4.4 Shift-invariant reconstruction of separator classes in noncausal LPTV scaling and its implication

This section introduces the idea of shift-invariant reconstruction of separator classes. With this idea, the properties of noncausal LPTV scaling applied to LTI systems are clarified further, particularly from the viewpoint of its possible ability in replacing the conventional frequency-dependent (i.e., dynamic causal LTI) scaling.

4.4.1 Shift-invariant reconstruction of separator classes

The preceding section discussed by introducing the (backward) timing-shift matrix the properties and effectiveness of noncausal LPTV scaling applied to LPTV systems. In particular, a central issue there was on the difference in the properties between noncausal LPTV scaling and causal LPTV or LTI scaling, and it was studied from the viewpoint of lifting timing and its shift. An important key in that study was whether the separator class taken in noncausal LPTV scaling is shift-invariant with respect to lifting timing. Motivated by this observation, suppose we are given a (not necessarily shift-invariant) class of noncausal

LPTV separators denoted by $\widehat{\boldsymbol{\Theta}}_0^{\text{noncausal}}(z)$, and let us construct the separator class

$$\widehat{\boldsymbol{\Theta}}(z) := \left\{ \frac{1}{N} \sum_{l=0}^{N-1} (\mathcal{S}(z)^l)^* \widehat{\Theta}(z) \mathcal{S}(z)^l \;\middle|\; \widehat{\Theta}(z) \in \widehat{\boldsymbol{\Theta}}_0^{\text{noncausal}}(z) \right\}. \tag{4.34}$$

Then, every separator in $\widehat{\boldsymbol{\Theta}}(z)$ is a noncausal LPTV separator by (4.21), and is shift-invariant by (4.23). Hence, $\widehat{\boldsymbol{\Theta}}(z)$ is strongly shift-invariant. Furthermore, it is easy to see that $\widehat{\boldsymbol{\Theta}}(z) = \widehat{\boldsymbol{\Theta}}_0^{\text{noncausal}}(z)$ if and only if $\widehat{\boldsymbol{\Theta}}_0^{\text{noncausal}}(z)$ is strongly shift-invariant. Hence, $\widehat{\boldsymbol{\Theta}}(z) \neq \widehat{\boldsymbol{\Theta}}_0^{\text{noncausal}}(z)$ whenever $\widehat{\boldsymbol{\Theta}}_0^{\text{noncausal}}(z)$ is not shift-invariant. We thus call the separator class $\widehat{\boldsymbol{\Theta}}(z)$ the (strongly) shift-invariant reconstruction of the separator class $\widehat{\boldsymbol{\Theta}}_0^{\text{noncausal}}(z)$. Similarly, we call

$$\frac{1}{N} \sum_{l=0}^{N-1} (\mathcal{S}(z)^l)^* \widehat{\Theta}(z) \mathcal{S}(z)^l \tag{4.35}$$

the shift-invariant reconstruction of the separator $\widehat{\Theta}(z)$.

This section is primarily concerned with the case when Σ is LTI, and provides some discussions related to shift-invariant reconstruction so that further properties of noncausal LPTV scaling applied to LTI systems can be clarified. In particular, we discuss the relationship between noncausal LPTV scaling based on $\widehat{\boldsymbol{\Theta}}(z)$ and causal LTI scaling based on the separator class $\boldsymbol{\Theta}(\zeta)$ we have introduced earlier in (4.20). Note that both $\widehat{\boldsymbol{\Theta}}(z)$ and $\boldsymbol{\Theta}(\zeta)$ are constructed from the same class $\widehat{\boldsymbol{\Theta}}_0^{\text{noncausal}}(z)$. What we establish in this section is that, even though a direct relationship between the classes $\boldsymbol{\Theta}(\zeta)$ and $\widehat{\boldsymbol{\Theta}}_0^{\text{noncausal}}(z)$ is still open, a direct relationship between the former class $\boldsymbol{\Theta}(\zeta)$ and the shift-invariant reconstruction $\widehat{\boldsymbol{\Theta}}(z)$ of the latter class can be clarified completely. Implications of the success in this direction will also be discussed.

Remark 4.2 There is no inclusion relation between $\widehat{\boldsymbol{\Theta}}_0^{\text{noncausal}}(z)$ and its shift-invariant reconstruction $\widehat{\boldsymbol{\Theta}}(z)$, in general (see Figure 4.1). This can be seen by considering the case $\widehat{\boldsymbol{\Theta}}_0^{\text{noncausal}}(z) = \widehat{\boldsymbol{\Theta}}_{\text{static}}^{\text{noncausal}}$. In this case, $\widehat{\boldsymbol{\Theta}}_{\text{static}}^{\text{noncausal}}$ includes static noncausal LPTV separators that are not shift-invariant (hence do not belong to $\widehat{\boldsymbol{\Theta}}(z)$) and result in dynamic separators (hence do not belong to $\widehat{\boldsymbol{\Theta}}_{\text{static}}^{\text{noncausal}}$) when shift-invariant reconstruction is applied to them. This does imply the lack of mutual inclusion, but the intersection $\widehat{\boldsymbol{\Theta}}(z) \cap \widehat{\boldsymbol{\Theta}}_{\text{static}}^{\text{noncausal}}$ is nonempty because it equals the class $\widehat{\boldsymbol{\Theta}}_{\text{static}}^{\text{LTI}}$ of static causal LTI separators (in the lifting-based framework).

4.4.2 Properties of shift-invariant reconstruction in noncausal LPTV scaling

The following theorem plays a crucial role in this section.

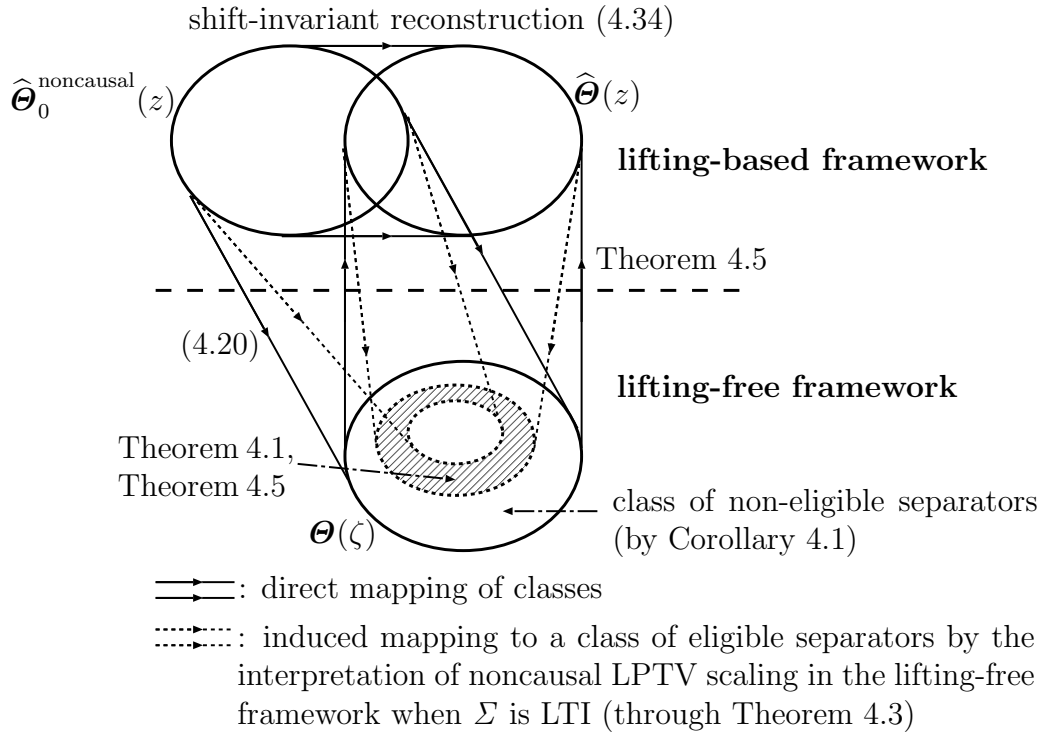

Figure 4.1: Relationship between some classes of separators and its implication in noncausal LPTV scaling.

Theorem 4.5 Given a noncausal LPTV separator $\widehat{\Theta}(z)$, consider the causal LTI separator $\Theta(\zeta)$ induced in the lifting-free framework by (4.19). Then, the equivalent separator $\widehat{\mathrm{E}}[\Theta(\zeta)]$ in the lifting-based framework coincides with the shift-invariant reconstruction (4.35) of $\widehat{\Theta}(z)$.

Proof. The noncausal LPTV separator $\widehat{\Theta}(z)$ can be described by

$$\widehat{\Theta}(z) = \Big(\widehat{\Theta}_{ij}(z)\Big)_{i,j=1,2}, \quad \widehat{\Theta}_{ij}(z) = \widehat{V}_i(z)^* \Gamma \widehat{V}_j(z) \tag{4.36}$$

where $\widehat{V}(z) =: [\widehat{V}_1(z)\ \widehat{V}_2(z)]$. Hence, $\Theta(\zeta)$ given by (4.19) is described by

$$\Theta(\zeta) = (\Theta_{ij}(\zeta))_{i,j=1,2} = \Big(T_p(\zeta)^* \widehat{V}_i(\zeta^N)^* \Gamma \widehat{V}_j(\zeta^N) T_p(\zeta)\Big)_{i,j=1,2}. \tag{4.37}$$

According to the discussion in Section 4.2, the derivation of the equivalent causal LTI separator $\widehat{\Theta}(z) = \widehat{\mathrm{E}}[\Theta(\zeta)]$ in the lifting-based framework corresponding to $\Theta(\zeta)$ amounts to

representing $(1/N)U_p(\zeta)\underline{\Theta_{ij}(\zeta)}U_p(\zeta)^*$ in terms of ζ^N. Regarding this issue, we have

$$\begin{aligned}
U_p(\zeta)\underline{\Theta_{ij}(\zeta)}U_p(\zeta)^* =& U_p(\zeta)\underline{T_p(\zeta)}^*\underline{\widehat{V}_i(\zeta^N)^*\Gamma\widehat{V}_j(\zeta^N)}\,\underline{T_p(\zeta)}U_p(\zeta)^* \\
=& \widehat{T}_p(\zeta^N)^*U_p(\zeta)\underline{\widehat{V}_i(\zeta^N)^*\Gamma\widehat{V}_j(\zeta^N)}U_p(\zeta)^*\widehat{T}_p(\zeta^N) \\
=& \widehat{T}_p(\zeta^N)^*\{I_N\otimes(\widehat{V}_i(\zeta^N)^*\Gamma\widehat{V}_j(\zeta^N))\}\widehat{T}_p(\zeta^N) \qquad (4.38)\\
=& \widehat{T}_p(\zeta^N)^*\{I_N\otimes\widehat{\Theta}_{ij}(\zeta^N)\}\widehat{T}_p(\zeta^N) \quad (\forall\zeta\in\partial\mathbf{D}), \qquad (4.39)
\end{aligned}$$

where $\otimes$ denotes the Kronecker product; in the reduction to (4.38), note that $\widehat{V}_i(\zeta^N)^*\Gamma\widehat{V}_j(\zeta^N)$ is invariant under the replacement of ζ by $\phi\zeta$ and that its size is $p\times p$, which is the same as that of the identity matrices in $T_p(\cdot)$ contained in $U_p(\zeta)$. Hence, the causal LTI separator $\widehat{\mathrm{E}}[\Theta(\zeta)]$ in the lifting-based framework equivalent to $\Theta(\zeta)$ in the lifting-free framework is given by

$$\widehat{\Theta}(z)=\left(\frac{1}{N}\widehat{T}_p(z)^*\{I_N\otimes\widehat{\Theta}_{ij}(z)\}\widehat{T}_p(z)\right)_{i,j=1,2}. \qquad (4.40)$$

To describe this separator in a simpler form, we first aim at giving an explicit form of $\widehat{T}_p(z)$. By the definition of $T_p(\zeta)$, it can be realized with

$$\left[\begin{array}{c|c} A_T & B_T \\ \hline C_T & D_T \end{array}\right] := \left[\begin{array}{cc|c} & I_{(N-2)p} & 0_{(N-2)p\times p} \\ 0_p & & I_p \\ \hline I_p & & 0_p \\ & I_{(N-2)p} & 0_{(N-2)p\times p} \\ & 0_{p\times(N-2)p} & I_p \end{array}\right]. \qquad (4.41)$$

Hence, by the definition of lifting of systems, $\widehat{T}_p(z)$ can be realized with $(\widehat{A}_T,\widehat{B}_T,\widehat{C}_T,\widehat{D}_T)$ given by

$$\left[\begin{array}{c|cccc} A_T^N & A_T^{N-1}B_T & A_T^{N-2}B_T & \dots & B_T \\ \hline C_T & D_T & & & \\ C_TA_T & C_TB_T & \ddots & & \\ \vdots & \vdots & \ddots & \ddots & \\ C_TA_T^{N-1} & C_TA_T^{N-2}B_T & \dots & C_TB_T & D_T \end{array}\right]. \qquad (4.42)$$

By direct calculations, we can obtain

$$A_T^m=\begin{bmatrix} & I_{(N-1-m)p} \\ 0_{mp} & \end{bmatrix},\quad A_T^mB_T=\begin{bmatrix} 0_{(N-2-m)p\times p} \\ I_p \\ 0_{mp\times p}\end{bmatrix}, \qquad (4.43)$$

$$C_TA_T^m=\begin{bmatrix} & I_{(N-1-m)p} \\ 0_{(m+1)p} & \end{bmatrix},\quad C_TA_T^mB_T=\begin{bmatrix} 0_{(N-2-m)p\times p} \\ I_p \\ 0_{(m+1)p\times p}\end{bmatrix}. \qquad (4.44)$$

In particular, $A_T^N = 0$. Therefore, we obtain

$$\widehat{T}_p(z) = z^{-1}\widehat{C}_T\widehat{B}_T + \widehat{D}_T = \begin{bmatrix} S_p(z)^{N-1} \\ \vdots \\ S_p(z) \\ I_{Np} \end{bmatrix}. \tag{4.45}$$

Substituting (4.45) into (4.40) immediately leads to (4.35). This completes the proof. Q.E.D.

This theorem together with (4.20) and (4.34) implies that the shift-invariant reconstruction $\widehat{\boldsymbol{\Theta}}(z)$ of the separator class $\widehat{\boldsymbol{\Theta}}_0^{\text{noncausal}}(z)$ is nothing but the class $\{\widehat{\mathrm{E}}[\Theta(\zeta)] \,|\, \Theta(\zeta) \in \boldsymbol{\Theta}(\zeta)\}$ of equivalent embedded causal LTI separators in the lifting-based framework (see Figure 4.1).

Combining our preceding arguments, we are led immediately to the following result about the robust stability analysis of the LTI system Σ.

Corollary 4.1 Suppose that G is LTI, and $\boldsymbol{\Delta}$ satisfies Assumption 2. Given a noncausal LPTV separator $\widehat{\Theta}(z)$, the associated $\Theta(\zeta)$ in (4.19) is eligible in the lifting-free framework if and only if the shift-invariant reconstruction (4.35) of $\widehat{\Theta}(z)$ is eligible in the lifting-based framework. In particular, given $\widehat{\boldsymbol{\Theta}}_0^{\text{noncausal}}(z)$, the induced class $\boldsymbol{\Theta}(\zeta)$ is eligible in the lifting-free framework if and only if $\widehat{\boldsymbol{\Theta}}(z)$ is in the lifting-based framework.

Proof. Necessity follows from Theorem 4.1 and Theorem 4.5, while sufficiency follows from Theorem 4.2 and Theorem 4.5. Q.E.D.

4.4.3 Implication of the properties of shift-invariant reconstruction in noncausal LPTV scaling

In the above, we have shown Theorem 4.5 and Corollary 4.1 as the main results in this section. We next discuss some facts revealed by these new results so that the significance of these results can be demonstrated. We refer to Figure 4.1 to this end, in which the upper part is related to the use of Theorem 2.2 (i.e., the lifting-based framework), while the lower part is related to the use of Theorem 2.3 (i.e., the lifting-free framework).

The classes $\boldsymbol{\Theta}_0(\zeta)$ and $\boldsymbol{\Theta}_1(\zeta)$, their inclusion relation, and their relevance to shift-invariant reconstruction

Let us consider the two subclasses contained in $\boldsymbol{\Theta}(\zeta)$ in this figure. The inner subclass is denoted by $\boldsymbol{\Theta}_0(\zeta)$ while the outer by $\boldsymbol{\Theta}_1(\zeta)$. By definition, $\boldsymbol{\Theta}_0(\zeta)$ is such a set of the eligible separators in the lifting-free framework that are obtained by applying (4.19) to all *eligible separators* $\widehat{\Theta}(z) \in \widehat{\boldsymbol{\Theta}}_0^{\text{noncausal}}(z)$ in the lifting-based framework. $\boldsymbol{\Theta}_1(\zeta)$ is defined similarly by replacing $\widehat{\boldsymbol{\Theta}}_0^{\text{noncausal}}(z)$ with its shift-invariant reconstruction $\widehat{\boldsymbol{\Theta}}(z)$. The introduction of the class $\boldsymbol{\Theta}_0(\zeta)$ is motivated by Theorem 4.3, but it is not ensured that $\boldsymbol{\Theta}_0(\zeta)$ coincides with the subset consisting of all eligible separators in $\boldsymbol{\Theta}(\zeta)$. This is because of the lack of the converse assertion in this theorem. This implies that the lifting-based framework with $\widehat{\boldsymbol{\Theta}}_0^{\text{noncausal}}(z)$ is not always equivalent to the lifting-free framework with $\boldsymbol{\Theta}(\zeta)$, but could in fact be more conservative. As we have discussed in Section 4.2, we have been interested in analyzing such a gap. The purpose of this subsection is to show that the preceding arguments in this section about shift-invariant reconstruction successfully lead to clarifying the gap. In fact, it will turn out that the separator class $\boldsymbol{\Theta}_1(\zeta)$ (and thus the shift-invariant reconstruction of $\widehat{\boldsymbol{\Theta}}_0^{\text{noncausal}}(z)$) plays a crucial role in characterizing the gap.

Before proceeding, we first remark that the inclusion between $\boldsymbol{\Theta}_0(\zeta)$ and $\boldsymbol{\Theta}_1(\zeta)$ implicitly asserted in Figure 4.1 is not trivial since there is generally no inclusion between $\widehat{\boldsymbol{\Theta}}_0^{\text{noncausal}}(z)$ and $\widehat{\boldsymbol{\Theta}}(z)$ (Remark 4.2). However, we indeed have $\boldsymbol{\Theta}_0(\zeta) \subset \boldsymbol{\Theta}_1(\zeta)$, and Theorem 4.5 plays a crucial role in its proof as follows. Let us take an arbitrary separator $\Theta(\zeta) \in \boldsymbol{\Theta}_0(\zeta)$. By the definition of $\boldsymbol{\Theta}_0(\zeta)$, there exists an eligible separator $\widehat{\Theta}(z) \in \widehat{\boldsymbol{\Theta}}_0^{\text{noncausal}}(z)$ such that the above $\Theta(\zeta)$ is represented by (4.19). On the other hand, the equivalent separator $\widehat{\mathrm{E}}[\Theta(\zeta)]$ in the lifting-based framework corresponding to $\Theta(\zeta)$ eligible in the lifting-free framework is eligible by Theorem 4.1, and it belongs to $\widehat{\boldsymbol{\Theta}}(z)$ by Theorem 4.5. By the definition of $\boldsymbol{\Theta}_1(\zeta)$, this implies that $\boldsymbol{\Theta}_0(\zeta) \subset \boldsymbol{\Theta}_1(\zeta)$. This inclusion implies that we can carry out robust stability analysis in a less conservative fashion by dealing with the shift-invariant reconstruction of separator classes in the lifting-based framework (at the possible expense of increased complexity in the search of eligible separators).

Implication and significance of shift-invariant reconstruction

Regarding the significance suggested above about the introduction of the shift-invariant reconstruction $\widehat{\boldsymbol{\Theta}}(z)$ and the corresponding class $\boldsymbol{\Theta}(\zeta)$ in the lifting-free framework, we can reveal a much more important and stronger result. In fact, it follows immediately from Corollary 4.1 that $\boldsymbol{\Theta}_1(\zeta)$ coincides with the class of all eligible separators in $\boldsymbol{\Theta}(\zeta)$. The implication of this fact on the properties of noncausal LPTV scaling is as follows.

As we have discussed earlier, this chapter is motivated by the possible ability of (static) noncausal LPTV scaling in replacing the conventional frequency-dependent (i.e., dynamic causal LTI) scaling, as suggested by Theorem 2.5 (and thus Theorem 4.3). Due to the lack of the converse assertion of that theorem, however, the degree of such an ability has not been fully clarified. In particular, it has not been clear if (under some conditions) noncausal LPTV scaling with the separator class $\widehat{\boldsymbol{\Theta}}_0^{\mathrm{noncausal}}(z)$ is equivalent to the conventional causal LTI scaling with the separator class $\boldsymbol{\Theta}(\zeta)$ derived from $\widehat{\boldsymbol{\Theta}}_0^{\mathrm{noncausal}}(z)$ as in (4.20). What is established by the above observation is that, even though a direct answer to the above question is still open, replacing $\widehat{\boldsymbol{\Theta}}_0^{\mathrm{noncausal}}(z)$ with its shift-invariant reconstruction $\widehat{\boldsymbol{\Theta}}(z)$ in noncausal LPTV scaling does lead, when it is interpreted in the lifting-free framework, equivalently to causal LTI scaling with $\boldsymbol{\Theta}(\zeta)$.

Before closing this section, we note that we could also derive the following result that is somewhat relevant to the inclusion $\boldsymbol{\Theta}_0(\zeta) \subset \boldsymbol{\Theta}_1(\zeta)$, as an immediate consequence of Theorem 4.4.

Corollary 4.2 Suppose that G is LTI, $\boldsymbol{\Delta}$ satisfies Assumption 2, and a class $\widehat{\boldsymbol{\Theta}}_0^{\mathrm{noncausal}}(z)$ of noncausal LPTV separators is given. If the class $\widehat{\boldsymbol{\Theta}}_0^{\mathrm{noncausal}}(z)$ is eligible, the class $\widehat{\boldsymbol{\Theta}}(z)$ is also eligible.

We have seen in the above the significance of the main results of this chapter (Theorem 4.5 and Corollary 4.1) in clarifying the ability of noncausal LPTV scaling applied to the robust stability analysis of LTI systems. This clearly demonstrates that the lifting timing, timing-shift matrix and shift-invariant reconstruction of separator classes are quite important also in the robust stability analysis of the LTI system Σ, in spite of the fact that the lifted representations of LTI systems are independent of lifting timing. As such, the arguments of this chapter are expected to provide a basis for further studies on the properties and effectiveness of noncausal LPTV scaling applied to LTI systems as well as LPTV systems.

4.4.4 Numerical confirmation of theoretical results

This subsection numerically confirms the inclusion relationship $\boldsymbol{\Theta}_0(\zeta) \subset \boldsymbol{\Theta}_1(\zeta)$ and the equivalence relationship between noncausal LPTV scaling based on $\widehat{\boldsymbol{\Theta}}(z)$ and causal LTI scaling based on $\boldsymbol{\Theta}(\zeta)$ in terms of conservativeness in robust stability analysis, which are shown in Figure 4.1.

We consider the internally stable LTI system G given by

$$\left[\begin{array}{c|c} A & B \\ \hline C & D \end{array}\right] = \left[\begin{array}{ccccc|cc} 0 & 1 & 0 & 0 & 0 & 0 & 0 \\ 0 & 0 & 1 & 0 & 0 & 0 & 0 \\ 0 & 0 & 0 & 1 & 0 & 0 & 0 \\ 0 & 0 & 0 & 0 & 1 & 0 & 0.1 \\ -0.2 & -0.62 & 0.01 & 0.6 & -0.7 & 0.1 & 0 \\ \hline 1 & 1 & 1 & 0 & 0 & 0.1 & 0.2 \\ 0 & 0 & 0 & 1 & 1 & 0 & 0 \end{array}\right]. \tag{4.46}$$

In addition, we assume the corresponding uncertainties Δ are static LTI and structured as given by $\Delta = \mathrm{diag}[\delta_1\ \delta_2]$. The purpose here is to compute (a lower bound of) the maximal $\overline{\delta}$ such that the closed-loop system Σ is robustly stable with respect to the uncertainty set $\boldsymbol{\Delta} = \{\Delta : \|\Delta\| < \overline{\delta}\}$. In such analysis, we employ the idea of the (D, G)-scaling approach [13] and take the following four types of separator classes: the first one is the class $\widehat{\boldsymbol{\Theta}}^{\mathrm{noncausal}}_{\mathrm{static},(D,G)}$ of static noncausal LPTV separators of the (D, G)-scaling type under a prescribed N (which we take equal to 6), which we view as $\widehat{\boldsymbol{\Theta}}^{\mathrm{noncausal}}_0(z)$ in the preceding arguments. The other three are the class $\boldsymbol{\Theta}(\zeta)$ constructed from the above class through (4.20), the class $\widehat{\boldsymbol{\Theta}}(z)$ constructed from the same class through (4.34), and the class $\boldsymbol{\Theta}_{\mathrm{static},(D,G)}$ of static causal LTI separators of the (D, G)-scaling type.

Note that the second and fourth are separator classes for the lifting-free framework; the reason why we take the fourth is as follows: since the second is induced by *static separators* in the lifting-based framework (and the third is asserted to have an ability equivalent to the second), we also take, for reference, the fourth one so that we can also demonstrate the advantage of the lifting-based framework over the lifting-free framework *under the common setting using only static separators*.

Remark 4.3 Separators in $\boldsymbol{\Theta}(\zeta)$ are dynamic, in general, and thus this class is less tractable than the above two classes of static separators. However, since free parameters in such separators are contained only in its "numerator part" by (4.19), no essential difference arises from the case of static separators. That is, eligibility of $\boldsymbol{\Theta}(\zeta)$ can be checked without conservativeness through the KYP lemma [34] applied to inequality (2.15), because (2.16) is satisfied automatically for any $\widehat{\Theta} \in \widehat{\boldsymbol{\Theta}}^{\mathrm{noncausal}}_{\mathrm{static},(D,G)}$, thanks to the properties of (D, G)-scaling. To avoid distraction and concentrate on demonstrating the significance of the preceding arguments in this section, however, the details are omitted about the numerical search process of separators (see Chapter 6 for details). Essentially the same comment applies to the treatment of $\widehat{\boldsymbol{\Theta}}(z)$.

The numerical results of the analysis of $\overline{\delta}$ are shown in Table 4.2, from which we can first confirm that static noncausal LPTV scaling is less conservative than static causal LTI

Table 4.2: Robust stability analysis with each class of separators ($N = 6$)

Separator class	$\widehat{\boldsymbol{\Theta}}^{\text{noncausal}}_{\text{static},(D,G)}$	$\boldsymbol{\Theta}(\zeta)$	$\widehat{\boldsymbol{\Theta}}(z)$	$\boldsymbol{\Theta}_{\text{static},(D,G)}$
$\overline{\delta}$	1.4091	1.4942	1.4942	1.2115

scaling in the lifting-free framework. However, we also see that the former is still more conservative than the dynamic causal LTI scaling in the lifting-free framework based on $\boldsymbol{\Theta}(\zeta)$. In other words, this is an example in which noncausal LPTV scaling with the separator class $\widehat{\boldsymbol{\Theta}}^{\text{noncausal}}_0(z)$ fails to equivalently check eligibility of the associated separator class $\boldsymbol{\Theta}(\zeta)$ in the lifting-free framework. However, it can be also confirmed from Table 4.2 that the result obtained through noncausal LPTV scaling based on $\widehat{\boldsymbol{\Theta}}(z)$, which is the shift-invariant reconstruction of $\widehat{\boldsymbol{\Theta}}^{\text{noncausal}}_{\text{static},(D,G)}$, is no more conservative than that of causal LTI scaling based on $\boldsymbol{\Theta}(\zeta)$. This confirms not only the inclusion relationship $\boldsymbol{\Theta}_0(\zeta) \subset \boldsymbol{\Theta}_1(\zeta)$ but also the equivalence in the ability of the two scaling approaches with the separator classes $\boldsymbol{\Theta}(\zeta)$ and $\widehat{\boldsymbol{\Theta}}(z)$ defined in the lifting-free framework and lifting-based framework, respectively.

4.5 Concluding remarks

This chapter developed a new direction for studying the properties of noncausal LPTV scaling, which has been introduced as a new method for robust stability analysis by applying the separator-type robust stability theorem and the discrete-time lifting technique. A key idea in this direction was to consider the timing of lifting, and shift invariance of separator classes was introduced as a key notion relevant to the lifting timing. It was then discussed that, compared with causal LPTV scaling and the conventional frequency-dependent scaling (i.e., causal LTI scaling), noncausal LPTV scaling has, in general, different properties about the shift invariance of the separator classes it deals with. It was also discussed how taking a different lifting timing in noncausal LPTV scaling could affect the robust stability analysis of LPTV systems. The robust stability analysis of LTI systems with noncausal LPTV scaling, on the other hand, is not affected by the lifting timing. This, however, never implies that the idea of lifting timing is meaningful only in the treatment of LPTV systems. Instead, it was established that the idea of shift-invariant reconstruction of separator classes plays an important role in clarifying further properties of noncausal LPTV scaling applied to LTI systems. In particular, we have given a partial answer to the open question about static noncausal LPTV scaling, i.e., how substantial and promising its ability is in equivalently inducing frequency-dependent scaling in the conventional lifting-free framework.

Chapter 5

Unified Treatment of Robust Stability Conditions through an Infinite Matrix Framework

5.1 Introduction

This chapter is concerned with robust stability analysis of LTI closed-loop systems employing the separator-type robust stability theorem. Properties of noncausal LPTV scaling for such analysis have been studied in the preceding chapter from the frequency-domain viewpoint through introducing the timing-shift matrix $S_p(z)$. This chapter, on the other hand, studies such properties from another viewpoint through introducing what we call an infinite matrix framework.

Robust stability can be analyzed by searching for eligible separators in both the lifting-free and lifting-based frameworks. To achieve nonconservative robust stability analysis, however, such a search must work on all frequency-dependent (i.e., dynamic) separators without any constraint, but this is not feasible from computational viewpoints. Thus, a tractable class of separators is introduced in practice, only on which the search of eligible separators is carried out, whichever framework we may employ. This generally results in conservativeness in robust stability analysis.

As such tractable classes, for example, we can introduce those of static separators in both causal LTI and noncausal LPTV scaling approaches, and the relationship between the corresponding two scaling approaches has been already studied, as reviewed in Chapter 2. However, if we take more general but tractable classes of separators in these approaches, it has not been easy to directly compare them as in the case of static separators. This difficulty can largely be attributed to the fact that they are dealt with in two different (i.e., lifting-free and lifting-based) frameworks and their frequency-domain properties are not easy

to compare in a straightforward fashion.

This chapter aims at developing a new unified framework for dealing with these two approaches that can facilitate their mutual comparison and relevant studies in a very comprehensible and intuitive manner. More explicitly, by means of infinite matrix representations of systems [15],[8], restatements of the robust stability conditions associated with the conventional causal LTI scaling and the lifting-based noncausal LPTV scaling are established in a unified fashion in Section 5.2. This leads to the notion of infinite-dimensional separators, whose specific forms are studied in Section 5.3 by confining ourselves to the tractable classes of separators characterized by finite impulse response, both in the conventional causal LTI scaling and noncausal LPTV scaling approaches. Section 5.4 combines these arguments to address the main problem. Specifically, it is demonstrated that the infinite matrix framework developed in this chapter is very comprehensible and useful in the theoretical study on the mutual relationship between causal LTI and noncausal LPTV scaling approaches. Theoretical benefit of the infinite matrix framework is further demonstrated as to its usefulness in isolating the effects of time dependence and frequency dependence in scaling through the structure of infinite-dimensional separators.

We use the following notation in this chapter. $\mathbf{N}_0$ denotes the set of nonnegative integers, and $l_2(\mathbf{N}_0, \mathbf{R}^q)$ denotes the set of unilateral infinite series of vectors $v_k \in \mathbf{R}^q$ such that $\sum_{k=0}^{\infty} \|v_k\|^2 < \infty$.

5.2 Robust stability conditions based on infinite matrix representations

This section employs infinite matrix representations of systems [15],[8], and introduces different forms of robust stability conditions under such treatment. The infinite matrix framework of such new conditions will turn out to provide a unified medium for directly comparing the lifting-free framework and the lifting-based framework in robust stability analysis. Hence, such a unified framework facilitates further studies on clarifying the relationship between the conventional causal LTI scaling and noncausal LPTV scaling. At the same time, such a framework is also effective for comparing the effect of frequency dependence in scaling (i.e., dealing with dynamic separators, as is often the case in the conventional lifting-free framework) and that of time dependence in scaling (which includes noncausal operations naturally introduced by the application of noncausal LPTV scaling). The introduction of robust stability conditions through infinite matrix representations will constitute the basis of the subsequent arguments in this chapter.

5.2.1 Robust stability analysis problem for LTI closed-loop systems

This subsection explicitly states the problem studied in this chapter. Let us consider the discrete-time closed-loop system Σ (Figure 2.3) consisting of the discrete-time nominal system G and the discrete-time uncertainty Δ. The system G is assumed to be internally stable, finite-dimensional, LTI, and represented by

$$x_{k+1} = Ax_k + Bw_k, \quad z_k = Cx_k + Dw_k \tag{5.1}$$

with $x_k \in \mathbf{R}^n$, $w_k \in \mathbf{R}^p$ and $z_k \in \mathbf{R}^p$. On the other hand, Δ is assumed to belong to a given set $\boldsymbol{\Delta}$ satisfying Assumption 2 (i.e., LTI uncertainties).

This chapter studies the problem of deciding whether the above LTI closed-loop system Σ is robustly stable with respect to the given set $\boldsymbol{\Delta}$.

5.2.2 Infinite matrix representations of systems

This subsection introduces infinite vector representations of input/output signals and the associated infinite matrix representations of systems [15],[8]. They will be a basis for introducing a different form of robust stability condition in this section.

Let us consider the infinite vector representation of w, the input of the nominal system G, and denote it by

$$\widetilde{w} = [w_0^T,\ w_1^T,\ w_2^T,\ \cdots]^T. \tag{5.2}$$

We also define $\widetilde{z}$ similarly. Assuming that the initial state of G is zero, these representations lead us to the formal description

$$\widetilde{z} = \widetilde{G}\widetilde{w} \tag{5.3}$$

of the input-output relation of the nominal system G, where the infinite matrix $\widetilde{G}$ is given by

$$\widetilde{G} = \begin{bmatrix} D & 0 & 0 & 0 & \cdots \\ CB & D & 0 & 0 & \ddots \\ CAB & CB & D & 0 & \ddots \\ CA^2B & CAB & CB & D & \ddots \\ \vdots & \ddots & \ddots & \ddots & \ddots \end{bmatrix} \tag{5.4}$$

with block Toeplitz and lower triangular structure. The infinite matrix representation $\widetilde{\Delta}$ of the uncertainty Δ is defined similarly.

5.2.3 Robust stability condition based on infinite matrix representations

This subsection is devoted to introducing a robust stability condition based on the infinite matrix representations of G and Δ. The condition introduced here may be, in a sense, simply a restatement of that in Theorem 2.3. Moreover, the restated infinite matrix condition might be less useful if its value were assessed only from a practical point of view. Nonetheless, significance of the extension toward such a direction with infinite matrix representations lies in the fact that a parallel and unified extension can also be achieved about Theorem 2.2 leading to noncausal LPTV scaling. We will indeed see this parallelism in the following subsection, and further see in Section 5.4 that such extensions effectively facilitate us to have a fresh and clear insight into the relationship between causal LTI scaling and noncausal LPTV scaling.

We begin our discussions with the following key lemma. It follows by applying the Fourier expansion, but requires rigorous arguments to circumvent mathematical subtleties; the detailed proof will be given in Subsection 5.2.5.

Lemma 5.1 Suppose that $M(\zeta)$ is a stable rational transfer matrix with q columns, and $L = L^*$ is a constant matrix. For a given $\alpha \in \mathbf{R}$,

$$M(\zeta)^* L M(\zeta) \geq \alpha I \quad (\forall \zeta \in \partial \mathbf{D}) \tag{5.5}$$

if and only if

$$\widetilde{M}^* \widetilde{L} \widetilde{M} \geq \alpha \widetilde{I} \tag{5.6}$$

on $l_2(\mathbf{N}_0, \mathbf{R}^q)$, where $\widetilde{M}$, $\widetilde{L}$ and $\widetilde{I}$ are the infinite matrix representations of $M(\zeta)$, L and I, respectively.

In (5.6), the inequality is in terms of non-negativeness of quadratic forms on $l_2(\mathbf{N}_0, \mathbf{R}^q)$. An implication of the above theorem is that the ζ-dependence in inequality (5.5) may be removed if one accepts to work on infinite matrix inequality (5.6). A direct application of the above lemma leads to the following proposition.

Proposition 5.1 Suppose that G is internally stable and the separator $\Theta(\zeta)$ is given by

$$\Theta(\zeta) = \begin{bmatrix} V_1(\zeta) & V_2(\zeta) \end{bmatrix}^* \Lambda \begin{bmatrix} V_1(\zeta) & V_2(\zeta) \end{bmatrix} \tag{5.7}$$

with a constant matrix $\Lambda = \Lambda^*$ and stable transfer matrices $V_1(\zeta)$ and $V_2(\zeta)$. Then, the robust stability conditions (2.15) and (2.16) hold if and only if the infinite matrix inequalities

$$\begin{bmatrix} \widetilde{I} \\ \widetilde{G} \end{bmatrix}^* \widetilde{\Theta} \begin{bmatrix} \widetilde{I} \\ \widetilde{G} \end{bmatrix} \leq 0, \tag{5.8}$$

$$\begin{bmatrix} \widetilde{\Delta} \\ \widetilde{I} \end{bmatrix}^* \widetilde{\Theta} \begin{bmatrix} \widetilde{\Delta} \\ \widetilde{I} \end{bmatrix} \geq \epsilon(\Delta)\widetilde{I} \quad \begin{pmatrix} \forall \Delta \in \boldsymbol{\Delta}, \\ \exists \epsilon(\Delta) > 0 \end{pmatrix} \tag{5.9}$$

hold on $l_2(\mathbf{N}_0, \mathbf{R}^p)$ for the infinite matrix

$$\widetilde{\Theta} = \begin{bmatrix} \widetilde{V}_1 & \widetilde{V}_2 \end{bmatrix}^* \widetilde{\Lambda} \begin{bmatrix} \widetilde{V}_1 & \widetilde{V}_2 \end{bmatrix} \tag{5.10}$$

where $\widetilde{V}_1$, $\widetilde{V}_2$ and $\widetilde{\Lambda}$ are the infinite matrix representations of $V_1(\zeta)$, $V_2(\zeta)$ and Λ, respectively.

In view of the role of the infinite matrix $\widetilde{\Theta}$ in inequalities (5.8) and (5.9), we call it a separator in the framework of infinite matrix representations, or simply an infinite-dimensional separator. Furthermore, we call the particular separator $\widetilde{\Theta}$ given in (5.10) the infinite matrix representation of the separator (5.7).

We have assumed in the above proposition that $V_1(\zeta)$ and $V_2(\zeta)$ are stable. This obviously leads to restricting the class of separators from which eligible separators in the lifting-free framework are searched for. Fortunately, however, such restriction is known to lead to no conservativeness in the robust stability analysis [25]. Hence, Theorem 2.3 and Proposition 5.1 lead immediately to the following robust stability theorem.

Theorem 5.1 Suppose that G is internally stable, and $\boldsymbol{\Delta}$ satisfies Assumption 2. Then, Σ is robustly (well-posed and) stable with respect to $\boldsymbol{\Delta}$ if and only if there exists $\widetilde{\Theta}$ that satisfies (5.8) and (5.9) on $l_2(\mathbf{N}_0, \mathbf{R}^p)$ and is in the form of (5.10), where $\widetilde{V}_1$ and $\widetilde{V}_2$ are the infinite matrix representations of stable transfer matrices $V_1(\zeta)$ and $V_2(\zeta)$, respectively, and $\widetilde{\Lambda}$ is the infinite matrix representation of a static system Λ.

5.2.4 Generalization of the class of infinite-dimensional separators

The preceding subsection studied introducing the infinite matrix representation counterpart to causal LTI scaling supported by Theorem 2.3, and gave infinite matrix representations of causal LTI separators. This subsection extends the study to noncausal LPTV scaling supported by Theorem 2.2, gives infinite matrix representations of noncausal LPTV separators, and observes how these representations are different from those of causal LTI separators.

The extension to noncausal LPTV scaling is essentially just to repeat in the lifting-based framework the same arguments as those in the preceding subsection. In other words, the

key in the extension is to apply Lemma 5.1 with $M(\zeta)$ replaced by the transfer matrix $\widehat{M}(z)$ defined on the lifted time axis. This naturally leads to an infinite matrix inequality on $l_2(\mathbf{N}_0, \mathbf{R}^{Np})$, but this space is isometrically isomorphic to $l_2(\mathbf{N}_0, \mathbf{R}^p)$ used in that lemma. Hence, these two spaces may be identified with each other, and thus it is not always necessary to distinguish an infinite matrix inequality on one space from the one on the other. Similarly, the infinite vector representation $\widetilde{w}$ of w and that of the lifted counterpart $\widehat{w}$ are essentially the same, and they need not be distinguished; we denote both of them by $\widetilde{w}$ without introducing the bothering notation $\widetilde{\widehat{w}}$. Similar comments apply also to the lifted representations of systems; the infinite matrix representation of G and that of the lifted counterpart of G may also be identified, and both of them are denoted by $\widetilde{G}$.

With the preceding arguments and notation, we are led to the following infinite matrix representation counterpart of Theorem 2.2 about noncausal LPTV scaling.

Theorem 5.2 Suppose that G is internally stable, and $\boldsymbol{\Delta}$ satisfies Assumption 2. Then, Σ is robustly (well-posed and) stable with respect to $\boldsymbol{\Delta}$ if and only if there exists $\widetilde{\Theta}$ that satisfies (5.8) and (5.9) on $l_2(\mathbf{N}_0, \mathbf{R}^{Np})$ and is in the form of

$$\widetilde{\Theta} = \begin{bmatrix} \widetilde{V}_1 & \widetilde{V}_2 \end{bmatrix}^* \widetilde{\Gamma} \begin{bmatrix} \widetilde{V}_1 & \widetilde{V}_2 \end{bmatrix} \tag{5.11}$$

where $\widetilde{V}_1$ and $\widetilde{V}_2$ are the infinite matrix representations of stable transfer matrices $\widehat{V}_1(z)$ and $\widehat{V}_2(z)$ *defined directly on the lifted time axis*, respectively, and $\widetilde{\Gamma}$ is the infinite matrix representation of a static system Γ.

Since $l_2(\mathbf{N}_0, \mathbf{R}^p)$ and $l_2(\mathbf{N}_0, \mathbf{R}^{Np})$ may essentially be identified as stated earlier, the difference between Theorem 5.1 about causal LTI scaling and Theorem 5.2 lies only in the forms of the infinite-dimensional separators $\widetilde{\Theta}$ in these theorems. In Theorem 5.1 (or (5.10)), $\widetilde{V}_1$ and $\widetilde{V}_2$ are related to stable LTI systems V_1 and V_2 (defined on the lifting-free time axis), and $\widetilde{\Lambda}$ is related to a constant matrix Λ whose size is compatible with the number of rows of V_1 and V_2. In Theorem 5.2, on the other hand, $\widetilde{V}_1$ and $\widetilde{V}_2$ are related to stable LTI systems $\widehat{V}_1$ and $\widehat{V}_2$ *defined on the lifted time axis*, and $\widetilde{\Gamma}$ is related to a constant matrix Γ whose size is compatible with the number of rows of $\widehat{V}_1$ and $\widehat{V}_2$. Therefore, in comparison with Theorem 5.1, Theorem 5.2 can be interpreted as relaxing the assumptions on the systems constituting the separator by allowing them to have N-periodicity. Moreover, some sort of noncausality is also allowed by introducing them directly on the lifted time axis. These differences lead to the enhanced ability of noncausal LPTV scaling, but they are simply natural consequences since the motivation behind introducing the idea of noncausal LPTV scaling underlying Theorem 5.2 has been nothing but such enhancement.

In the following arguments, if the infinite-dimensional separator $\tilde{\Theta}$ satisfies (5.8) and (5.9), then we say that it is eligible in the infinite matrix framework.

5.2.5 Proof of Lemma 5.1

This subsection gives the proof of the key lemma shown in Subsection 5.2.3. Throughout this subsection, ζ is confined to $\partial\mathbf{D}$. Consider the infinite-dimensional vectors

$$\widetilde{x} = \begin{bmatrix} x_0^T & x_1^T & \cdots & x_K^T & 0 & \cdots \end{bmatrix}^T, \quad x_i \in \mathbf{R}^q \ (i = 0, \ldots, K), \quad \exists K < \infty, \tag{5.12}$$

and let l_0 denote the set of all infinite-dimensional vectors given by (5.12). This l_0 is obviously a dense subset of $l_2(\mathbf{N}_0, \mathbf{R}^q)$. It is easy to see that it suffices to prove Lemma 5.1 only for $\alpha = 0$.

Necessity proof:
Let $\alpha = 0$ and suppose that (5.5) holds. For the infinite matrix

$$T^\infty(\zeta) = \begin{bmatrix} I & \zeta^{-1}I & \zeta^{-2}I & \cdots \end{bmatrix}, \tag{5.13}$$

it is obvious that $T^\infty(\zeta)\widetilde{x}$, which by definition is an infinite series if $\widetilde{x} \in l_2(\mathbf{N}_0, \mathbf{R}^q)$, is convergent for $\widetilde{x} \in l_0$, and belongs to $\mathbf{C}^q$. Hence, it follows from (5.5) that

$$\widetilde{x}^T T^\infty(\zeta)^* M(\zeta)^* L M(\zeta) T^\infty(\zeta)\widetilde{x} \geq 0 \quad (\forall \zeta \in \partial\mathbf{D}, \ \forall \widetilde{x} \in l_0). \tag{5.14}$$

Since $M(\zeta)$ is stable, it admits the expansion

$$M(\zeta) = M_0 + \zeta^{-1}M_1 + \zeta^{-2}M_2 + \cdots \quad (\zeta \in \partial\mathbf{D}). \tag{5.15}$$

This implies that $T^\infty(\zeta)\widetilde{M}$ is convergent, which immediately justifies that

$$T^\infty(\zeta)\widetilde{M} = M(\zeta)T^\infty(\zeta) \tag{5.16}$$

if we note that the right-hand side involves no infinite series. By substituting this relation into (5.14), we have

$$\widetilde{x}^T \widetilde{M}^* T^\infty(\mathrm{e}^{\mathrm{i}\theta})^* L T^\infty(\mathrm{e}^{\mathrm{i}\theta})\widetilde{M}\widetilde{x} \geq 0 \quad (0 \leq \forall\theta \leq 2\pi, \ \forall \widetilde{x} \in l_0), \tag{5.17}$$

where i denotes the imaginary unit. Integrating both sides over $[0, 2\pi]$ leads to

$$\widetilde{x}^T \widetilde{M}^* \int_0^{2\pi} T^\infty(\mathrm{e}^{\mathrm{i}\theta})^* L T^\infty(\mathrm{e}^{\mathrm{i}\theta}) d\theta \widetilde{M}\widetilde{x} \geq 0 \quad (\forall \widetilde{x} \in l_0), \tag{5.18}$$

where a direct computation yields

$$\int_0^{2\pi} T^\infty(\mathrm{e}^{\mathrm{i}\theta})^* L T^\infty(\mathrm{e}^{\mathrm{i}\theta}) d\theta = 2\pi \widetilde{L}. \tag{5.19}$$

Hence,

$$\widetilde{x}^T \widetilde{M}^* \widetilde{L} \widetilde{M} \widetilde{x} \geq 0 \quad (\forall \widetilde{x} \in l_0). \tag{5.20}$$

Since $\widetilde{M}$ and $\widetilde{L}$ are bounded on $l_2(\mathbf{N}_0, \mathbf{R}^q)$, and since l_0 is dense in $l_2(\mathbf{N}_0, \mathbf{R}^q)$, inequality (5.20) holds also for all $\widetilde{x} \in l_2(\mathbf{N}_0, \mathbf{R}^q)$. This completes the proof.

Sufficiency proof:
We let $\alpha = 0$ and show that (5.6) fails if (5.5) fails. If

$$M(\mathrm{e}^{\mathrm{i}\theta})^* L M(\mathrm{e}^{\mathrm{i}\theta}) \not\geq 0 \quad (0 \leq \exists \theta \leq 2\pi), \tag{5.21}$$

there exists $\theta = \theta_0$ $(0 < \theta_0 < 2\pi)$ and v_0 such that

$$v_0^* M(e^{\mathrm{i}\theta_0})^* L M(e^{\mathrm{i}\theta_0}) v_0 < 0. \tag{5.22}$$

Since $M(\mathrm{e}^{\mathrm{i}\theta})^* L M(\mathrm{e}^{\mathrm{i}\theta})$ is continuous with respect to θ because $M(\zeta)$ is rational, there exist θ_1 and θ_2 such that

$$v_0^* M(e^{\mathrm{i}\theta})^* L M(e^{\mathrm{i}\theta}) v_0 < 0, \quad \theta \in [\theta_1, \theta_2], \quad 0 < \theta_1 < \theta_0 < \theta_2 < 2\pi. \tag{5.23}$$

If we consider approximating v_0 for $\theta \in [\theta_1, \theta_2]$ and 0 otherwise with a continuous complex vector function on $[0, 2\pi]$, we readily see the existence of continuous $x(\theta)$ such that $x(0) = x(2\pi)$ and

$$\int_0^{2\pi} x(\theta)^* M(\mathrm{e}^{\mathrm{i}\theta})^* L M(\mathrm{e}^{\mathrm{i}\theta}) x(\theta) d\theta < 0. \tag{5.24}$$

By Fejér's theorem [3], for any $\epsilon > 0$, there exists a finite series

$$S(\theta) = \sum_{i=-m}^{m} c_i \mathrm{e}^{\mathrm{i}i\theta}, \quad c_i \in \mathbf{C}^q \ (i = -m, \ldots, m) \tag{5.25}$$

such that

$$\|x(\theta) - S(\theta)\| < \epsilon \quad (0 \leq \forall \theta \leq 2\pi). \tag{5.26}$$

By taking ϵ small enough, we can have

$$\int_0^{2\pi} S(\theta)^* M(\mathrm{e}^{\mathrm{i}\theta})^* L M(\mathrm{e}^{\mathrm{i}\theta}) S(\theta) d\theta < 0, \tag{5.27}$$

which in turn implies that

$$\int_0^{2\pi} S(\theta)^* \mathrm{e}^{\mathrm{i}m\theta} M(\mathrm{e}^{\mathrm{i}\theta})^* L M(\mathrm{e}^{\mathrm{i}\theta}) \mathrm{e}^{-\mathrm{i}m\theta} S(\theta) d\theta < 0. \tag{5.28}$$

Noting that

$$\mathrm{e}^{-\mathrm{i}m\theta} S(\theta) = T^{\infty}(\mathrm{e}^{\mathrm{i}\theta}) \widetilde{x}_{c,m}, \tag{5.29}$$

for

$$\widetilde{x}_{c,m} := \begin{bmatrix} c_m^T & c_{m-1}^T & \cdots & c_{-m}^T & 0 & \cdots \end{bmatrix}^T, \tag{5.30}$$

we readily have

$$\int_0^{2\pi} \widetilde{x}_{c,m}^* T^{\infty}(\mathrm{e}^{\mathrm{i}\theta})^* M(\mathrm{e}^{\mathrm{i}\theta})^* L M(\mathrm{e}^{\mathrm{i}\theta}) T^{\infty}(\mathrm{e}^{\mathrm{i}\theta}) \widetilde{x}_{c,m} d\theta < 0. \tag{5.31}$$

This, together with (5.16) and (5.19), implies that

$$\widetilde{x}_{c,m}^* \widetilde{M}^* \widetilde{L} \widetilde{M} \widetilde{x}_{c,m} < 0. \tag{5.32}$$

Although $\widetilde{x}_{c,m}$ belongs to $l_2(\mathbf{N}_0, \mathbf{C}^q)$ (rather than $l_2(\mathbf{N}_0, \mathbf{R}^q)$), its decomposition into $\widetilde{x}_{c,m} = \widetilde{x}_{\mathrm{rl},m} + \mathrm{j}\widetilde{x}_{\mathrm{im},m}$ with $\widetilde{x}_{\mathrm{rl},m}, \widetilde{x}_{\mathrm{im},m} \in l_0$ leads to

$$\widetilde{x}_{c,m}^* \widetilde{M}^* \widetilde{L} \widetilde{M} \widetilde{x}_{c,m} = \widetilde{x}_{\mathrm{rl},m}^T \widetilde{M}^* \widetilde{L} \widetilde{M} \widetilde{x}_{\mathrm{rl},m} + \widetilde{x}_{\mathrm{im},m}^T \widetilde{M}^* \widetilde{L} \widetilde{M} \widetilde{x}_{\mathrm{im},m}. \tag{5.33}$$

Therefore, at least one of $\widetilde{x}_{\mathrm{rl},m}^T \widetilde{M}^* \widetilde{L} \widetilde{M} \widetilde{x}_{\mathrm{rl},m}$ and $\widetilde{x}_{\mathrm{im},m}^T \widetilde{M}^* \widetilde{L} \widetilde{M} \widetilde{x}_{\mathrm{im},m}$ must be negative. This completes the proof.

5.3 Infinite matrix representations of causal LTI and noncausal LPTV separators characterized by finite impulse response

This section first deals with a dynamic LTI separator in the lifting-free framework characterized by finite impulse response (FIR), for simplicity, and gives its infinite matrix representation. The arguments reveal in the framework of infinite matrix representations an implication of frequency dependence (or dynamics) of separators. The arguments are then extended to a separator in the lifting-based framework characterized by FIR, and the infinite matrix representation of a noncausal LPTV separator is also given. Such a separator has not only frequency dependence but also time dependence resulting from its N-periodicity,

in general. An implication of such N-periodicity in contrast with frequency dependence will also be interpreted in the infinite matrix framework. These interpretations will be crucial as preliminary observations for the arguments in the following section. In fact, the mutual relationship between causal LTI separators and noncausal LPTV separators will be discussed there in an intuitive fashion by the use of the infinite matrix framework.

5.3.1 Causal LTI separator characterized by finite impulse response

In this subsection, we consider the dynamic causal LTI separator $\Theta_{\mathrm{FIR}}(\zeta) = \Theta_{\mathrm{FIR}}(\zeta)^*$ (defined for $\zeta \in \partial\mathbf{D}$ in the lifting-free framework) given by

$$\begin{aligned}
&\Theta_{\mathrm{FIR}}(\zeta) = (\Theta_{\mathrm{FIR},ij}(\zeta))_{i,j=1,2}\,,\\
&\Theta_{\mathrm{FIR},ij}(\zeta) = \Theta_{ij}^{[0]} + \sum_{k=1}^{K}\left(\Theta_{ij}^{[-k]}\zeta^{-k} + \Theta_{ij}^{[k]}(\zeta^*)^{-k}\right),\\
&\Theta_{ij}^{[k]} = \left(\Theta_{ji}^{[-k]}\right)^T \in \mathbf{R}^{p\times p}\ (k = 0, 1, \ldots, K).
\end{aligned} \tag{5.34}$$

We call it a causal LTI separator characterized by FIR, or simply a causal LTI FIR separator, and we refer to K as its order, assuming that $\Theta_{ij}^{[K]} \neq 0$ for some $i, j = 1, 2$; a causal LTI separator $V(\zeta)^*\Gamma V(\zeta)$ is in the form of (5.34) if and only if $V(\zeta)$ has an FIR. Since we have assumed in Theorem 5.1 that $V_1(\zeta)$ and $V_2(\zeta)$ are stable and thus their impulse responses converge to zero, it would not be extremely restrictive to confine ourselves to such a class of separators by taking a large enough K. This subsection is devoted to giving an explicit form of the infinite matrix representation of the dynamic causal LTI FIR separator (5.34).

The separator (5.34) defined on $\partial\mathbf{D}$ can be rearranged as

$$\Theta_{\mathrm{FIR}}(\zeta) = \left(T_p(\zeta)^*\Theta_{ij}^{[\mathrm{FIR}]}T_p(\zeta)\right)_{i,j=1,2} \tag{5.35}$$

where

$$T_p(\zeta) = \begin{bmatrix}\zeta^{-K}I_p\\ \vdots\\ \zeta^{-1}I_p\\ I_p\end{bmatrix},\quad \Theta_{ij}^{[\mathrm{FIR}]} = \begin{bmatrix}\Theta_{ij}^{[0]} & \Theta_{ij}^{[1]} & \cdots & \Theta_{ij}^{[K]}\\ \Theta_{ij}^{[-1]} & 0 & \cdots & 0\\ \vdots & \vdots & \ddots & \vdots\\ \Theta_{ij}^{[-K]} & 0 & \cdots & 0\end{bmatrix}. \tag{5.36}$$

Hence by (5.10), the infinite matrix representation of $\Theta_{\mathrm{FIR}}(\zeta)$ is given by

$$\widetilde{\Theta}_{\mathrm{FIR}} = \left(\widetilde{T}_p^*\widetilde{\Theta}_{ij}^{[\mathrm{FIR}]}\widetilde{T}_p\right)_{i,j=1,2}, \tag{5.37}$$

where $\widetilde{T}_p$ and $\widetilde{\Theta}_{ij}^{[\mathrm{FIR}]} = \mathrm{diag}[\Theta_{ij}^{[\mathrm{FIR}]}, \Theta_{ij}^{[\mathrm{FIR}]}, \cdots]$ are the infinite matrix representations of $T_p(\zeta)$ and $\Theta_{ij}^{[\mathrm{FIR}]}$, respectively. The explicit form of the former is given by

$$\widetilde{T}_p = \begin{bmatrix} T_{p,0} & 0 & \cdots \\ \vdots & T_{p,0} & \ddots \\ T_{p,K} & \vdots & \ddots \\ 0 & T_{p,K} & \ddots \\ \vdots & \ddots & \ddots \end{bmatrix}, \tag{5.38}$$

if we introduce the matrices

$$T_{p,i} = \begin{bmatrix} \delta_{Ki} I_p \\ \vdots \\ \delta_{1i} I_p \\ \delta_{0i} I_p \end{bmatrix}, \ i = 0, 1, \ldots, K \tag{5.39}$$

with the Kronecker delta δ_{ij}. Hence, it follows that $\widetilde{\Theta}_{\mathrm{FIR}} = \left(\widetilde{\Theta}_{\mathrm{FIR},ij}\right)_{i,j=1,2}$, where

$$\widetilde{\Theta}_{\mathrm{FIR},ij} = \begin{bmatrix} \Theta_{ij}^{[0]} & \Theta_{ij}^{[1]} & \cdots & \Theta_{ij}^{[K]} & 0 & \cdots \\ \Theta_{ij}^{[-1]} & \Theta_{ij}^{[0]} & \Theta_{ij}^{[1]} & \cdots & \Theta_{ij}^{[K]} & \ddots \\ \vdots & \Theta_{ij}^{[-1]} & \ddots & \ddots & \ddots & \ddots \\ \Theta_{ij}^{[-K]} & \vdots & \ddots & & & \\ 0 & \Theta_{ij}^{[-K]} & \ddots & & & \\ \vdots & \ddots & \ddots & & & \end{bmatrix}. \tag{5.40}$$

It should be noted that the above infinite matrix is block Toeplitz, which is obtained by repeatedly shifting the matrix $\Theta_{ij}^{[\mathrm{FIR}]}$ toward the right-lower direction by one block and then superposing the resulting matrices. Since only $\Theta_{ij}^{[k]} \in \mathbf{R}^{p\times p},\ k = 0, \pm 1, \ldots, \pm K$ are nonzero submatrices in $\widetilde{\Theta}_{\mathrm{FIR},ij}$, we simply say that $\widetilde{\Theta}_{\mathrm{FIR}}$ has band structure with one-side width K *with respect to the size of* $\mathbf{R}^{p\times p}$.

In the special case of a static causal LTI separator, i.e., when $K = 0$, each block of $\widetilde{\Theta}_{\mathrm{FIR}}$ reduces to an infinite block diagonal (and Toeplitz) matrix. Increasing K leads to the increase in the one-side width of (or the freedom in) the band structure associated with the infinite-dimensional separator $\widetilde{\Theta}_{\mathrm{FIR}}$. We could formally regard the limit of such band structure for $K \to \infty$ to be a general block Toeplitz structure.

5.3.2 Noncausal LPTV separator characterized by finite impulse response

Next, let us consider the noncausal LPTV FIR separator $\widehat{\Theta}_{\mathrm{FIR}}(z) = \widehat{\Theta}_{\mathrm{FIR}}(z)^*$ (defined for $z \in \partial\mathbf{D}$ in the lifting-based framework), which is given by $\widehat{\Theta}_{\mathrm{FIR}}(z) = \left(\widehat{\Theta}_{\mathrm{FIR},ij}(z)\right)_{i,j=1,2}$, where $\widehat{\Theta}_{\mathrm{FIR},ij}(z)$ is given by $\Theta_{\mathrm{FIR},ij}(\zeta)$ with ζ replaced by z and $\Theta_{ij}^{[k]}$ replaced by $\widehat{\Theta}_{ij}^{[k]}$ in (5.34). By parallel arguments to those in the preceding subsection, the infinite matrix representation of this separator is given by $\widetilde{\Theta}_{\mathrm{FIR}} = \left(\widetilde{\Theta}_{\mathrm{FIR},ij}\right)_{i,j=1,2}$ with $\widetilde{\Theta}_{\mathrm{FIR},ij}$ given by (5.40) whose $\Theta_{ij}^{[k]}$ is replaced by $\widehat{\Theta}_{ij}^{[k]}$ again. Hence, it is obvious that this infinite-dimensional separator also has band structure with one-side width K *with respect to the size of* $\mathbf{R}^{Np\times Np}$. That is, the structure depends on both K and N, which are related to frequency dependence and time dependence, respectively.

The preceding subsection observed that the infinite matrix representation of the causal LTI FIR separator (5.34) has band structure with one-side width K with respect to the size of $\mathbf{R}^{p\times p}$. The degree of freedom in its structure can be increased by taking larger K (the index for frequency dependence). The size of matrices constituting the band, however, remains the same regardless of K. For a noncausal LPTV FIR separator, on the other hand, the role of K remains the same, while the size of matrices constituting the band structure depends on N (the index for time dependence). Hence, even under fixed K (e.g., $K = 0$ leading to static separators), the degree of freedom in the associated band structure can be increased as the lifting period N increases. An important question about noncausal LPTV scaling would be whether there can be established some explicit relationship between the freedom with respect to K (relevant to frequency dependence) and that with respect to N (relevant to time dependence). We demonstrate in the following section that the framework of infinite matrix representations developed in this chapter provides a very clear and intuitive insight that is helpful to studying such issues.

5.4 Comparison of different scaling approaches through infinite matrix framework

The purpose of this section is to demonstrate the usefulness of the framework of infinite matrix representations developed in this chapter, as a unified medium for dealing with lifting-free (i.e., causal LTI) and lifting-based (i.e., noncausal LPTV) scaling approaches to robust stability analysis.

In the following arguments, we occasionally refer to the schematic picture of the infinite-dimensional separator $\widetilde{\Theta}_{ij}$ as in Figure 5.1 to ease descriptions and help intuitive under-

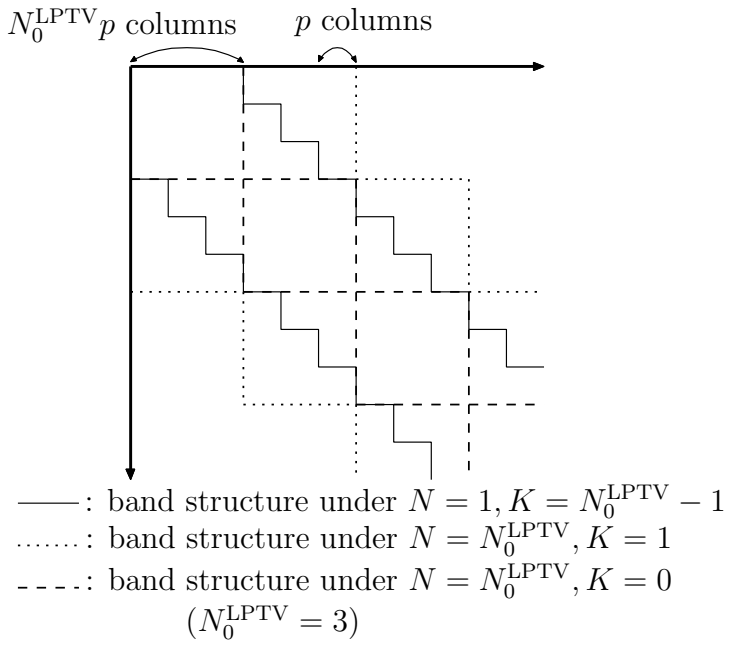

Figure 5.1: Schematic picture of infinite matrix representation $\widetilde{\Theta}_{ij}$.

standing; this picture assumes the case of noncausal LPTV scaling with $N = N_0^{\mathrm{LPTV}}$ for $N_0^{\mathrm{LPTV}} = 3$, but it applies at the same time to causal LTI scaling (i.e., with $N = 1$) by considering $p \times p$ submatrices in this figure. An explicit description about our standing assumption (on the stability of the transfer matrices contained in separators) is suppressed for conciseness in this section.

5.4.1 Noncausal LPTV separator induced by causal LTI separator

In this subsection, we assume that the infinite matrix representation (5.10) of a causal LTI separator $\Theta(\zeta)$ is eligible in the infinite matrix framework. Our purpose here is to discuss what implications will follow (what separators may be induced equivalently) under the interpretation of $\Theta(\zeta)$ from the noncausal LPTV scaling viewpoint.

Here, recall that the infinite matrix representation of a system and that of its N-lifted description coincide with each other, regardless of N. This, together with the inspection of the infinite matrix representations (5.10) and (5.11), leads immediately to the following result.

Theorem 5.3 Suppose the infinite-dimensional separator (5.10) associated with the causal LTI separator (5.7) is eligible. Then, the infinite matrix representation of the lifted counterpart $\widehat{\mathrm{E}}[\Theta(\zeta)]$ (see Section 4.2 for the definition of the embedding mapping $\widehat{\mathrm{E}}[\cdot]$) of $\Theta(\zeta)$ is also eligible.

We need no manipulations of equations to prove this theorem, and it just suffices to

change the way to view infinite matrices by taking different partitioning. Indeed, if the band structure in Figure 5.1 shown with solid lines is block Toeplitz in terms of submatrices in $\mathbf{R}^{p\times p}$, then it can also be viewed as block Toeplitz in terms of submatrices in $\mathbf{R}^{Np\times Np}$ (consider the band structure in Figure 5.1 shown with dot lines), and this together with close inspection of the forms of the latter submatrices completes the proof. We can easily see that the converse assertion of the above theorem also holds.

Remark 5.1 The implication of the above theorem is essentially the same as that of Theorems 4.1 in the preceding chapter, even though the assertion in the latter has been stated without introducing the infinite matrix framework. The role of this new framework in the above theorem and its proof is believed to be transparent and much more intuitive and comprehensible compared with the techniques in the preceding chapter based on the frequency-domain properties of lifted systems.

We see that $\widehat{\mathrm{E}}[\Theta(\zeta)]$ is a causal LPTV separator. Hence by Theorem 5.3, if (i) there exists an eligible causal LTI separator in the lifting-free framework, then (ii) there exists an eligible causal LPTV separator in the lifting-based framework, while it is obvious that the condition (ii) implies (iii) there exists an eligible noncausal LPTV separator. If we apply the technique with $\widetilde{S}_p$ introduced in the following subsection, we can readily establish that (iii) implies (i). Hence, these three conditions are in fact equivalent.

Since we have started our arguments from two robust stability theorems, each of which gives an apparently different but *necessary and sufficient* condition for robust stability, the mere observation above is actually a trivial consequence. The value of the above theorem rather lies in that it clarifies an explicit mutual correspondence among eligible separators in different frameworks.

In spite of the equivalence of the above conditions (i)–(iii), however, it does not simply imply that noncausal LPTV scaling offers no advantage over causal LTI scaling even in a practical sense. Indeed, a more substantial comparison should be made about different scaling approaches under the practical situation in which the search of eligible separators can only be carried out within some restricted but tractable class. As a matter of fact, the most fundamental motivation of the present chapter lies in the comparison of causal LTI and noncausal LPTV scaling approaches under such a viewpoint.

As an example of restricted but tractable classes, we consider a class of causal LTI FIR separators with the order $K = K_0^{\mathrm{LTI}}$. Then, the following theorem holds.

Theorem 5.4 If there exists an eligible causal LTI FIR separator with $K = K_0^{\mathrm{LTI}}$ in the lifting-free framework, there exists an eligible noncausal LPTV FIR separator with $N =$

N_0^{LPTV} and $K = K_0^{\mathrm{LPTV}}$ in the lifting-based framework, provided that

$$K_0^{\mathrm{LPTV}} N_0^{\mathrm{LPTV}} \geq K_0^{\mathrm{LTI}}. \tag{5.41}$$

To see the assertion, consider the band structure with one-side width K with respect to the size of $\mathbf{R}^{p\times p}$, and suppose that it is included in the band structure with one-side width K_0^{LPTV} with respect to the size of $\mathbf{R}^{N_0^{\mathrm{LPTV}}p\times N_0^{\mathrm{LPTV}}p}$. It is easy to see that the maximal value of such K equals $K_0^{\mathrm{LPTV}} N_0^{\mathrm{LPTV}}$, and this immediately leads to the assertion. The fact provided in this theorem is not obvious without exploiting the infinite matrix framework, and this clearly demonstrates a situation in which the new unified framework is quite useful.

5.4.2 Causal LTI separator induced by noncausal LPTV separator

The preceding subsection was under the existence assumption of the eligible infinite matrix representation of a causal LTI separator. In contrast, this subsection assumes that the infinite matrix representation of an eligible noncausal LPTV separator is given, and studies what implications will follow by interpreting it in the causal LTI scaling viewpoint.

Let us introduce the infinite matrix[1]

$$\widetilde{S}_p = \begin{bmatrix} 0_{p\times\infty} \\ \widetilde{I} \end{bmatrix} \tag{5.42}$$

where $\widetilde{I}$ denotes the infinite matrix representation of the identity system with p inputs and outputs. Since $\widetilde{G}$ is block Toeplitz, it is easy to see that

$$\widetilde{G}\widetilde{S}_p = \begin{bmatrix} 0_{p\times\infty} \\ \widetilde{G} \end{bmatrix} = \widetilde{S}_p\widetilde{G}. \tag{5.43}$$

The same arguments apply also to the uncertainty Δ. Hence, by post-multiplying $\widetilde{S}_p$ and pre-multiplying its adjoint on (5.8) and (5.9), we see that the infinite-dimensional separator

$$\mathrm{diag}[\widetilde{S}_p, \widetilde{S}_p]^* \widetilde{\Theta} \mathrm{diag}[\widetilde{S}_p, \widetilde{S}_p] = \left(\widetilde{S}_p^* \widetilde{\Theta}_{ij} \widetilde{S}_p\right)_{i,j=1,2} \tag{5.44}$$

is also eligible. The submatrix $\widetilde{S}_p^* \widetilde{\Theta}_{ij} \widetilde{S}_p$ is nothing but the infinite matrix obtained by removing the first p rows and columns of $\widetilde{\Theta}_{ij}$ (and then by shifting the result toward the left-upper direction to stay at the same position); note by the assumption on $\widetilde{\Theta}$ that $\widetilde{\Theta}_{ij}$ is block Toeplitz in terms of submatrices in $\mathbf{R}^{Np\times Np}$, and the above p rows and columns removed correspond to only a fraction of the underlying block. Hence, we can repeat applying

[1]The matrix $\widetilde{S}_p$ is in fact the infinite matrix representation of the timing-shift matrix $S_p(z)$ introduced in the preceding chapter.

diag$[\widetilde{S}_p, \widetilde{S}_p]$ on the resulting "shifted infinite-dimensional separator" for N times, when the resulting shifted separator reverts to the original $\widetilde{\Theta}$. We will thus have N distinguishable eligible infinite-dimensional separators (including the original one) in this process, and their average (this is nothing but the shift-invariant reconstruction of the infinite-dimensional separator) is also eligible since the conditions are affine with respect to the separator.

For example, if the original $\widetilde{\Theta}$ corresponds to a static noncausal LPTV separator (i.e., $K = 0$ as in the band structure in Figure 5.1 shown with dash lines), then we can see that the above averaged infinite-dimensional separator will have the band structure with respect to the size of $\mathbf{R}^{p\times p}$ (this in particular implies that it is block Toeplitz) shown in solid lines in the figure. In other words, the existence of an eligible static noncausal LPTV separator under the lifting period $N = N_0^{\mathrm{LPTV}}$ ensures that of an eligible (dynamic) causal LTI FIR separator with K not exceeding $N_0^{\mathrm{LPTV}} - 1$. Extending this observation to the case of general noncausal LPTV FIR separators readily leads to the following result.

Theorem 5.5 If there exists an eligible noncausal LPTV FIR separator with $N = N_0^{\mathrm{LPTV}}$ and $K = K_0^{\mathrm{LPTV}}$ in the lifting-based framework, there exists an eligible causal LTI FIR separator with $K = K_0^{\mathrm{LTI}}$ in the lifting-free framework, provided that

$$K_0^{\mathrm{LTI}} + 1 \geq (K_0^{\mathrm{LPTV}} + 1)N_0^{\mathrm{LPTV}}. \tag{5.45}$$

This theorem gives a class of causal LTI FIR separators with which the associated causal LTI scaling is ensured to be less conservative than (to be more precise, at least as effective as) noncausal LPTV FIR scaling with $N = N_0^{\mathrm{LPTV}}$ and $K = K_0^{\mathrm{LPTV}}$, while Theorem 5.4 discusses the opposite direction. More specifically, the implications of these two theorems can be summarized as follows. With respect to the conservativeness of robust stability analysis, noncausal LPTV FIR scaling with $N = N_0^{\mathrm{LPTV}}$ and $K = K_0^{\mathrm{LPTV}}$ is superior to (at least, not inferior to) causal LTI FIR scaling with $K = K_0^{\mathrm{LPTV}} N_0^{\mathrm{LPTV}}$. However, the former is inferior to (at least, not superior to) another enhanced causal LTI FIR scaling with K increased by $N_0^{\mathrm{LPTV}} - 1$, i.e., with K given by $K = (K_0^{\mathrm{LPTV}} + 1)N_0^{\mathrm{LPTV}} - 1$.

From the two theorems in this section, we can see how the conservativeness of the causal LTI and noncausal LPTV FIR scaling approaches varies with the order K for frequency dependence and the lifting period N, and the comparison of such conservativeness can be carried out through the conditions (5.41) and (5.45) in an explicit fashion. Although this is only a discussion for the relationship between causal LTI and noncausal LPTV FIR scaling approaches, the infinite matrix framework is equally effective for comparing other particular scaling approaches defined in the lifting-free and lifting-based frameworks.

5.5 Concluding remarks

Aiming at developing a framework for facilitating further clarification of the relationships between the conventional lifting-free causal LTI scaling and lifting-based noncausal LPTV scaling approaches, this chapter first gave the infinite matrix representation counterparts of the robust stability conditions underlying these approaches. This successfully led to a unified framework for dealing with the two approaches through the idea of infinite-dimensional separators. Explicit forms of the infinite-dimensional separators were given for these approaches, and were shown to have mutually different types of block Toeplitz (band) structure. The arguments also showed how noncausal and time-varying nature as well as frequency dependence introduced into scaling is reflected on the (band) structure. It was then demonstrated that the difference in the structure provides us with a very clear and intuitive interpretation on the difference in the two scaling approaches, and some relationship between these approaches was understood with the infinite matrix framework in a very comprehensible way. The benefit of developing the infinite matrix framework is thus clear, and this framework is believed to be very useful in further theoretical studies.

Chapter 6

Robust Stability Analysis Based on Noncausal LPTV FIR Scaling

6.1 Introduction

Chapters 4 and 5 studied the properties of dynamic noncausal LPTV scaling from theoretical viewpoints. This chapter, on the other hand, discusses the scaling approach from the viewpoint of how to exploit it in actual analysis problems in an efficient fashion.

The necessary and sufficient condition in the (lifting-based) separator-type robust stability theorem consists of two types of inequalities, one for the nominal system while the other for uncertainties, where the latter consists of infinitely many inequalities, in accordance with the fact that there are infinitely many possible uncertainties. To handle these inequalities, a restricted but tractable class of separators is usually introduced satisfying the following properties: (i) the class can be represented with a finite number of parameters; (ii) the infinitely many inequalities for uncertainties are satisfied on the class in a sufficient fashion. Such treatment, however, leads to conservativeness in robust stability analysis. For less conservative robust stability analysis, this chapter confines itself to what we call noncausal LPTV FIR separators, which satisfy (i), and develops a framework called noncausal LPTV FIR scaling for exploiting such separators through the lifting-based treatment. Regarding such discussions, once a basis for numerical treatment of (lifting-free) causal LTI FIR scaling is established, noncausal LPTV FIR scaling can essentially be dealt with as its extension. Hence, developing an explicit procedure of robust stability analysis based on causal LTI FIR scaling is important as a preliminary step for the discussions in this chapter, and thus we first study it.

This chapter begins by briefly discussing through the basic idea of (D, G)-scaling [13] what constraints should be placed on causal LTI FIR separators so that the property (ii) is satisfied, and gives explicit structure of the class of causal LTI FIR separators dealt with

in this chapter. This explicit structure, in principle, immediately leads us to a systematic method for searching for an eligible (i.e., satisfying the condition for robust stability) causal LTI FIR separator; indeed, applying the KYP lemma [34] readily converts the search, without any conservativeness, to an LMI problem involving the static coefficient matrices of FIR separators. To avoid undue increase in the computational load for solving the LMI, however, an explicit but nontrivial minimal realization is further derived about an augmented system to which the KYP lemma will be applied. This is a crucial step not merely from a practical point of view but also from a theoretical point of view. It is partly because employing a minimal realization maximally improves the ability of causal LTI FIR scaling, and theoretically clarifying its order could provide us with an estimate of the associated computational load. Based on these discussions, we further develop an explicit procedure of robust stability analysis based on noncausal LPTV FIR scaling, and numerically demonstrate its effectiveness through the comparison with the conventional static LTI scaling and μ-analysis. Note that the relationship between causal LTI and noncausal LPTV FIR scaling approaches with respect to conservativeness in the analysis has been theoretically studied as Theorems 5.4 and 5.5 in the preceding chapter. Hence, the validity of these results will also be confirmed with an example in this chapter.

This chapter is organized as follows. Section 6.2 states the robust stability problem dealt with in this chapter, and revisits the definition of causal LTI FIR scaling. This section then considers restricting the class of causal LTI FIR separators to the (D, G)-scaling type, and clarifies the structure of the (D, G)-scaling type causal LTI FIR separators suitable for dealing with a given set of structured uncertainties. On the basis of this step, Section 6.3 shows a method of searching for an eligible causal LTI FIR separator. In particular, from the computational viewpoint, this section derives a minimal realization of an augmented system involved in the analysis, and gives an LMI condition. Section 6.4 extends the developed analysis procedure to that of noncausal LPTV FIR scaling through employing the lifting-based treatment. Section 6.5 demonstrates with numerical examples the effectiveness of noncausal LPTV FIR scaling, and also numerically confirms the theoretical results shown in the preceding chapter.

6.2 Basic idea of robust stability analysis with causal LTI FIR scaling

In this section, we first state the problem studied in this chapter. Then, as a preliminary step for developing an explicit robust stability analysis method based on noncausal LPTV FIR scaling, we introduce causal LTI FIR scaling without lifting-based treatment. We also

consider restricting the associated causal LTI FIR separators to (D, G)-scaling type for actual analysis problems, and explicitly show an appropriate structure of the separators that is crucial for dealing with the structured uncertainties.

6.2.1 Robust stability analysis problem with LTI structured uncertainty

Let us consider the discrete-time closed-loop system Σ (Figure 2.3) consisting of the nominal system G and the uncertainty Δ. The system G is assumed to be internally stable, finite-dimensional, LTI, and represented by (5.1) with $x_k \in \mathbf{R}^n$, $u_k \in \mathbf{R}^p$ and $y_k \in \mathbf{R}^p$. On the other hand, Δ is assumed to belong to a given set $\boldsymbol{\Delta}$ satisfying the following assumption.

Assumption 3 Every $\Delta \in \boldsymbol{\Delta}$ is finite-dimensional and LTI, and the corresponding transfer matrix has the block-diagonal structure

$$\Delta(\zeta) = \mathrm{diag}[\delta_1 I_{m_1}, \cdots, \delta_S I_{m_S}, \Delta_1, \cdots, \Delta_F, \Delta_1(\zeta), \cdots, \Delta_Z(\zeta)], \tag{6.1}$$

with $\delta_i \in \mathbf{R}$ $(i = 1, \ldots, S)$, $\Delta_i \in \mathbf{R}^{n_i \times n_i}$ $(i = 1, \ldots, F)$ and $\Delta_i(\zeta) \in \mathbf{RH}_\infty^{l_i \times l_i}$ $(i = 1, \ldots, Z)$. In addition, every $\Delta \in \boldsymbol{\Delta}$ satisfies the H_∞ norm condition $\|\Delta\|_\infty < 1/\gamma$ for a given $\gamma > 0$.

This chapter studies the problem of numerically deciding whether the above closed-loop system Σ is robustly stable with respect to $\boldsymbol{\Delta}$ for a given γ.

6.2.2 Causal LTI FIR scaling

Since causal LTI scaling corresponds to a generalization of the conventional frequency-dependent scaling such as D-scaling, its fundamental idea is not necessarily novel, yet a method for exploiting the idea in the actual problems has not been deeply developed. This is because the class consisting of all causal LTI separators is very large, and it is hard to develop a systematic way to search, in a necessary and sufficient fashion, for an eligible separator from that class. An easy direction to circumvent the difficulty at the price of possible conservativeness in analysis is to fix $V(\zeta)$ of the causal LTI separator

$$\Theta(\zeta) = V(\zeta)^* \Lambda V(\zeta). \tag{6.2}$$

More precisely, if a proper and stable transfer matrix $V(\zeta)$ is given, then it follows from the KYP lemma [34] that the problem of searching for a separator (6.2) satisfying (2.15), the condition for the nominal system G, reduces to an LMI problem with respect to the constant matrix Λ. This problem should be much easier than dealing directly with $\Theta(\zeta)$ with arbitrary $V(\zeta)$. To exploit such an idea, we confine ourselves to the class of special

causal LTI separators $\Theta_{\mathrm{FIR}}(\zeta) = \Theta_{\mathrm{FIR}}(\zeta)^*$ ($\zeta \in \partial\mathbf{D}$) given by (5.34). If $V(\zeta)$ in (6.2) is given by the z-transform of an FIR, the separator $\Theta(\zeta)$ can be represented in the form of (5.34). Conversely, every separator in the form (5.34) can be represented in the form of (6.2) for the fixed $V(\zeta)$ given by

$$V(\zeta) := \begin{bmatrix} V_1(\zeta) & V_2(\zeta) \end{bmatrix} = \mathrm{diag}[T_p(\zeta), T_p(\zeta)],\ T_p(\zeta) = \begin{bmatrix} \zeta^{-K} I_p \\ \vdots \\ \zeta^{-1} I_p \\ I_p \end{bmatrix}, \tag{6.3}$$

which is the z-transform of an FIR. Thus, we call a separator given by (5.34) a causal LTI FIR separator, as introduced in the preceding chapter. Causal LTI FIR scaling is the approach to robust stability analysis based on causal LTI FIR separators. A rationale for our confining to causal LTI FIR scaling can be given by the fact that every causal LTI separator with a given stable transfer matrix $V(\zeta)$ and a given Λ can be approximated by a causal LTI FIR separator with large enough "order" K, whereas, once the order K is fixed, the class of such causal LTI FIR separators can be described with a finite number of matrices $\Theta_{ij}^{[k]}$ and thus should be easy to deal with (compared with the class of dynamic causal LTI separators with $V(\zeta)$ confined to a given class). In this connection, it is known that the necessity assertion of Theorem 2.3 remains true even if $V(\zeta)$ is confined to stable transfer matrices. Hence, causal LTI FIR scaling is expected to alleviate the difficulties in the search of an eligible dynamic separator without introducing excessive conservativeness. This advantage is expected to be inherited in the analysis with the extended noncausal LPTV FIR scaling.

Remark 6.1 The causal LTI separator (2.29) induced from the static noncausal LPTV separator $\widehat{\Theta}$ in Theorem 2.5 is nothing but a causal LTI FIR separator, noting that $\zeta^*\zeta = 1$ on $\partial\mathbf{D}$. Although we introduced causal LTI FIR scaling as a preliminary step toward the discussions about noncausal LPTV FIR scaling in this chapter, the former scaling thus has also been a key concept throughout the thesis.

6.2.3 (D, G)-scaling type of causal LTI FIR separators

To exploit causal LTI FIR scaling in a tractable way, we next introduce a particular class of causal LTI FIR separators. Specifically, we consider restricting the class of causal LTI FIR separators to (D, G)-scaling type, and describe explicit constraints on the (D, G)-scaling type causal LTI FIR separators under which inequality (2.16) is automatically satisfied for the given uncertainty set $\boldsymbol{\Delta}$. Introducing such a class is crucial since robust stability analysis can then be tackled by searching, within the restricted class, for an (eligible) separator satisfying

the other inequality (2.15) about the nominal system, as stated in Chapter 3 in the case of static scaling.

Let us take the γ in Assumption 3 and consider the separator of the (D, G)-scaling type given by

$$\Theta(\zeta) = \begin{bmatrix} -\gamma^2 \Theta_D(\zeta) & \Theta_G(\zeta) \\ \Theta_G(\zeta)^* & \Theta_D(\zeta) \end{bmatrix}, \tag{6.4}$$

$$\Theta_D(\zeta) > 0 \ \ (\forall \zeta \in \partial \mathbf{D}). \tag{6.5}$$

Suppose that $\Theta_D(\zeta)$ and $\Theta_G(\zeta)$ satisfy

$$\Theta_D(\zeta)\Delta(\zeta) = \Delta(\zeta)\Theta_D(\zeta) \ \ (\forall \Delta \in \boldsymbol{\Delta}, \forall \zeta \in \partial \mathbf{D}), \tag{6.6}$$

$$\Theta_G(\zeta)^* \Delta(\zeta) + \Delta(\zeta)^* \Theta_G(\zeta) = 0 \ \ (\forall \Delta \in \boldsymbol{\Delta}, \forall \zeta \in \partial \mathbf{D}). \tag{6.7}$$

As is well known, inequality (2.16) then reduces to $\|\Delta(\zeta)\|_\infty < 1/\gamma$ and thus it does hold by Assumption 3. Therefore, robust stability can easily be analyzed by searching for a (D, G)-scaling type separator (6.4) satisfying (2.15) together with constraints (6.5)–(6.7). A class of causal LTI FIR separators of order K (thus $V(\zeta)$ is given by (6.3)) that lead to $\Theta_D(\zeta)$ and $\Theta_G(\zeta)$ satisfying (6.6) and (6.7) can easily be constructed as

$$\boldsymbol{\Theta}_{\mathrm{FIR}}(\zeta) = \left\{ \mathrm{diag}[T_p(\zeta), T_p(\zeta)]^* \Theta^{[\mathrm{FIR}]} \mathrm{diag}[T_p(\zeta), T_p(\zeta)] \,\middle|\, \Theta^{[\mathrm{FIR}]} \in \boldsymbol{\Theta}^{[\mathrm{FIR}]} \right\} \tag{6.8}$$

where $\boldsymbol{\Theta}^{[\mathrm{FIR}]}$ denotes the set of constant matrices $\Theta^{[\mathrm{FIR}]}$ such that

$$\Theta^{[\mathrm{FIR}]} = \begin{bmatrix} -\gamma^2 \Theta_D^{[\mathrm{FIR}]} & \Theta_G^{[\mathrm{FIR}]} \\ (\Theta_G^{[\mathrm{FIR}]})^T & \Theta_D^{[\mathrm{FIR}]} \end{bmatrix}, \tag{6.9}$$

$$\Theta_D^{[\mathrm{FIR}]} = (\Theta_D^{[\mathrm{FIR}]})^T \in \boldsymbol{\Theta}_D^{[\mathrm{FIR}]}, \ \ \Theta_G^{[\mathrm{FIR}]} = -(\Theta_G^{[\mathrm{FIR}]})^T \in \boldsymbol{\Theta}_G^{[\mathrm{FIR}]} \tag{6.10}$$

with $\boldsymbol{\Theta}_D^{[\mathrm{FIR}]}$ defined as the set of matrices

$$\Theta_K = \begin{bmatrix} \Theta^{[0]} & \Theta^{[1]} & \cdots & \Theta^{[K]} \\ \Theta^{[-1]} & 0 & \cdots & 0 \\ \vdots & \vdots & \ddots & \vdots \\ \Theta^{[-K]} & 0 & \cdots & 0 \end{bmatrix} \in \mathbf{R}^{(K+1)p \times (K+1)p}, \tag{6.11}$$

$$\Theta^{[k]} = \mathrm{diag}[\Theta_1^{[k]}, \cdots, \Theta_S^{[k]}, \theta_{\mathrm{s}1}^{[k]} I_{n_1}, \cdots, \theta_{\mathrm{s}F}^{[k]} I_{n_F}, \theta_{\mathrm{d}1}^{[k]} I_{l_1}, \cdots, \theta_{\mathrm{d}Z}^{[k]} I_{l_Z}] \in \mathbf{R}^{p \times p}, \tag{6.12}$$

$$\Theta_i^{[k]} \in \mathbf{R}^{m_i \times m_i} \ \ (i = 1, \ldots, S), \tag{6.13}$$

$$\theta_{\mathrm{s}i} \in \mathbf{R} \ \ (i = 1, \ldots, F), \tag{6.14}$$

$$\theta_{\mathrm{d}i} \in \mathbf{R} \ \ (i = 1, \ldots, Z) \tag{6.15}$$

and $\boldsymbol{\Theta}_G^{[\mathrm{FIR}]}$ as the set of Θ_K with $\Theta^{[k]}$ replaced by

$$\Theta^{[k]} = \mathrm{diag}[\Theta_1^{[k]}, \cdots, \Theta_S^{[k]}, 0_{n_1}, \cdots, 0_{n_F}, 0_{l_1}, \cdots, 0_{l_Z}]. \tag{6.16}$$

Indeed, we can readily see that every $\Theta_{\mathrm{FIR}}(\zeta) \in \boldsymbol{\Theta}_{\mathrm{FIR}}(\zeta)$ is a (Hermitian) causal LTI FIR separator with $\Theta_{\mathrm{FIR},ij}(\zeta)$ (i.e., the resulting $\Theta_D(\zeta)$ and $\Theta_G(\zeta)$) being block diagonal since $\Theta^{[k]}$ is. A close inspection of the structure of $\Theta_D(\zeta)$ and $\Theta_G(\zeta)$ readily leads to (6.6) and (6.7) if we note the second equation in (6.10).

Summarizing the above arguments, we see that it suffices to search for such a causal LTI FIR separator $\Theta(\zeta) = \Theta_{\mathrm{FIR}}(\zeta)$ in the class $\boldsymbol{\Theta}_{\mathrm{FIR}}(\zeta)$ satisfying (2.15) as well as the remaining constraint (6.5). The first constraint (2.15) can readily be rewritten as

$$G_{\mathrm{a}}(\zeta)^* \Theta^{[\mathrm{FIR}]} G_{\mathrm{a}}(\zeta) \leq 0 \quad (\forall \zeta \in \partial\mathbf{D}), \tag{6.17}$$

where

$$G_{\mathrm{a}}(\zeta) := \mathrm{diag}[T_p(\zeta), T_p(\zeta)] \begin{bmatrix} I \\ G(\zeta) \end{bmatrix}. \tag{6.18}$$

A similar comment applies also to the second constraint (6.5); it is obviously equivalent to

$$T_p(\zeta)^* \Theta_D^{[\mathrm{FIR}]} T_p(\zeta) > 0 \quad (\forall \zeta \in \partial\mathbf{D}). \tag{6.19}$$

Hence, the problem to be solved for exploiting causal LTI FIR (D, G)-scaling is to search for a static matrix $\Theta^{[\mathrm{FIR}]}$ satisfying the frequency-dependent conditions (6.17) and (6.19) under the structural constraints (6.9) and (6.10).

6.3 LMI reformulation of causal LTI FIR scaling

6.3.1 Minimal realization of the augmented system $G_{\mathrm{a}}(\zeta)$

Once we obtain a realization of the augmented system $G_{\mathrm{a}}(\zeta)$ introduced in (6.18), the frequency-dependent inequality (6.17) immediately reduces to an LMI condition by the KYP lemma, and a similar argument applies also to (6.19). A minimal realization of $T_p(\zeta)$ in (6.19) can readily be obtained. Thus, we confine this subsection to the derivation of a minimal realization of $G_{\mathrm{a}}(\zeta)$. Such a discussion is important not only from a practical viewpoint but also from a theoretical viewpoint since clarifying the order of the minimal realization could provide us with an estimate of the associated computational load in the analysis.

Although it is straightforward to construct a realization of $G_{\mathrm{a}}(\zeta)$ with order $2Kp + n$, where n denotes the order of a minimal realization of $G(\zeta)$, the resulting realization can

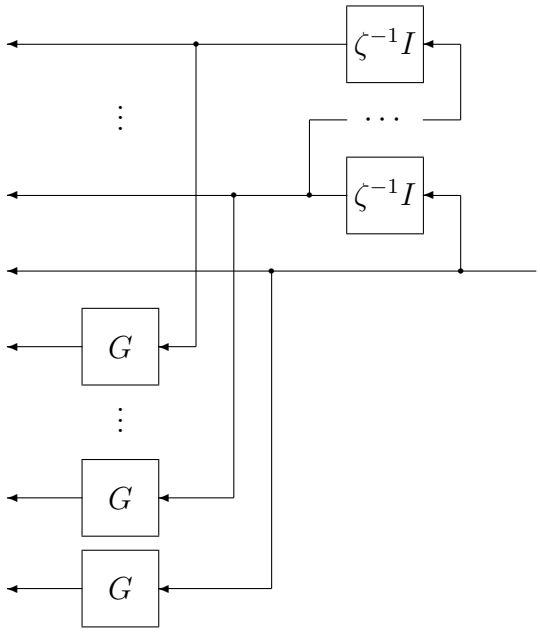

Figure 6.1: Nominal system G_{a} for FIR scaling.

be confirmed to non-minimal when $K \geq 1$. Still worse, it seems hard to derive a closed-form minimal realization by eliminating redundant states in such a non-minimal realization. Hence, we begin by introducing another non-minimal realization of $G_{\mathrm{a}}(\zeta)$ suitable as an initial step for deriving a minimal realization of it. We see that G_{a} can be represented by the block diagram in Figure 6.1. From this block diagram, we can readily obtain a realization of $G_{\mathrm{a}}(\zeta)$ given by

$$(A_{\mathrm{a}0}, B_{\mathrm{a}0}, C_{\mathrm{a}0}, D_{\mathrm{a}0}) := \left[\begin{array}{cc:c:c} 0_{(K-1)p\times p} & I_{(K-1)p} & 0 & 0_{(K-1)p\times p} \\ 0_p & 0_{p\times(K-1)p} & & I_p \\ \hdashline I_K \otimes B & & I_{K+1}\otimes A & 0_{Kn\times p} \\ 0_{n\times Kp} & & & B \\ \hline I_{Kp} & & 0 & 0_{Kp\times p} \\ 0_{p\times Kp} & & & I_p \\ \hdashline I_K \otimes D & & I_{K+1}\otimes C & 0_{Kp\times p} \\ 0_{p\times Kp} & & & D \end{array}\right], \tag{6.20}$$

where (A, B, C, D) denotes a minimal realization of $G(\zeta)$. Note that the order of the above realization is $(Kp + n) + Kn$.

Taking account of the structure of the reachability matrix associated with the realization

(6.20), we define the similarity transformation matrix

$$V = \left[\begin{array}{ccccc:ccccc} & & I_{Kp} & & & & & 0 & & \\ \hdashline 0_{n\times p} & & & & & I_n & & & & \\ B & & & & & A & \ddots & & & \\ AB & & \ddots & & & A^2 & \ddots & \ddots & & \\ \vdots & & \ddots & \ddots & & \vdots & \ddots & \ddots & \ddots & \\ A^{K-1}B & \cdots & AB & B & & A^K & \cdots & A^2 & A & I_n \end{array}\right]. \tag{6.21}$$

Indeed, the first K block columns of V correspond to those of the reachability matrix (lined up in the reverse order), while the remaining columns are chosen to make V nonsingular; V is in fact constructed in such a way that V^{-1} has a closed-form representation given by

$$V^{-1} = \left[\begin{array}{ccccc:ccccc} & & I_{Kp} & & & & & 0 & & \\ \hdashline 0_{n\times p} & & & & & I_n & & & & \\ -B & & & & & -A & \ddots & & & \\ & \ddots & & & & & \ddots & \ddots & & \\ & & & -B & & & & -A & I_n & \end{array}\right]. \tag{6.22}$$

Applying the similarity transformation with this V to the realization (6.20) leads to

$$V^{-1}A_{\mathrm{a0}}V = \left[\begin{array}{cc:c} 0_{(K-1)p\times p} & I_{(K-1)p} & 0 \\ 0_p & 0_{p\times(K-1)p} & \\ \hdashline B & 0 & \\ 0 & 0_{Kn\times(K-1)p} & I_{K+1}\otimes A \end{array}\right], \tag{6.23}$$

$$V^{-1}B_{\mathrm{a0}} = \left[\begin{array}{c} 0_{(K-1)p\times p} \\ I_p \\ \hdashline 0_{(K+1)n\times p} \end{array}\right]. \tag{6.24}$$

It is obvious from the structure of the above matrices that the last Kn states of the new realization are unreachable and thus may be discarded. We can readily see that this leads to the following closed-form realization with the order $Kp+n$.

$$\left[\begin{array}{ccccc:c|c} 0_{(K-1)p\times p} & & I_{(K-1)p} & & & 0 & 0_{(K-1)p\times p} \\ 0_p & & 0_{p\times(K-1)p} & & & 0 & I_p \\ \hdashline B & & 0_{n\times(K-1)p} & & & A & 0 \\ \hline & & I_{Kp} & & & 0 & 0_{Kp\times p} \\ & & 0_{p\times Kp} & & & 0 & I_p \\ \hdashline D & & & & & C & \\ CB & \ddots & & & & CA & \\ CAB & \ddots & D & & & \vdots & 0_{Kp\times p} \\ \vdots & \ddots & CB & D & & \vdots & \\ CA^{K-1}B & \ldots & CAB & CB & & CA^K & D \end{array}\right] \tag{6.25}$$

We can see that this realization is reachable and observable, and thus is minimal; we denote it by $(A_{\rm a}, B_{\rm a}, C_{\rm a}, D_{\rm a})$ in the following.

6.3.2 LMI condition for robust stability analysis with causal LTI FIR scaling

Once a minimal realization of $G_{\rm a}(\zeta)$ is given, the following lemma is a direct consequence of the KYP lemma [34].

Lemma 6.1 Suppose that G (and thus $G_{\rm a}$) is internally stable. Then, $G_{\rm a}(\zeta)$ satisfies (6.17) if and only if there exists a real symmetric matrix $P \in \mathbf{R}^{(Kp+n)\times(Kp+n)}$ satisfying

$$\begin{bmatrix} I & 0 \\ A_{\rm a} & B_{\rm a} \\ C_{\rm a} & D_{\rm a} \end{bmatrix}^* \mathrm{diag}\left[-P, P, \Theta^{[\mathrm{FIR}]}\right] \begin{bmatrix} I & 0 \\ A_{\rm a} & B_{\rm a} \\ C_{\rm a} & D_{\rm a} \end{bmatrix} \leq 0. \tag{6.26}$$

By this lemma, we can search for a causal LTI FIR separator satisfying (6.17) and thus (2.15) by solving the LMI (6.26) for $\Theta^{[\mathrm{FIR}]}$ and P.

The remaining constraint (6.5), or equivalently (6.19), is satisfied if and only if there exists a real symmetric matrix $P_T \in \mathbf{R}^{Kp\times Kp}$ such that

$$\begin{bmatrix} I & 0 \\ A_T & B_T \\ C_T & D_T \end{bmatrix}^* \mathrm{diag}\left[-P_T, P_T, -\Theta_D^{[\mathrm{FIR}]}\right] \begin{bmatrix} I & 0 \\ A_T & B_T \\ C_T & D_T \end{bmatrix} < 0, \tag{6.27}$$

where (A_T, B_T, C_T, D_T) denotes the minimal realization of $T_p(\zeta)$ given by

$$\left[\begin{array}{c|c} A_T & B_T \\ \hline C_T & D_T \end{array}\right] = \left[\begin{array}{cc|c} 0_{(K-1)p\times p} & I_{(K-1)p} & 0_{(K-1)p\times p} \\ 0_p & 0_{p\times(K-1)p} & I_p \\ \hline \multicolumn{2}{c|}{I_{Kp}} & 0_{Kp\times p} \\ \multicolumn{2}{c|}{0_{p\times Kp}} & I_p \end{array}\right]. \tag{6.28}$$

Combining all the preceding arguments, we have developed a framework for analyzing robust stability of the closed-loop system Σ with causal LTI FIR (D, G)-scaling; Σ is robustly stable with respect to $\boldsymbol{\Delta}$ satisfying Assumption 3 if the two LMIs (6.26) and (6.27) are solvable for $\Theta^{[\mathrm{FIR}]}$, P and P_T, where $\Theta^{[\mathrm{FIR}]}$ is confined to have the structure given by (6.9) and (6.10).

6.4 Extension to noncausal LPTV FIR scaling

In this section, based on the arguments about causal LTI FIR scaling, we further develop a robust stability analysis method with noncausal LPTV FIR scaling. We first discuss the

(D, G)-scaling type constraint on noncausal LPTV FIR separators defined in the lifting-based framework, and show the specific restricted structure of the separators satisfying such a constraint for the given $\boldsymbol{\Delta}$. We then briefly state the LMI condition for noncausal LPTV FIR scaling in the lifting-based framework.

6.4.1 Constraints on (D, G)-scaling type noncausal LPTV FIR separators

Let us consider the noncausal LPTV FIR separator $\widehat{\Theta}_{\mathrm{FIR}}(z) = \widehat{\Theta}_{\mathrm{FIR}}(z)^*$ (defined for $z \in \partial\mathbf{D}$ in the lifting-based framework), which is given by $\widehat{\Theta}_{\mathrm{FIR}}(z) = \left(\widehat{\Theta}_{\mathrm{FIR},ij}(z)\right)_{i,j=1,2}$, where $\widehat{\Theta}_{\mathrm{FIR},ij}(z)$ is given by $\Theta_{\mathrm{FIR},ij}(\zeta)$ with ζ replaced by z and $\Theta_{ij}^{[k]}$ replaced by $\widehat{\Theta}_{ij}^{[k]}$ in (5.34). This subsection discusses the structure that noncausal LPTV FIR separators have to take so that (2.14) is automatically satisfied with respect to $\boldsymbol{\Delta}$ satisfying Assumption 3.

As a step toward such discussions, we first consider confining the separators to the following (D, G)-scaling type.

$$\widehat{\Theta}_{\mathrm{FIR}}(z) = \begin{bmatrix} -\gamma^2\widehat{\Theta}_D(z) & \widehat{\Theta}_G(z) \\ \widehat{\Theta}_G(z)^* & \widehat{\Theta}_D(z) \end{bmatrix}, \tag{6.29}$$

$$\widehat{\Theta}_D(z) > 0 \quad (\forall z \in \partial\mathbf{D}) \tag{6.30}$$

Then, if $\widehat{\Theta}_D(z)$ and $\widehat{\Theta}_G(z)$ satisfy the conditions

$$\widehat{\Theta}_D(z)\widehat{\Delta}(z) = \widehat{\Delta}(z)\widehat{\Theta}_D(z) \quad (\forall \Delta \in \boldsymbol{\Delta}), \tag{6.31}$$

$$\widehat{\Theta}_G(z)^*\widehat{\Delta}(z) + \widehat{\Delta}(z)^*\widehat{\Theta}_G(z) = 0 \quad (\forall \Delta \in \boldsymbol{\Delta}) \tag{6.32}$$

for the N-lifted transfer matrix $\widehat{\Delta}(z)$ of Δ, inequality (2.14) reduces to $\|\widehat{\Delta}(z)\|_\infty < 1/\gamma$ (i.e., $\|\Delta(\zeta)\|_\infty < 1/\gamma$), and thus it does hold by Assumption 3. Hence, we further confine ourselves to those $\widehat{\Theta}_D(z)$ and $\widehat{\Theta}_G(z)$ satisfying (6.31) and (6.32), as is the case with causal LTI FIR scaling. An inconvenient aspect in dealing with these constraints, however, is that the structure of the lifted $\widehat{\Delta}(z)$ is different from that of the original $\Delta(\zeta)$ in (6.1). For example, if $\Delta(\zeta) = \mathrm{diag}[\delta_1, \delta_2]$ with independent δ_1 and δ_2, its lifted representation with $N = 2$ becomes $\widehat{\Delta}(z) = \mathrm{diag}[\delta_1, \delta_2, \delta_1, \delta_2]$. If this $\widehat{\Delta}(z)$ is represented as the right hand side of (6.1) with ζ replaced by z, we are forced to taking $S = 4$, but this leads to ignoring the fact that both δ_1 and δ_2 appear twice in $\widehat{\Delta}(z)$. To circumvent such inconvenience, we first apply the block checker/diagonal transformation introduced in [20].

For $N \in \mathbf{N}$, $\nu \in \mathbf{N}$ and $\alpha_i \in \mathbf{N}$ $(i = 1, \ldots, \nu)$ with the set $\mathbf{N}$ of positive integers, the permutation matrix

$$E_N(\alpha_1, \cdots, \alpha_\nu) = [E_N^{(1)}(\alpha_1, \cdots, \alpha_\nu), \cdots, E_N^{(\nu)}(\alpha_1, \cdots, \alpha_\nu)] \in \mathbf{R}^{\alpha N \times \alpha N} \tag{6.33}$$

with $\alpha := \sum_{i=1}^{\nu} \alpha_i$ is called a block checker/diagonal transformation matrix, where $E_N^{(i)}(\alpha_1, \cdots, \alpha_\nu)$ $(i = 1, \ldots, \nu)$ is defined as

$$E_N^{(i)}(\alpha_1, \cdots, \alpha_\nu) = I_N \otimes E^{(i)}(\alpha_1, \cdots, \alpha_\nu) \tag{6.34}$$

through the decomposition of the identity matrix I_α into

$$I_\alpha =: [E^{(1)}(\alpha_1, \cdots, \alpha_\nu), \cdots, E^{(\nu)}(\alpha_1, \cdots, \alpha_\nu)], \tag{6.35}$$

with $E^{(i)}(\alpha_1, \cdots, \alpha_\nu) \in \mathbf{R}^{\alpha \times \alpha_i}$ $(i = 1, \ldots, \nu)$. By virtue of

$$E_N^{\Delta} := E_N(m_1, \cdots, m_S, n_1, \cdots, n_F, l_1, \cdots, l_Z), \tag{6.36}$$

we have

$$\begin{aligned} \widehat{\Delta}(z)\grave{} &:= (E_N^{\Delta})^T \widehat{\Delta}(z) E_N^{\Delta} \\ &= \mathrm{diag}[\delta_1 I_{Nm_1}, \cdots, \delta_S I_{Nm_S}, I_N \otimes \Delta_1, \cdots, I_N \otimes \Delta_F, \widehat{\Delta}_1(z), \cdots, \widehat{\Delta}_Z(z)], \end{aligned} \tag{6.37}$$

where $\widehat{\Delta}_i(z)$ is the lifted representation of $\Delta_i(\zeta)$. The structure of $\widehat{\Delta}(z)\grave{}$ is very close to that of $\Delta(\zeta)$ given by (6.1), and the only essential deference between the two structures is that $\Delta_1, \ldots, \Delta_F$ in (6.1) are replaced with $I_N \otimes \Delta_1, \ldots, I_N \otimes \Delta_F$ in (6.37), respectively.

Here, by post-multiplying E_N^{Δ} and pre-multiplying its transpose on (6.31) and (6.32), we have the equivalent conditions

$$\widehat{\Theta}_D(z)\grave{}\widehat{\Delta}(z)\grave{} = \widehat{\Delta}(z)\grave{}\widehat{\Theta}_D(z)\grave{} \quad (\forall \Delta \in \boldsymbol{\Delta}), \tag{6.38}$$

$$\left(\widehat{\Theta}_G(z)\grave{}\right)^* \widehat{\Delta}(z)\grave{} + \left(\widehat{\Delta}(z)\grave{}\right)^* \widehat{\Theta}_G(z)\grave{} = 0 \quad (\forall \Delta \in \boldsymbol{\Delta}), \tag{6.39}$$

where $\widehat{\Theta}_D(z)\grave{} = (E_N^{\Delta})^T \widehat{\Theta}_D(z) E_N^{\Delta}$ and $\widehat{\Theta}_G(z)\grave{} = (E_N^{\Delta})^T \widehat{\Theta}_G(z) E_N^{\Delta}$. Therefore, we can replace the problem of finding the structure of $\widehat{\Theta}_D(z)$ and $\widehat{\Theta}_G(z)$ satisfying (6.31) and (6.32) with the problem of finding the structure of $\widehat{\Theta}_D(z)\grave{}$ and $\widehat{\Theta}_G(z)\grave{}$ satisfying (6.38) and (6.39). The latter problem is essentially the same as the corresponding problem that also arose in causal LTI FIR scaling. Hence, we can readily have an answer to the former problem, whose details will be given in the following subsection.

6.4.2 Specific structure of (D, G)-scaling type noncausal LPTV FIR separators

Let us consider the class of noncausal LPTV FIR separators

$$\widehat{\Theta}_{\rm FIR}(z) = \Big(T_{Np}(z)^* \widehat{\Theta}_{ij}^{[\rm FIR]} T_{Np}(z)\Big)_{i,j=1,2}, \tag{6.40}$$

$$T_{Np}(z) = \begin{bmatrix} z^{-K} I_{Np} \\ \vdots \\ z^{-1} I_{Np} \\ I_{Np} \end{bmatrix}, \ \widehat{\Theta}_{ij}^{[\rm FIR]} = \begin{bmatrix} \widehat{\Theta}_{ij}^{[0]} & \widehat{\Theta}_{ij}^{[1]} & \cdots & \widehat{\Theta}_{ij}^{[K]} \\ \widehat{\Theta}_{ij}^{[-1]} & 0 & \cdots & 0 \\ \vdots & \vdots & \ddots & \vdots \\ \widehat{\Theta}_{ij}^{[-K]} & 0 & \cdots & 0 \end{bmatrix}, \tag{6.41}$$

with

$$\widehat{\Theta}_{22}^{[\rm FIR]} = (\widehat{\Theta}_{22}^{[\rm FIR]})^T \in \widehat{\boldsymbol{\Theta}}_D^{[\rm FIR]}, \tag{6.42}$$

$$\widehat{\Theta}_{12}^{[\rm FIR]} = -(\widehat{\Theta}_{12}^{[\rm FIR]})^T \in \widehat{\boldsymbol{\Theta}}_G^{[\rm FIR]}, \tag{6.43}$$

$$\widehat{\Theta}_{11}^{[\rm FIR]} = -\gamma^2 \widehat{\Theta}_{22}^{[\rm FIR]}, \tag{6.44}$$

$$\widehat{\Theta}_{21}^{[\rm FIR]} = (\widehat{\Theta}_{12}^{[\rm FIR]})^T, \tag{6.45}$$

$$T_{Np}(z)^* \widehat{\Theta}_{22}^{[\rm FIR]} T_{Np}(z) > 0 \ \ (\forall z \in \partial \mathbf{D}), \tag{6.46}$$

where $\widehat{\boldsymbol{\Theta}}_D^{[\rm FIR]}$ is the set consisting of all the matrices given by

$$\widehat{\Theta}_K = \begin{bmatrix} \widehat{\Theta}^{[0]} & \cdots & \widehat{\Theta}^{[K]} \\ \vdots & 0 & 0 \\ \widehat{\Theta}^{[-K]} & 0 & 0 \end{bmatrix}, \tag{6.47}$$

$$\widehat{\Theta}^{[k]} = E_N^{\Delta} {\rm diag}[\widehat{\Theta}_1^{[k]}, \cdots, \widehat{\Theta}_S^{[k]}, \widehat{\Theta}_{\rm s1}^{[k]}, \cdots, \widehat{\Theta}_{{\rm s}F}^{[k]}, \theta_{\rm d1}^{[k]} I_{Nl_1}, \cdots, \theta_{{\rm d}Z}^{[k]} I_{Nl_Z}](E_N^{\Delta})^T, \tag{6.48}$$

$$\widehat{\Theta}_i^{[k]} \in \mathbf{R}^{Nm_i \times Nm_i} \ \ (i = 1, \ldots, S), \tag{6.49}$$

$$\widehat{\Theta}_{\rm si}^{[k]} = \begin{bmatrix} \theta_{{\rm si},11}^{[k]} I_{n_i} & \cdots & \theta_{{\rm si},1N}^{[k]} I_{n_i} \\ \vdots & \ddots & \vdots \\ \theta_{{\rm si},N1}^{[k]} I_{n_i} & \cdots & \theta_{{\rm si},NN}^{[k]} I_{n_i} \end{bmatrix}, \tag{6.50}$$

and $\widehat{\boldsymbol{\Theta}}_G^{[\rm FIR]}$ is the set consisting of all the matrices given by the above $\widehat{\Theta}_K$ with $\widehat{\Theta}^{[k]}$ replaced by

$$\widehat{\Theta}^{[k]} = E_N^{\Delta} {\rm diag}[\widehat{\Theta}_1^{[k]}, \cdots, \widehat{\Theta}_S^{[k]}, 0_{Nn_1}, \cdots, 0_{Nn_F}, 0_{Nl_1}, \cdots, 0_{Nl_Z}](E_N^{\Delta})^T. \tag{6.51}$$

Then, (2.14) reduces to $\|\widehat{\Delta}(z)\|_\infty < 1/\gamma$ (i.e., $\|\Delta(\zeta)\|_\infty < 1/\gamma$), and it is automatically satisfied for the given uncertainty set $\boldsymbol{\Delta}$. The essential difference between the above structure and that of (D, G)-scaling type causal LTI FIR separators is only $\widehat{\Theta}_{\rm s1}^{[k]}, \ldots, \widehat{\Theta}_{{\rm s}F}^{[k]}$ in (6.48) whose structure is given by (6.50) associated with the blocks $I_N \otimes \Delta_1, \ldots, I_N \otimes \Delta_F$ of the structured uncertainty in (6.37).

6.4.3 LMI condition for robust stability analysis with noncausal LPTV FIR scaling

The preceding subsection stated that if we confine ourselves to noncausal LPTV FIR separators given by (6.40) satisfying (6.42)–(6.46), then (2.14) in the separator-type robust stability theorem is automatically satisfied. Therefore, for robust stability analysis based on noncausal LPTV FIR scaling, it suffices to search for $\widehat{\Theta}^{[\mathrm{FIR}]} = \left(\widehat{\Theta}_{ij}^{[\mathrm{FIR}]}\right)_{i,j=1,2}$ satisfying (6.42)–(6.46) such that the separator $\widehat{\Theta}(z) = \widehat{\Theta}_{\mathrm{FIR}}(z)$ resulting from (6.40) satisfies the remaining condition (2.13). When $N = 1$ (i.e., in causal LTI scaling), a method of searching for such $\widehat{\Theta}_{\mathrm{FIR}}(= \Theta_{\mathrm{FIR}})$ leading to $\Theta(\zeta)$ satisfying (2.15) has been already discussed in the preceding section. This subsection extends the result to the case of noncausal LPTV FIR scaling.

Substituting $\widehat{\Theta}_{\mathrm{FIR}}(z)$ given by (6.40) into $\widehat{\Theta}(z)$, we can rewrite (2.13) as

$$\widehat{G}_{\mathrm{a}}(z)^* \widehat{\Theta}^{[\mathrm{FIR}]} \widehat{G}_{\mathrm{a}}(z) \le 0 \quad (\forall z \in \partial\mathbf{D}), \tag{6.52}$$

where $\widehat{G}_{\mathrm{a}}(z) := [T_{Np}(z)^T \;\; (T_{Np}(z)\widehat{G}(z))^T]^T$. A realization of $\widehat{G}_{\mathrm{a}}(z)$ is given by

$$\left[\begin{array}{cccc:c:c}
0_{(K-1)Np\times Np} & I_{(K-1)Np} & & & 0 & 0_{(K-1)Np\times Np} \\
0_{Np} & 0_{Np\times(K-1)Np} & & & 0 & I_{Np} \\
\hdashline
\widehat{B} & 0_{n\times(K-1)Np} & & & \widehat{A} & 0 \\
\hline
\multicolumn{3}{c}{I_{KNp}} & & 0 & 0_{KNp\times Np} \\
\multicolumn{3}{c}{0_{Np\times KNp}} & & 0 & I_{Np} \\
\hdashline
\widehat{D} & & & & \widehat{C} & \\
\widehat{C}\widehat{B} & \ddots & & & \widehat{C}\widehat{A} & \\
\widehat{C}\widehat{A}\widehat{B} & \ddots & \widehat{D} & & \vdots & 0_{KNp\times Np} \\
\vdots & \ddots & \widehat{C}\widehat{B} & \widehat{D} & \vdots & \\
\widehat{C}\widehat{A}^{K-1}\widehat{B} & \dots & \widehat{C}\widehat{A}\widehat{B} & \widehat{C}\widehat{B} & \widehat{C}\widehat{A}^{K} & \widehat{D}
\end{array}\right] \tag{6.53}$$

which is minimal if (A, B) is reachable and (C, A) is observable. We denote it by $(\widehat{A}_{\mathrm{a}}, \widehat{B}_{\mathrm{a}}, \widehat{C}_{\mathrm{a}}, \widehat{D}_{\mathrm{a}})$, where $\widehat{A}_{\mathrm{a}} \in \mathbf{R}^{(KNp+n)\times(KNp+n)}$, $\widehat{B}_{\mathrm{a}} \in \mathbf{R}^{(KNp+n)\times Np}$, $\widehat{C}_{\mathrm{a}} \in \mathbf{R}^{2(K+1)Np\times(KNp+n)}$ and $\widehat{D}_{\mathrm{a}} \in \mathbf{R}^{2(K+1)Np\times Np}$.

Then, by the KYP lemma, we immediately have the following result.

Lemma 6.2 Assume that G (i.e., $\widehat{G}_{\mathrm{a}}(z)$) is internally stable. Then, $\widehat{G}_{\mathrm{a}}(z)$ satisfies (6.52) if and only if there exists a real symmetric matrix $P \in \mathbf{R}^{(KNp+n)\times(KNp+n)}$ satisfying

$$\begin{bmatrix} I & 0 \\ \widehat{A}_{\mathrm{a}} & \widehat{B}_{\mathrm{a}} \\ \widehat{C}_{\mathrm{a}} & \widehat{D}_{\mathrm{a}} \end{bmatrix}^* \mathrm{diag}\left[-P, P, \widehat{\Theta}^{[\mathrm{FIR}]}\right] \begin{bmatrix} I & 0 \\ \widehat{A}_{\mathrm{a}} & \widehat{B}_{\mathrm{a}} \\ \widehat{C}_{\mathrm{a}} & \widehat{D}_{\mathrm{a}} \end{bmatrix} \le 0. \tag{6.54}$$

By this lemma, we can find through (6.40) a noncausal LPTV FIR separator $\widehat{\Theta}(z) = \widehat{\Theta}_{\mathrm{FIR}}(z)$ satisfying (2.13) by solving the LMI (6.54). Regarding the inequality condition (6.46) on $\widehat{\Theta}_{22}^{[\mathrm{FIR}]}$, we can also reduce it to the LMI condition (6.27) with (A_T, B_T, C_T, D_T) replaced by a minimal realization of $T_{Np}(z)$.

To summarize, we can analyze robust stability of the closed-loop system by solving the above two LMIs under the constraints (6.42)–(6.45), and this establishes an explicit and feasible method for robust stability analysis with noncausal LPTV FIR scaling.

6.5 Numerical examples

This section numerically demonstrates the effectiveness of the developed framework for robust stability analysis with noncausal LPTV FIR scaling. We also confirm with a numerical example the theoretical results shown in Theorems 5.4 and 5.5 about conservativeness of noncausal LPTV FIR scaling relative to that of causal LTI FIR scaling.

6.5.1 Numerical demonstration of effectiveness of noncausal LPTV FIR scaling

Let us consider the stable LTI system G given by

$$A = \begin{bmatrix} 0 & I_3 \\ 0.1 & a^T \end{bmatrix},\ a^T = \begin{bmatrix} 0.3 & -0.6 & 0.8 \end{bmatrix},$$
$$B = \begin{bmatrix} 0_2 \\ 0.1 I_2 \end{bmatrix},\ C = \begin{bmatrix} I_2 & 0_2 \end{bmatrix},\ D = 0 \tag{6.55}$$

and the uncertainty set $\boldsymbol{\Delta} = \{\Delta \,\big|\, \|\Delta\| < \overline{\delta},\ \Delta = \mathrm{diag}[\delta_1, \delta_2],\ \delta_i \in \mathbf{R}\ (i = 1, 2)\}$ with given $\overline{\delta}$ $(= 1/\gamma)$. The problem we study here is to find (a lower bound of) the maximal $\overline{\delta}$ such that the closed-loop system Σ consisting of G and Δ $(\in \boldsymbol{\Delta})$ is robustly stable.

For this problem, we first analyze the maximal $\overline{\delta}$ by static causal LTI scaling. Then, we have a lower bound $\overline{\delta} = 2.0849$. Next, we analyze it by noncausal LPTV FIR scaling with $(N, K) = (2, 1)$. Then, we have a less conservative lower bound $\overline{\delta} = 3.2587$. This clearly demonstrates that introducing frequency dependence and time dependence into scaling (i.e., taking $K > 0$ and $N > 1$) is very effective. To confirm the improvement of the analysis results more visually, we show in Figure 6.2 the robust stability regions of (δ_1, δ_2) ensured by the above analysis results, where the outer solid line and inner dashed line correspond to $(N, K) = (2, 1)$ (i.e., noncausal LPTV FIR scaling) and $(N, K) = (1, 0)$ (i.e., static causal LTI scaling), respectively. The outer shaded area represents the instability region computed with a fine-grid analysis. We can see that noncausal LPTV FIR scaling drastically improves the analysis and gives an (almost) exact stability radius.

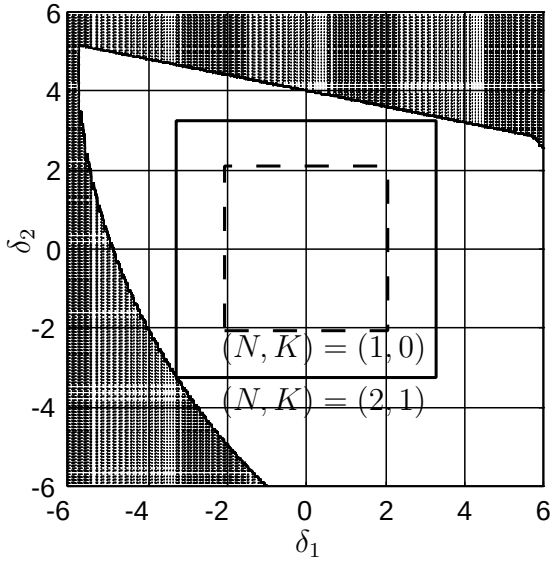

Figure 6.2: Robust stability domain for the closed-loop system.

6.5.2 Comparison with μ-analysis

The preceding subsection has demonstrated the effectiveness of noncausal LPTV FIR scaling through comparison with static causal LTI scaling. This subsection proceeds to numerical comparison with the conventional dynamic (D, G)-scaling approach of μ-analysis [51], where we use the μ-analysis and synthesis toolbox [2] of MATLAB. μ-analysis tackles the robust stability problem of closed-loop systems through calculating the structured singular value at each frequency. We take 1000 points between 10^{-2} and $\pi/T_{\rm s}$ ($\approx 3.14 \times 10^3$) (with equal distance in the logarithmic scale) as angular frequency points at which the structured singular values are computed, assuming that Σ has sampling period $T_{\rm s} = 0.001$. Then, we have the frequency plot of an upper bound $\overline{\mu}$ of the structured singular values for the nominal system G shown in Figure 6.3, and from its peak value 0.3048, an estimate of a lower bound of $\overline{\delta}$ becomes 3.2811 as its reciprocal.

Even though the above value is larger than the upper bound 3.2587 with noncausal LPTV FIR scaling, it does not immediately imply that μ-analysis has achieved a less conservative

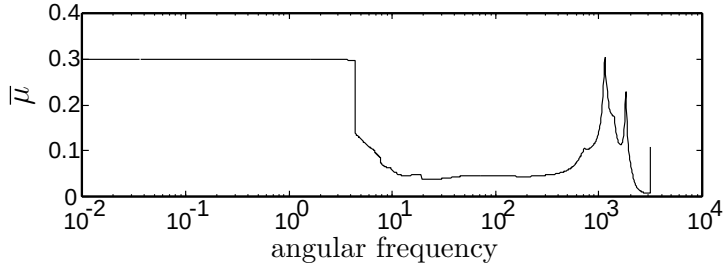

Figure 6.3: Upper bound $\overline{\mu}$ of the structured singular value.

analysis. Indeed, we have seen that the above noncausal LPTV FIR scaling has succeeded in an almost exact analysis, and hence it would be contradicting if we could have such a discernibly larger lower bound of the maximal $\overline{\delta}$. What the above numerical result with μ-analysis reminds us is that it can only give an *estimate* of a lower bound, and it changes with the angular frequencies at which the structured singular values are computed. For example, to detect the peak of the upper bound $\overline{\mu}$ around 10^3 more accurately, suppose we take 1000 points between 10^3 and $10^{3.1}$. Then, the resulting estimate of a lower bound of $\overline{\delta}$ reduces to 3.2528, which turns smaller than the lower bound obtained by noncausal LPTV FIR scaling.

In contrast to such an essentially approximate nature in μ-analysis, checking the existence of an eligible noncausal LPTV FIR separator can be carried out in a necessary and sufficient fashion (for each fixed N and K of noncausal LPTV FIR scaling), and once an eligible separator turns out to exist, it immediately ensures robust stability rigorously. The framework presented in this chapter would be much more reliable than μ-analysis in this regard.

Remark 6.2 Although the above μ-analysis with the toolbox seems to have almost no advantage over the LMI-based noncausal LPTV FIR scaling with respect to both the computational complexity and the reliability, these drawbacks have been studied and resolved, e.g., in [28],[16],[35],[36]. In particular, these articles study μ-analysis methods that do not require such typical frequency grids for calculating μ as those employed in this subsection, and succeed in reducing the computational complexity as well as improving the reliability. Although the approaches to robust stability analysis discussed in this thesis and those papers are completely different, it is considered to be important to further sophisticate our scaling approach, so as to be applied to much wider classes of problems.

6.5.3 Numerical confirmation of theoretical results on the effect of introducing time dependence into scaling

The preceding two subsections have demonstrated the effectiveness of noncausal LPTV FIR scaling by comparing it with static causal LTI scaling and μ-analysis. This subsection takes several pairs of (N, K) for noncausal LPTV FIR scaling, and confirms the theoretical results shown in Theorems 5.4 and 5.5 numerically.

Let us consider the stable LTI system G given by

$$A = \begin{bmatrix} 0 & I_5 \\ 0.1 & a^T \end{bmatrix},\ a^T = \begin{bmatrix} -0.2 & -0.3 & 0.3 & -0.6 & 0.8 \end{bmatrix},$$
$$B = \begin{bmatrix} 0_{2\times 4} \\ 0.1 I_4 \end{bmatrix},\ C = \begin{bmatrix} I_4 & 0_{4\times 2} \end{bmatrix},\ D = 0 \tag{6.56}$$

Table 6.1: Analysis results by noncausal LPTV FIR scaling

(N, K)	(1, 0)	(2, 0)	(1, 1)	(1, 2)	(2, 1)	(1, 3)
$\overline{\delta}$ $(= 1/\gamma)$	0.8449	1.0041	1.2036	1.4563	1.4563	1.4563

and the uncertainty set $\boldsymbol{\Delta} = \{\Delta \big|\ \|\Delta\| < \overline{\delta},\ \Delta = \mathrm{diag}[\delta_1, \delta_2, \delta_3, \delta_4],\ \delta_i \in \mathbf{R}\ (i = 1, \ldots, 4)\}$. We study the problem of finding (a lower bound of) the maximal $\overline{\delta}$ such that the closed-loop system Σ consisting of G and Δ $(\in \boldsymbol{\Delta})$ is robustly stable.

The analysis results of the maximal $\overline{\delta}$ obtained by noncausal LPTV FIR scaling (and causal LTI FIR scaling as a special case) are shown in Table 6.1. In this table, the pairs (N, K) are aligned in such an order that the corresponding analysis result for one pair should be less conservative (more precisely, should not degrade) than that for the pair to the left of it, according to the assertions of Theorems 5.4 and 5.5. We can confirm that the results in this table indeed demonstrate the assertions.

Remark 6.3 Since we have restricted separators to (D, G)-scaling type in this example, their infinite matrix counterparts are led to have an associated structure. This situation possibly affects the discussions about Theorems 5.4 and 5.5, whose proofs in the preceding chapter were based on the assumption that the infinite-dimensional FIR separator has no structural constraint in causal LTI scaling and noncausal LPTV scaling. Fortunately, however, the assertions of Theorems 5.4 and 5.5 can be confirmed to hold, by essentially the same arguments, even under the above restriction on the separators, provided that uncertainties are static (i.e., $Z = 0$). This can be immediately confirmed through deriving the infinite matrix counterparts of (D, G)-scaling type causal LTI FIR separators and (D, G)-scaling type noncausal LPTV FIR separators (and comparing their structures in the infinite matrix framework).

6.6 Concluding remarks

In this chapter, we have first established a systematic framework for robust stability analysis based on causal LTI FIR scaling. To develop such a framework, we first introduced an appropriate class of (D, G)-scaling type of causal LTI FIR separators associated with the given structure of uncertainties. We then provided an explicit LMI condition for searching for an eligible FIR separator, together with a minimal realization of the augmented system $G_{\mathrm{a}}(\zeta)$ involved in the LMI condition. The latter contributes to reducing the computation load in robust stability analysis.

Then, based on these arguments, we have further developed a robust stability analysis method based on lifting-based noncausal LPTV FIR scaling. Numerical examples were also given to demonstrate the effectiveness of the developed method. The examples show that noncausal LPTV FIR scaling surely reduces conservativeness in robust stability analysis, and is practically tractable and reliable compared with the conventional μ-analysis, as long as the use of the MATLAB toolbox is concerned. The validity of the theoretical results shown in the preceding chapter has been also confirmed numerically. The theoretical results in Chapter 4 can also be demonstrated in a similar fashion, and thus we have actually given in the chapter a numerical example in which the idea of FIR scaling is exploited in numerical computations.

Chapter 7

Conclusion

This thesis studied robustness analysis and controller synthesis based on discrete-time noncausal LPTV scaling for closed-loop systems with structured uncertainties. We summarize main contributions of this thesis in the following.

In Chapter 2, we reviewed the definition of noncausal LPTV scaling, and discussed its effectiveness in robust stability analysis. In particular, we showed theoretical results indicating that noncausal LPTV scaling induces dynamic scaling in the lifting-free framework even when it is taken to be static in the lifting-based framework. This property indeed contributes to reducing conservativeness in robust stability analysis, and we demonstrated it with numerical examples.

In Chapter 3, we considered exploiting static noncausal LPTV scaling, which has such a promising property, in robust controller synthesis. If we take account of only robust stability in the synthesis, however, the responses of the resulting control systems may become very oscillatory because of the periodicity of the controllers naturally designed under the lifting-based treatment. To avoid this problem, we developed a lifting-based controller synthesis method taking account of not only robust stability but robust H_∞ performance. We numerically demonstrated that the developed method can achieve good robust stability with successfully alleviating the oscillations. We further demonstrated by control experiments with a cart inverted pendulum that the developed method is indeed practical and has potentials for tackling actual control problems.

In Chapter 4, to clarify further properties of noncausal LPTV scaling, whose effectiveness has already been confirmed in both analysis and synthesis problems, we introduced the concept called shift invariance with respect to lifting timing, and studied its relationship to noncausal LPTV scaling. Then, we showed that noncausal LPTV scaling is not shift-invariant, in general, while causal LTI scaling is. In addition, we found that the operation called shift-invariant reconstruction plays an important role in clarifying properties of non-

causal LPTV scaling. More specifically, we theoretically showed that the gap (in terms of conservativeness in robust stability analysis) between some class of noncausal LPTV scaling and causal LTI scaling induced from the former scaling in the lifting-free framework can be interpreted in the lifting-based framework as that between the former scaling and its shift-invariant reconstruction. This means that the aforementioned gap can be completely characterized in the lifting-based framework, and the shift-invariant reconstruction plays a key role in exploiting full potential of (static) noncausal LPTV scaling.

In Chapter 5, as an alternative tool for studying properties of noncausal LPTV scaling, we considered the framework of representing systems by infinite matrices, and derived a separator-type robust stability condition in the framework. Such a new tool provides us with a unified treatment of lifting-free causal LTI scaling and lifting-based noncausal LPTV scaling, through deriving their infinite matrix counterparts. As tractable and practical classes, we introduced noncausal LPTV FIR scaling and causal LTI FIR scaling in the lifting-based and lifting-free frameworks, respectively, and compared them in the infinite matrix framework. Then, through the comparison, we clarified the effect of exploiting the lifting technique in reducing conservativeness of robust stability analysis. These discussions were carried out in a very intuitive manner with the new unified framework, which is expected to inspire further studies on properties of noncausal LPTV scaling.

In Chapter 6, we developed a numerical method for robust stability analysis based on noncausal LPTV FIR scaling whose properties have been discussed through the infinite matrix framework. We numerically demonstrated that conservativeness of the scaling approach can be reduced by increasing the lifting period and the order of the corresponding FIR separators. In addition, we also confirmed with a numerical example the validity of the theoretical results obtained through the infinite matrix framework. The theoretical results in Chapter 4 can also be numerically demonstrated in a similar fashion, and thus we have actually given in the chapter a numerical example in which the idea of FIR scaling is exploited in numerical computations.

We thus studied robustness analysis and controller synthesis based on noncausal LPTV scaling from both theoretical and practical viewpoints. Static noncausal LPTV scaling has been theoretically and numerically confirmed to be effective in robust stability analysis, compared with the conventional static causal LTI scaling, and its extension toward controller synthesis has also been discussed in Chapter 3 with demonstrating the effectiveness by control experiments. Therefore, the basis of *static* noncausal LPTV scaling is considered to be developed almost entirely. As future works around these discussions, for example, we can raise the issue of making the synthesis framework further practical (e.g., by considering the introduction of integral compensation) and that of studying whether introducing the

notion of (static) noncausal LPTV scaling is also effective for analysis frameworks other than (D, G)-scaling, which has been dealt with throughout this thesis.

Regarding *dynamic* noncausal LPTV scaling, on the other hand, its extension toward controller synthesis has not been discussed in this thesis, although robust stability analysis based on such scaling has in detail in Chapters 4–6. This was mainly attributed to a particular difficulty in exploiting (not necessarily lifting-based) dynamic scaling in controller synthesis in an LMI-based fashion. Regarding static scaling, the linearization techniques shown in [38] and [31] are known to be effective in deriving a BMI condition that can be exploited for output feedback full-order controller synthesis (which reduces to an LMI when the associated static separator is given and fixed). However, these techniques cannot be directly exploited for dynamic scaling. An obstacle for deriving an LMI (or BMI) condition for controller synthesis exploiting dynamic scaling is associated with a difficulty in ensuring internal stability of the nominal system in the closed-loop system. Fortunately, however, a solution to this issue has been provided in [39], in which a coupling condition is introduced between the two Lyapunov matrices in the associated inequality conditions for controller synthesis. On the basis of this result, the reference [41] has studied robust controller synthesis exploiting dynamic scaling. Even though these studies deal only with the continuous-time case, our discrete-time noncausal LPTV FIR scaling could also be exploited for controller synthesis, provided that a similar fundamental technique is established in the discrete-time case. Such discussions will also be future works related with the discussions in this thesis.

Bibliography

[1] Anderson, B. D. O., and Vongpanitlerd, S., *Network Analysis and Synthesis*, Prentice-Hall (1973).

[2] Balas, G. J., Doyle, J. C., Glover, K., Packard, A., and Smith, R., *μ-Analysis and Synthesis Toolbox User's Guide*, MUSYN Inc. and MathWorks (1994).

[3] Bhatia, R., *Fourier Series*, The Mathematical Association of America (2005).

[4] Bittanti, S., and Colaneri, P., Invariant representations of discrete-time periodic systems, *Automatica*, Vol. 36, No. 12, pp. 1777–1793 (2000).

[5] Bittanti, S., and Colaneri, P., *Periodic Systems: Filtering and Control*, Springer-Verlag (2009).

[6] Bode, H. W., *Network Analysis and Feedback Amplifier Design*, D. Van Nostrand Company, Inc. (1945).

[7] Boyd, S., El Ghaoui, L., Feron, E., and Balakrishnan, V., *Linear Matrix Inequalities in System and Control Theory*, Society for Industrial and Applied Mathematics (1994).

[8] Chen, T., and Francis, B., *Optimal Sampled-Data Control Systems*, Springer-Verlag (1995).

[9] Chilali, M., and Gahinet, P., H_∞ design with pole placement constraints: An LMI approach, *IEEE Transactions on Automatic Control*, Vol. 41, No. 3, pp. 358–367 (1996).

[10] Desoer, C. A., and Vidyasagar, M., *Feedback Systems: Input-Output Properties*, Academic Press (1975).

[11] Doyle, J., Analysis of feedback systems with structured uncertainties, *IEE Proceedings*, Vol. 129, No. 6, pp. 242–250 (1982).

[12] Doyle, J. C., Glover, K., Khargonekar, P. P., and Francis, B. A., State-space solutions to standard H_2 and H_∞ control problems, *IEEE Transactions on Automatic Control*, Vol. 34, No. 8, pp. 831–847 (1989).

[13] Fan, M. K. H., Tits, A. L., and Doyle, J. C., Robustness in the presence of mixed parametric uncertainty and unmodeled dynamics, *IEEE Transactions on Automatic Control*, Vol. 36, No. 1, pp. 25–38 (1991).

[14] Feintuch, A., and Francis, B. A., Uniformly optimal control of linear time-varying systems, *Systems & Control Letters*, Vol. 5, No. 1, pp. 67–71 (1984).

[15] Feintuch, A., Khargonekar, P., and Tannenbaum, A., On the sensitivity minimization problem for linear time-varying periodic systems, *SIAM Journal on Control and Optimization*, Vol. 24, No. 5, pp. 1076–1085 (1986).

[16] Ferreres, G., Magni, J. F., and Biannic, J.M., Robustness analysis of flexible structures: Practical algorithms, *International Journal of Robust and Nonlinear Control*, Vol. 13, No. 8, pp. 715–733 (2003).

[17] Fu, M., Dasgupta, S., and Chai Soh, Y., Integral quadratic constraint approach vs. multiplier approach, *Automatica*, Vol. 41, No. 2, pp. 281–287 (2005).

[18] Gahinet, P., Explicit controller formulas for LMI-based H_∞ synthesis, *Automatica*, Vol. 32, No. 7, pp. 1007–1014 (1996).

[19] Glover, K., and Doyle, J. C., State-space formulae for all stabilizing controllers that satisfy an H_∞-norm bound and relations to risk sensitivity, *Systems & Control Letters*, Vol. 11, No. 3, pp. 167–172 (1988).

[20] Hagiwara, T., Block checker/diagonal transformation matrices, their properties, and the interplay with fast-lifting, *International Journal of Systems Science*, Vol. 42, No. 8, pp. 1293–1303 (2011).

[21] Hagiwara, T., Note on well-posedness and separator-type robust stability theorem of LTI systems, *SICE Journal of Control, Measurement, and System Integration*, Vol. 5, No. 3, pp. 169–174 (2012).

[22] Hagiwara, T., and Ohara, Y., Noncausal linear periodically time-varying scaling for discrete-time systems, Proc. IFAC Workshop on Periodic Control Systems (2007).

[23] Hagiwara, T., and Ohara, Y., Noncausal linear periodically time-varying scaling for robust stability analysis of discrete-time systems: Frequency-dependent scaling induced by static separators, *Automatica*, Vol. 46, No. 1, pp. 167–173 (2010).

[24] Hosoe, Y., and Hagiwara, T., Robust stabilizing controller synthesis based on discrete-time noncausal linear periodically time-varying scaling (in Japanese), *Transactions of the Society of Instrument and Control Engineers*, Vol. 46, No. 4, pp. 219–228 (2010).

[25] Iwasaki, T., and Hara, S., Well-posedness of feedback systems: Insights into exact robustness analysis and approximate computations, *IEEE Transactions on Automatic Control*, Vol. 43, No. 5, pp. 619–630 (1998).

[26] Khargonekar, P. P., Poolla, K., and Tannenbaum, A., Robust control of linear time-invariant plants using periodic compensation, *IEEE Transactions on Automatic Control*, Vol. 30, No. 11, pp. 1088–1096 (1985).

[27] Kwakernaak, H., Robust control and H_∞-optimization—Tutorial paper, *Automatica*, Vol. 29, No. 2, pp. 255–273 (1993).

[28] Lawrence, C. T., Tits, A. L., and Van Dooren, P., A fast algorithm for the computation of an upper bound on the μ-norm, *Automatica*, Vol. 36, No. 3, pp. 449–456 (2000).

[29] Masubuchi, I., Ohara, A., and Suda, N., LMI-based controller synthesis: A unified formulation and solution, *International Journal of Robust and Nonlinear Control*, Vol. 8, No. 8, pp.669–686 (1998).

[30] Megretski, A., and Rantzer, A., System analysis via integral quadratic constraints, *IEEE Transactions on Automatic Control*, Vol. 42, No. 6, pp. 819–830 (1997).

[31] de Oliveira, M. C., Geromel, J. C., and Bernussou, J., Extended H_2 and H_∞ norm characterizations and controller parametrizations for discrete-time systems, *International Journal of Control*, Vol. 75, No. 9, pp. 666–679 (2002).

[32] Packard, A., and Doyle, J., The complex structured singular value, *Automatica*, Vol. 29, No. 1, pp. 71–109 (1993).

[33] Poljak, S., and Rohn, J., Checking robust nonsingularity is NP-hard, *Mathematics of Control, Signals, and Systems*, Vol. 6, No. 1, pp. 1–9 (1993).

[34] Rantzer, A., On the Kalman-Yakubovich-Popov lemma, *Systems & Control Letters*, Vol. 28, No. 1, pp. 7–10 (1996).

[35] Roos, C., and Biannic, J. M., Efficient computation of a guaranteed stability domain for a high-order parameter dependent plant, Proc. 2010 American Control Conference, pp. 3895–3900 (2010).

[36] Roos, C., Lescher, F., Biannic, J. M., Doll, C., and Ferreres, G., A set of μ-analysis based tools to evaluate the robustness properties of high-dimensional uncertain systems, Proc. IEEE Multi-Conference on Systems and Control, pp. 644–649 (2011).

[37] Safonov, M. G., *Stability and Robustness of Multivariable Feedback Systems*, MIT Press (1980).

[38] Scherer, C., Gahinet, P., and Chilali, M., Multiobjective output-feedback control via LMI optimization, *IEEE Transactions on Automatic Control*, Vol. 42, No. 7, pp. 896–911 (1997).

[39] Scherer, C. W., and Kose, I. E., Robustness with dynamic IQCs: An exact state-space characterization of nominal stability with applications to robust estimation, *Automatica*, Vol. 44, No. 7, pp. 1666–1675 (2008).

[40] Vaidyanathan, P. P., *Multirate Systems and Filter Banks*, Prentice-Hall (1993).

[41] Veenman, J., and Scherer, C. W., IQC-synthesis with general dynamic multipliers, Proc. 18th IFAC World Congress, pp. 4600–4605 (2011).

[42] Vidyasagar, M., *Nonlinear System Analysis* (2nd ed.), Prentice-Hall (1993).

[43] Willems, J. C., *The Analysis of Feedback Systems*, MIT Press (1971).

[44] Yakubovich, V. A., A frequency theorem for the case in which the state and control spaces are Hilbert spaces, with an application to some problems in the synthesis of optimal controls, Part I, *Siberian Mathematical Journal*, Vol. 15, No. 3, pp. 457–476 (1974).

[45] Yakubovich, V. A., A frequency theorem for the case in which the state and control spaces are Hilbert spaces, with an application to some problems in the synthesis of optimal controls, Part II, *Siberian Mathematical Journal*, Vol. 16, No. 5, pp. 828–845 (1975).

[46] Zames, G., On the input-output stability of time-varying nonlinear feedback systems—Part I: Conditions derived using concepts of loop gain, conicity, and positivity, *IEEE Transactions on Automatic Control*, Vol. 11, No. 2, pp. 228–238 (1966).

[47] Zames, G., On the input-output stability of time-varying nonlinear feedback systems—Part II: Conditions involving circles in the frequency plane and sector nonlinearities, *IEEE Transactions on Automatic Control*, Vol. 11, No. 3, pp. 465–476 (1966).

[48] Zames, G., Feedback and optimal sensitivity: Model reference transformations, multiplicative seminorms, and approximate inverses, *IEEE Transactions on Automatic Control*, Vol. 26, No. 2, pp. 301–320 (1981).

[49] Zames, G., Feedback and optimal sensitivity: Model reference transformations, weighted seminorms, and approximate inverses, Proc. 17th Allerton Conference, pp. 744–752 (1979).

[50] Zhang, J., and Zhang, C., Robustness of discrete periodically time-varying control under LTI unstructured perturbations, *IEEE Transactions on Automatic Control*, Vol. 45, No. 7, pp. 1370–1374 (2000).

[51] Zhou, K., and Doyle, J. C., *Essentials of Robust Control*, Prentice-Hall (1998).

Publications by the Author

Journal Papers

1. Y. Hosoe and T. Hagiwara, Robust stabilizing controller synthesis based on discrete-time noncausal linear periodically time-varying scaling (in Japanese), *Transactions of the Society of Instrument and Control Engineers*, Vol. 46, No. 4, pp. 219–228, 2010.

2. Y. Hosoe and T. Hagiwara, Properties of discrete-time noncausal linear periodically time-varying scaling and their relationship with shift-invariance in lifting-timing, *International Journal of Control*, Vol. 84, No. 6, pp. 1067–1079, 2011.

3. Y. Hosoe and T. Hagiwara, Robust performance controller synthesis based on discrete-time noncausal linear periodically time-varying scaling, *Asian Journal of Control*, Vol. 14, No. 5, pp. 1194–1204, 2012.

4. K. Katayama, Y. Hosoe and T. Hagiwara, Demonstrating the effectiveness of robust performance synthesis based on noncausal linear periodically time-varying scaling through control experiments of cart inverted pendulum (in Japanese), *Transactions of the Institute of Systems, Control, and Information Engineers*, Vol. 26, No. 5, pp. 165–173, 2013.

5. Y. Hosoe and T. Hagiwara, Unified treatment of robust stability conditions for discrete-time systems through an infinite matrix framework, *Automatica*, Vol. 49, No. 5, pp. 1488–1493, 2013.

6. Y. Hosoe and T. Hagiwara, Robust stability analysis based on finite impulse response scaling for discrete-time linear time-invariant systems, *IET Control Theory & Applications*, accepted for publication.

International Conference Papers

1. Y. Hosoe and T. Hagiwara, Effects induced by noncausality of scaling on robust stability analysis of discrete-time periodically time-varying systems, Proc. SICE Annual Conference 2010, SB07.01, pp. 3017–3023, Taipei, Taiwan, August 2010.

2. Y. Hosoe and T. Hagiwara, Synthesis of robust performance controllers based on discrete-time noncausal linear periodically time-varying scaling, Proc. IFAC International Workshop on Periodic Control Systems, Fr2B-79 (6 pages), Antalya, Turkey, August 2010.

3. Y. Hosoe and T. Hagiwara, Relationship between noncausal linear periodically time-varying scaling and causal linear time-invariant scaling for discrete-time systems, Proc. 18th IFAC World Congress, TuA06.6, pp. 3384–3391, Milano, Italy, August 2011.

4. Y. Hosoe and T. Hagiwara, Robust stability analysis with cycling-based LPTV scaling and its relationship with lifting-based approach, Proc. SICE Annual Conference 2011, FrA13-06, pp. 1782–1790, Tokyo, Japan, September 2011.

5. Y. Hosoe and T. Hagiwara, Infinite matrix representations of robust stability conditions for discrete-time systems, Proc. 50th IEEE Conference on Decision and Control and European Control Conference, MoB18.4, pp. 1359–1366, Orlando, USA, December 2011.

6. Y. Hosoe and T. Hagiwara, Robust stability analysis based on discrete-time FIR scaling, Proc. 2012 American Control Conference, FrB21.2, pp. 5972–5979, Montreal, Canada, June 2012.

7. Y. Hosoe and T. Hagiwara, Robust stability analysis based on noncausal LPTV FIR scaling: Explicit procedure and relationship with causal LTI FIR scaling, Proc. 51st IEEE Conference on Decision and Control, MoA06.5, pp. 240–247, Maui, USA, December 2012.

8. K. Katayama, Y. Hosoe and T. Hagiwara, Demonstrating the effectiveness of noncausal LPTV scaling through control experiments with cart inverted pendulum, Proc. 5th IFAC International Workshop on Periodic Control Systems, ThS6T1.4, pp. 143–148, Caen, France, July 2013.

9. T. Hikihara, Y. Hosoe and T. Hagiwara, Manipulation of fluxoid by electromagnetic perturbation, 2013 International Symposium on Nonlinear Theory and its Applications, Santa Fe, USA, September 2013 (to be presented).

10. R. Yamamoto, Y. Hosoe and T. Hagiwara, Introducing integral compensation into controller synthesis based on noncausal LPTV scaling and control experiments with cart inverted pendulum, SICE Annual Conference 2013, Nagoya, Japan, September 2013 (to be presented).

Domestic Conference Papers

1. Y. Hosoe, Y. Ohara, Y. Ebihara and T. Hagiwara, Discrete-time output-feedback controller synthesis satisfying inequality constraints represented by static separators (in Japanese), Proc. SICE Kansai Branch Symposium, pp. 9–12, Osaka, January 2009.

2. Y. Hosoe and T. Hagiwara, Discrete-time robust stabilizing controller synthesis based on noncausal linear periodically time-varying scaling (in Japanese), Proc. SICE 9th Annual Conference on Control Systems, TA5-4 (6 pages), Hiroshima, March 2009.

3. Y. Hosoe and T. Hagiwara, Properties of the robust controller design method based on discrete-time noncausal periodically time-varying scaling and their application (in Japanese), Proc. 38th SICE Symposium on Control Theory, pp. 195–200, Osaka, September 2009.

4. Y. Hosoe, T. Hagiwara and T. Hikihara, A numerical simulation of fluxoid manipulated by external perturbation (in Japanese), IEICE Technical Report, Vol. 109, No. 458, pp. 47–52, Tokyo, March 2010.

5. Y. Hosoe and T. Hagiwara, A study on robust stability analysis of discrete-time periodically time-varying systems via noncausal scaling (in Japanese), Proc. 54th Annual Conference of the Institute of Systems, Control and Information Engineers, W35-3, pp. 233–234, Kyoto, May 2010.

6. Y. Hosoe and T. Hagiwara, Relationship between noncausal linear periodically time-varying scaling and causal linear time-invariant scaling for discrete-time systems (in Japanese), Proc. 39th SICE Symposium on Control Theory, pp. 51–56, Osaka, September 2010.

7. Y. Hosoe and T. Hagiwara, Relationship of shift-invariance about timing of lifting to discrete-time noncausal linear periodically time-varying scaling (in Japanese), Proc. SICE 11th Annual Conference on Control Systems, 185-1-2 (8 pages), Okinawa, March 2011.

8. Y. Hosoe and T. Hagiwara, Robust stability condition of discrete-time systems based on infinite-dimensional matrix representation (in Japanese), Proc. SICE 11th Annual Conference on Control Systems, 185-1-3 (8 pages), Okinawa, March 2011.

9. Y. Hosoe and T. Hagiwara, Robust stability analysis based on discrete-time FIR scaling (in Japanese), Proc. 40th SICE Symposium on Control Theory, pp. 301–308, Osaka, September 2011.

10. Y. Hosoe and T. Hagiwara, FIR scaling exploited for dynamic parts of structured uncertainties (in Japanese), Proc. SICE 12th Annual Conference on Control Systems, 7 pages, Nara, March 2012.

11. K. Katayama, Y. Hosoe and T. Hagiwara, Verifying the effectiveness of robust performance synthesis based on noncausal linear periodically time-varying scaling through control experiment of cart inverted pendulum (in Japanese), Proc. 56th Annual Conference of the Institute of Systems, Control and Information Engineers, W42-1, pp. 587–588, Kyoto, May 2012.

12. Y. Hosoe and T. Hagiwara, Introduction of time dependence into FIR scaling for reducing conservativeness of robust stability analysis (in Japanese), Proc. 56th Annual Conference of the Institute of Systems, Control and Information Engineers, W42-2, pp. 589–590, Kyoto, May 2012.

13. M. Miyamoto, Y. Hosoe and T. Hagiwara, Robust stability analysis based on dynamic scaling employing Laguerre basis and Kautz basis (in Japanese), Proc. 57th Annual Conference of the Institute of Systems, Control and Information Engineers, 123-6 (4 pages), Hyogo, May 2013.

14. Y. Hosoe and T. Hagiwara, Robust stability analysis of discrete-time systems with polytopic stochastic uncertainties (in Japanese), Proc. 57th Annual Conference of the Institute of Systems, Control and Information Engineers, 213-6 (5 pages), Hyogo, May 2013.

15. R. Yamamoto, Y. Hosoe and T. Hagiwara, Introducing integral compensation into controller synthesis based on noncausal LPTV scaling and control experiments with cart inverted pendulum (in Japanese), Proc. 57th Annual Conference of the Institute of Systems, Control and Information Engineers, 333-3 (4 pages), Hyogo, May 2013.